Norwegian University
of Life Sciences

Master's Thesis 2018 30 ECTS
Department of Mathematical Science and Technology

Design and simulation of a grid-connected PV system in South Africa: technical, commercial and economical aspects

Marie Klever
Environmental Physics and Renewable Energy
Faculty of Science and Technology

Preface

This master's thesis finalizes my five-year masters degree in Environmental physics and renewable energy at the Norwegian University of Life Science (NMBU). The thesis was an initiative from Cathrine Nyquist, co-founder and managing director of Panthera Africa, regarding designing a photovoltaic (PV) system suited for Panthera Africa. It has been an exciting and challenging experience, filled with life lessons and acquired knowledge.

I would like to thank my supervisor, Espen Olsen, who introduced me to this thesis in the first place. He has contributed with his assistance and guidance during my work on the thesis. I would also like to thank Andreas Størdal, my co-supervisor and Power Production Analyst at Scatec Solar. Thank you for all information, ideas and advices during this process.

Furthermore, I would like to send a big thanks to Cathrine Nyquist, Lizaene Cornwall and all the other workers at Panthera Africa. I had a wonderful time when visiting and volunteering, due to all the amazing animals and people. Panthera Africa has the most peaceful atmosphere and gave me an inner calmness in the midst of writing my thesis. The field trip gave me a better understanding of who Panthera Africa is and what they do. A special thanks to Cathrine Nyquist for answering all my emails and questions, and providing me with the information needed to write my thesis. You have been supportive throughout this whole process and motivated me to do a better job.

For providing me with climatic information to my thesis I would like to thank the South African Weather Service (SAWS) and the Agricultural Research Council (ARC). The information gave me insight into the climatic conditions at Panthera Africa and provided me with relevant climatic data to use in the PV system simulation.

A special thanks to my mum and dad for your invaluable support and discussions during my master thesis. I would not have managed to do this without you. I would also like to thank Kari and Martine for good laughs, discussions and frustrations during the previous semester. It would not have been the same without you. Especially Martine, thank you so much for proofreading my thesis and giving me constructive feedback.

Ås, 14.02.2018

Marie Klever

Sammendrag

Formålet med denne masteroppgaven er å undersøke potensialet og lønnsomheten for å installere et nett tilknyttet fotovoltaisk (PV) anlegg hos Panthera Africa, lokalisert i Overstrand kommune i Sør Afrika. Panthera Africa har flere nordvendte tak overflater, samt et tilgjengelig bakkeareal. Energiforbruket er estimert til å være rundt 42.3 MWh årlig. Systemene er designet til å produsere 30 - 35 MWh, siden Overstrand kommune krever at PV system kunder må kjøpe mer elektrisitet enn de selger til kraftselskapet over en sammenhengende 12 måneders periode.

Værdata fra ulike databaser og værstasjoner vurderes for å bestemme den tilgjengelige solressursen. Den globale innstrålingen er mellom 1709 og 1854 kWh/m^2 årlig. Den gjennomsnittlige temperaturen er 16.9 °C og nedbør forekommer hovedsakelig om vinteren.

Simuleringsprogrammet PVsyst brukes for å designe og simulere PV systemene. Designparametere som modulorientering, skygging, system tap og avstand mellom PV modul rader evalueres. Skyggeanalysen viser at bakkemonterte moduler har de laveste skyggetapene. Skyggetapene foregår hovedsakelig om vinteren for bakkemonterte moduler og sommeren for takmonterte moduler.

En hovedsimulering gjennomføres med ulike PV moduler og vekselrettere for å finne det optimale systemet. Effekten av å bruke optimaliserere eller modul vekselrettere for å maksimere energiproduksjonen undersøkes. De bakkemonterte systemene har generelt en bedre systemytelse enn de takmonterte systemene. Et bakkemontert system med Solar Frontier moduler yter best. Det produserer 31.8 MWh og har en ytelse (PR) på 84.2%. Optimaliserere øker systemytelsen med 0.5% og modul vekselrettere øker systemytelsen med 3.6%, sammenlignet med streng vekselrettere. De største systemtapene er vekselretter tap og lavere modul effektivitet grunnet høye temperaturer. De bakkemonterte systemene har bedre korrelasjon mellom produksjon og forbruk, sammenlignet med taksystemene.

Faktorer som påvirker systemytelsen undersøkes i en sensitivitetsanalyse. Analysen viser at en endring i strålingsdata kan øke energiproduksjonen med 5%, mens endringer i tilsmussings tap og U-verdien hovedsakelig påvirker systemytelsen. Et aldringstap for systemet på 20 år minker systemytelsen med 6 - 9%, avhengig av hvilke moduler og invertere som brukes. Innstrålingstap og elektriske tap som skyldes gjensidig skygging avhenger sterkt av avstanden mellom PV modul radene, og øker med avtagende avstand.

Den økonomiske analysen viser at de beregnede elektrisitetskostnadende (LCoE) varierer mellom 1.4 - 1.8 R/kWh. Systemet med best ytelse er ikke det mest lønnsomme. Alle systemene har en negativ netto nåverdi og en tilbakebetalingstid som overstiger levetiden. Det er usikkerheter både i investeringskostnadene og de forhåndsdefinerte parameterne.

Abstract

The purpose of this thesis is to evaluate the potential and economic feasibility of installing a grid-connected photovoltaic (PV) system at Panthera Africa, located in Overstrand municipality in South Africa. Panthera Africa have several northward facing roof surfaces of limited area and an available ground area. The yearly energy demand is estimated to be around 42.3 MWh. As Overstrand municipality requires PV system customers to purchase more electricity from the utility than they feed back onto the grid on a consecutive 12 month period, the systems are designed to produce 30 - 35 MWh.

Climatic data at the site is assessed by comparing data from local weather station and different databases in order to determine the available solar resource. The yearly global horizontal irradiation is assumed to be between 1709 and 1854 kWh/m^2. The average temperature is found to be 16.9 °C, with rainfall mainly occurring during winter months.

PVsyst is used as the simulation software to design and simulate the PV systems. Design parameters such as module orientation, shading, inter-row spacing and loss factors are evaluated. A shading analysis shows that the ground area has the least amount of shading. Shading loss mainly occurs during winter for the ground area and summer for roof surfaces.

A base case simulation is performed using different module and inverter types to find the best performing system. The effect of using optimizers or module inverters to maximize energy production is investigated. The performance ratio is generally higher for ground mounted systems than for roof mounted systems. The best performing system is a ground mounted system having Solar Frontier modules. It produces 31.8 MWh and has a performance ratio (PR) of 84.2%. Using optimizers increases the performance by 0.5%, while module inverters increases the performance by 3.6%, compared to using string inverters. The main system losses are inverter losses and module efficiency loss due to temperatures different from STC. The ground mounted systems have a better correlation between the monthly production and consumption, compared with the roof mounted systems.

Different factors affecting the system performance are investigated in a sensitivity analysis. The analysis shows that a change in irradiation data could increase the system yield by 5%, while changes is soiling loss and the thermal parameter mainly affect the PR. When considering 20 years of ageing losses, the PR decreases by 6 - 9%, depending on the module and inverter used. The irradiance and electrical loss due to mutual shading strongly depends on the inter-row spacing, and increases with decreasing inter-row spacing.

The levelized cost of electricity varies between 1.4 - 1.8 R/kWh in the economical evaluation. The best performing system is not the most profitable. All systems have a negative net present value and a payback time exceeding the lifetime. There are uncertainties in the economical evaluation both in the investment costs and the predefined parameters.

Nomenclature

Symbols

α	Solar altitude anlge	$^\circ$
α_a	Absorption coefficient of solar irradiance	
β	Voltage temperature coefficient	$\%/^\circ C$
β_m	PV module tilt angle	$^\circ$
δ	Declination angle	$^\circ$
η	Conversion efficiency	%
η_m	Module efficiency	%
γ	Power temperature coefficient	$\%/^\circ C$
γ_m	PV module azimuth angle	$^\circ$
γ_s	Solar azimuth angle	$^\circ$
ν	Frequency	Hz
ρ_{cable}	Specific resistance of cable material	$\omega mm^2/m$
θ	Angle of incidence	$^\circ$
θ_z	Zenith angle	$^\circ$
A	Cross section of cable	mm
C_t	Cash flow in year t	R
$Costs_t$	Cash outflow in year t	R
d	System degradation rate	%
D_t	Decommissioning cost in year t	R
$D_{alt\,diff}$	Difference in altitude	m
D_{clim}	Climatic distance	m
D_{hor}	Horizontal distance	m
d_{row}	Inter-row spacing	m
DHI	Diffuse horizontal radiation	kWh/m^2

DNI	Direct normal radiation	kWh/m^2
E_c	Energy at bottom edge of conduction band	eV
E_g	Band gap energy	eV
E_{photon}	Photon energy	$J \cdot s \cdot Hz$
$E_{t=0}$	Initial yearly energy production of the system	kWh
E_v	Energy at top edge of valence band	eV
G	Terrestrial irradiance recieved on earth	W/m^2
G_t	Global tilted irradiance	W/m^2
G_{dif}	Diffuse irradiance	W/m^2
G_{dir}	Direct irradiance	W/m^2
G_{inc}	Incident solar irradiance	W/m^2
G_{ref}	Reflected irradiance	W/m^2
GHI	Global horizontal radiation	kWh/m^2
I_0	Investment cost	R
$I_{inv\,max}$	Maximum inverter input current	A
I_{SC}	Short circuit current	A
$I_{string\,max}$	Maximum string current	A
l	Cable length	m
M_t	Interest payments in year t	R
n_{max}	Maximum number of PV modules in a string	
n_{min}	Minimum number of PV modules in a string	
n_{string}	Maximum number of strings in an array	
O_t	Operation and maintenence cost in year t	R
$P_{inv\,AC}$	Nominal AC inverter power	W
P_{in}	Incident power at STC	W
P_{max}	Peak power	W
$P_{nom\,array}$	Nominal PV array power	W

$P_{nom\,ratio}$	Nominal power ratio	–
P_w	Wiring ohmic loss	W
r	Discount rate	%
R_w	Global wiring resistance	ω
R_{array}	PV array cabling resistance	ω
R_{sh}	Shunt resistance	ω
R_s	Series resistance	ω
$Revenue_t$	Cash inflow in year t	R
T	System lifetime	$year$
t	Year of operation	$year$
T_{amb}	Ambient temperature	$°C$
T_{module}	Module temperature	$°C$
T_{STC}	Operating temperature at STC	$°C$
U	Thermal loss factor	W/m^2K
U_c	Constant thermal loss factor	W/m^2K
U_v	Wind dependent thermal loss factor	$W/m^2K/m/s$
v	Wind speed	m/s
$V_{inv\,max}$	Maximum DC input voltage of the inverter	V
$V_{inv\,mpp\,min}$	Minimum voltage at which the inverter can search for the MPP	V
$V_{module\,max}$	Maximum PV array voltage	V
$V_{mpp\,STC}$	MPP voltage of PV module at STC	V
$V_{OC\,STC}$	Open circuit voltage of PV module at STC	V
V_{OC}	Open circuit voltage	V
w_m	Module width	m
Y_a	Array yield	kWh/kWp
Y_f	Specific yield	kWh/kWp
Y_r	Reference yield	kWh/kWp

UV	Ultra violet	

Constants

G_{NOCT}	Irradiance at NOCT	$800\,W/m^2$
G_{SC}	Solar constant	$1361\,W/m^2$
h	Planck constant	$6.626 \times 10^{-34}\,Js$

Abbreviations

AC	Alternating current
AM	Air mass
ARC	Agricultural research council
BAPV	Building adapted photovoltaics
BIPV	Building integrated photovoltaics
BoS	Balance of system
c-Si	Crystalline silicon
DC	Direct current
DoE	Department of energy
DPE	Department of public enterprice
EDGE	Excellence in design for greater efficiency
FF	Fill factor
FiT	Feed-in-tariff
GIR	Global incident radiation
IAM	Incidence angle modifier
IEA	International energy agency
LCoE	Levelized cost of electricity
LID	Light induced degradation
MPP	Maximum power point
MPPT	Maximum power point tracker
NERSA	National energy regulator of South Africa

NOCT	Nominal operating cell temperature
NPV	Net present value
NREL	National renewable energy laboratory
PID	Potential induced degradation
PR	Performance ratio
PV	Photovoltaic
ROI	Return on investment
RV	Residual value
SARS	South African revenue service
SAWS	South African weather service
SSEG	Small scale embedded generation
STC	Standard test conditions
SURAN	South African universities radiometric network

Table of Contents

Preface i
Sammendrag ii
Abstract iii
Nomenclature iv

1 Introduction **3**
1.1 Background 3
1.1.1 Small scale embedded generation 4
1.2 Objectives 4
1.3 Panthera Africa - Big Cat Sanctuary 4
1.4 Structure 5

2 Theory **7**
2.1 Solar resources 7
2.1.1 Solar radiation 7
2.1.2 Terrestrial solar radiation 7
2.1.3 Seasonal, daily and latitudinal variations 8
2.1.4 Position of the Sun and PV module 9
2.1.5 Solar irradiance on a tilted PV module 9
2.2 PV system technology 10
2.2.1 The photovoltaic cell 10
2.2.2 The PV module 13
2.2.3 Inverters 15
2.2.4 Mounting system 17
2.2.5 Other BoS components 17
2.3 Grid-connected PV system design and evaluation 19
2.3.1 Site assessment 19
2.3.2 Shading analysis 19
2.3.3 Climatic data acquisition 20
2.3.4 Module orientation and inter-row spacing 21
2.3.5 Module and inverter selection 22
2.3.6 Array to inverter matching 22
2.3.7 PV system performance 25
2.3.8 PV system losses 26
2.4 Economical evaluation of a PV system 27
2.4.1 Payback time 28
2.4.2 Net Present Value (NPV) 28
2.4.3 Levelized cost of electricity 28
2.4.4 Funding and compensation schemes 30
2.5 Policies and regulations 31

3 Methodology **34**
3.1 Simulation Software: PVsyst . . . 34
3.1.1 Project design . . . 34
3.1.2 Project specification . . . 35
3.1.3 System variant management . . . 36
3.1.4 Accuracy of PVsyst . . . 39
3.2 Site assessment . . . 40
3.2.1 Geographical location . . . 40
3.2.2 Available area specifications and orientations . . . 40
3.2.3 Near shading items . . . 41
3.2.4 Location of BoS components . . . 42
3.2.5 Electricity consumption and grid connection . . . 42
3.3 Climatic data acquisition . . . 43
3.3.1 Local weather stations . . . 43
3.3.2 Databases . . . 45
3.3.3 Data comparison and analysis . . . 46
3.3.4 Choosing meteorological datasets and albedo values . . . 47
3.4 Module orientation and inter-row spacing . . . 48
3.4.1 Roof mounted PV system . . . 49
3.4.2 Ground mounted PV system . . . 49
3.5 Shading . . . 50
3.5.1 Near shading on buildings . . . 50
3.5.2 Near shading on ground area . . . 51
3.5.3 Far shading . . . 52
3.6 Selection of modules and inverters . . . 52
3.6.1 Selecting modules . . . 53
3.6.2 Selecting inverters . . . 54
3.7 System design . . . 55
3.7.1 Matching energy production and consumption . . . 55
3.7.2 Design temperatures . . . 56
3.7.3 Array to inverter matching . . . 56
3.7.4 System design configuration . . . 57
3.8 System losses . . . 59
3.9 Sensitivity analysis . . . 61
3.9.1 Irradiation data sensitivity . . . 61
3.9.2 Soiling loss sensitivity . . . 61
3.9.3 Thermal parameter sensitivity . . . 62
3.9.4 Ageing sensitivity . . . 62
3.9.5 Ground mounted orientation sensitivity . . . 62
3.10 Economical evaluation . . . 63

4 Simulation results and discussion **66**
4.1 Base case simulation . . . 66
4.1.1 Roof mounted system results . . . 67

4.1.2 Ground mounted system results . . . 69
4.1.3 Discussion . . . 69
4.2 Irradiation data sensitivity . . . 73
4.2.1 Discussion . . . 73
4.3 Soiling loss sensitivity . . . 74
4.3.1 Discussion . . . 74
4.4 Thermal parameter sensitivity . . . 76
4.4.1 Discussion . . . 76
4.5 Ageing sensitivity . . . 77
4.5.1 Discussion . . . 78
4.6 Ground mounted orientation sensitivity . . . 78
4.6.1 Inter-row spacing sensitivity . . . 78
4.6.2 Azimuth angle sensitivity . . . 79
4.7 Economical evaluation . . . 80
4.7.1 Comparing production and consumption . . . 80
4.7.2 Economical evaluation . . . 81

5 Conclusion **85**
5.1 Further work . . . 86

Bibliography **87**

A Meteorological data **93**

B Component specifications **95**

C Economical assumptions **103**

D Roof mounted system results for the individual buildings **105**

E Simulation results **106**

F Energy amount to buy or sell **108**

G Economical evaluation **109**

Chapter 1

Introduction

1.1 Background

The South African electricity sector is dominated by the state-owned utility supplier Eskom. The utility generates about 95% of the electricity used in South Africa and is responsible for transmitting and distributing the electricity [1], in what is termed a monopolistic sector. Eskom has an energy mix of coal power stations, nuclear power plants, gas turbines, hydroelectric power stations, solar PV plants, wind turbine farms and concentrated solar power plants [2, 3]. The most abundant source of energy in South Africa is coal and about 90% of the electricity generated by Eskom is from coal fired power stations [3]. Even though coal is the dominant energy generation source, South Africa has an excellent solar resource. With an average yearly irradiation between 1750 and 2500 kWh/m^2 [4], the possibility of solar PV is great.

Due to the South African growing need for greater power system capacity, the Renewable Energy Independent Power Producers Procurement Program (REIPPPP) was introduced in 2011. The program focuses on using public-private partnerships with independent power producers (IPPs) to develop sustainable energy facilities [5]. The IPPs sign long-term power purchase agreements (PPAs) with Eskom to guarantee their revenue [6]. It aims to start the renewable energy industry in South Africa, as renewable energy is a mature, sustainable and increasingly competitive solution to increase electricity production [4]. The installed solar PV capacity in South African has increased under the REIPPPP, reaching 1474 MW at the end of December 2016 [7]. The program has run four competitive tenders/bidding rounds since 2011, resulting in price drops for electricity generated by solar PV and wind [6]. Electricity produced by solar PV has dropped by 71% in nominal terms [6].

South Africa is signatory on both the Kyoto Protocol and the Paris Agreement COP21. The Paris Agreement commits all countries to contribute to an ambitious greenhouse gas (GHG) emissions reduction goal and expects all signed parties to report regularly on the status of their emissions and implementation efforts. As the South Africa relies heavily on coal to produce energy, it is a high emitter of greenhouse gases. According to COP21, South Africa is responsible of 1.46% of the global greenhouse gas emission by the parties in the agreement [8]. The implementation of REIPPPP is a step towards increasing teh amount of renewable energy in the country's energy sector.

1.1.1 Small scale embedded generation

Small Scale Embedded Generation (SSEG) in South Africa refers to power generation under 1MWp which are located on residential, commercial or industrial sites where electricity is also consumed [9]. Even though the REIPPPP only made provisions for large scale PV plants, South Africa has seen an increase in the number of private PV systems installed on residential and commercial premises [10]. Increasing electricity prices, combined with supportive policy incentives and decreasing technology costs are prompting more consumers towards solar energy solutions. In addition, Energy Service Companies (ESCOs) offers customers end-to-end energy solutions, including energy audit, technical design, installation, operation and maintenance and financing.

Several municipalities in South Africa have already introduced rules and regulations to allow for small scale embedded generation. Some also offers incentives for residential and commercial customers such as feed-in-tariffs or net metering.

Despite the increase in SSEG installations in South Africa, there are challenges. Governmental regulations and policies regarding SSEG are needed. There is also a conflict regarding electricity prices. Energy prices in South Africa has risen significantly over the past decade as a result of Eskom's new build program and the cost of essential plant maintenance. As more consumers install PV systems, the revenue for Eskom will decrease, and the electricity prices will have to rise further, to compensate for the decrease in revenue. This will affect the low-end customers the most, as they often does not have the financial means to go solar.

1.2 Objectives

The thesis is written as a feasibility study, exploring possible PV system solutions for Panthera Africa. The objective of this thesis is to design a PV system suited for the needs at Panthera Africa and includes:

- Collecting and evaluating meteorological data for the site to determine the available solar resource and environmental conditions.
- Evaluating available roof surfaces and ground surfaces regarding the suitability of installing a PV system.
- Designing and simulating several possible PV systems suited to Panthera Africa's electricity need, while considering limitations and restrictions due to local guidelines regarding small scale embedded generation.
- Evaluating the economical feasibility of the PV systems designed.

1.3 Panthera Africa - Big Cat Sanctuary

Panthera Africa Big Cat Sanctuary is a non-profit company, founded by Lizaene Cornwall and Cathrine N. Nyquist, located in Overstrand municipality in the Western Cape in South Africa. It is one of seven ethical sanctuaries in South Africa for captive bred

big cats. They are a true sanctuary, meaning no breeding, trading or cub petting takes place. Panthera Africa focuses on being an educational platform and raising awareness about ethical animal treatment through educational visits, volunteering programs and educational presentations.

1.4 Structure

Chapter 1 gives an introduction to solar PV in South Africa, with a focus on small scale embedded generation. The objective of the thesis is also presented, as well as a description of Panthera Africa.

Chapter 2 provides theory regarding the solar resource, PV system technology, the design and evaluation of a grid-connected PV system, economical evaluation of a PV system, and policies and regulations regarding installing PV systems in South Africa.

Chapter 3 describes the methodology used in this thesis and gives an introduction to PVsyst, which is the simulation software used. It also presents system parameters to be further analyzed in a sensitivity analysis.

Chapter 4 presents the results from the main simulation, the results from all sensitivity analysis and the results from the economical evaluation. The discussion regarding each presented result is also included in this chapter.

Chapter 5 presents the main conclusion for this thesis and gives suggestions for further work.

Chapter 2
Theory

2.1 Solar resources

The theory in section 2.1 and 2.2 is mainly based on *Solar energy – the physics and engineering of photovoltaic conversion technologies and systems* [11], *PVeducation.org* [12] and *Renewable and efficient electric power systems* [13]. Other sources are specified.

To design and analyses a photovoltaic (PV) system we need to know how much sunlight is available at the location of the PV system. The solar irradiance that reaches the Earth's surface varies due to atmospheric effects, local variations in the atmosphere, latitude of the location and the season of the year and the time of day. These factors affect both the power density, the spectral distribution of the light and the angle from which light is incident on a surface.

2.1.1 Solar radiation

The Sun is the source of the solar radiation that hits the Earth. Nuclear fusion takes place in the center of the Sun, releasing a total power of about $3.8 \cdot 10^{26}$ W, where 98% is released as electromagnetic radiation. In addition to behaving as electromagnetic radiation, the light also behaves as particles, called photons. The photon energy, E_{photon}, is given by Planck's law

$$E_{photon} = h\nu, \tag{2.1}$$

where $h = 6.626 \cdot 10^{-34} J \cdot s$ is Planck's constant and ν is the frequency of the photon [Hz].

2.1.2 Terrestrial solar radiation

The Sun radiates power at an intensity of $6.4 \cdot 10^7 \mathrm{W/m^2}$ in all directions in space. As the distance from the Sun increases, the power intensity decreases. The solar irradiance fraction that reaches the Earth's atmosphere is called the extraterrestrial radiation. It fluctuates throughout the year because of the Earth's elliptical orbit. The yearly average value is called the *solar constant*, G_{sc}, and is illustrated in figure 2.1a. It has a value of 1361 $\mathrm{W/m^2}$ [11].

As light passes through the atmosphere, its power decreases and the spectral distribution changes. The light is attenuated due to scattering, absorption and reflection by gases, aerosols and dust particles. The attenuation amount depends on the distance the beam has to travel through the atmosphere. The major factor in reducing the power of the solar radiation is the path length of the sunlight through the atmosphere, described by

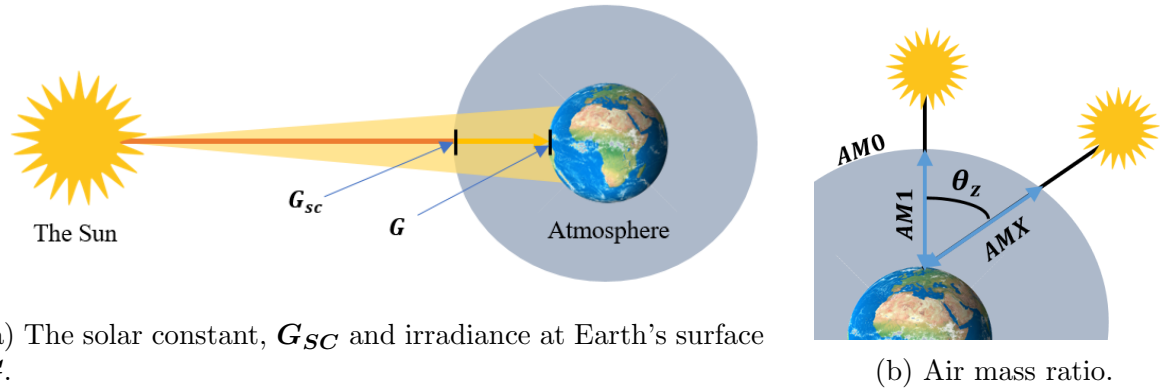

(a) The solar constant, G_{SC} and irradiance at Earth's surface G.

(b) Air mass ratio.

Figure 2.1: Illustration of (a) the solar constant and irradiance at Earth's surface and (b) air mass ratio, where AMX is the unknown air mass.

the air mass (AM). AM is the sunlight's path length divided by the minimum possible path length ($AM1$), which occurs when the Sun is at zenith, i.e. directly overhead. The air mass ratio can be expressed as

$$AM = \frac{1}{cos\theta_z}, \tag{2.2}$$

where θ_z is the angle from the vertical (the zenith angle) [°], as illustrated in figure 2.1b.

The terrestrial radiation G received at the surface of the Earth on a cloudless day is close to 1000 W/m^2 [11]. Clouds reduces the incident power and alters the proportion of direct and diffuse radiation. Absorption by gases such as H_2O, O_2, O_3 and CO_2 alters the spectral distribution of the terrestrial solar radiation, as illustrated in figure 2.2. The extraterrestrial solar spectrum is called AM0, because no atmosphere is traversed. A standard spectrum called AM1.5 is used to approximate the varying terrestrial spectrum. Both spectrums are illustrated in figure 2.2. The Sun's position and cloud cover influences the solar spectrum [14].

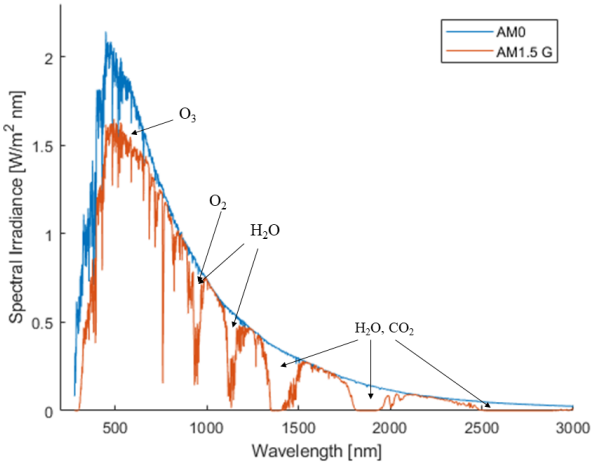

Figure 2.2: Illustrates spectrum AM0 and AM1.5. Different gases absorb light at different wavelengths, as shown by gaps in AM1.5. Data in the figure is downloaded from [15].

2.1.3 Seasonal, daily and latitudinal variations

Terrestrial irradiance varies with season, time of day and latitude of the location. The Earth circles around the Sun in an elliptical orbit and is tilted 23.45° with respect to the ecliptic plane, as shown in figure 2.3. This, together with the fact that the Earth revolves around its axis, causes seasons and therefore yearly variations in terrestrial solar radiation. Terrestrial radiation also varies with latitude.

The declination angle of the Sun, δ, is the angle between the equator and a line drawn from the center of the Earth to the center of the Sun. The declination angle in the Southern Hemisphere reaches a minimum of -23.45° at summer solstice, a maximum of +23.45° at winter solstice and is 0° at both equinoxes. An equinox is the time of year when day and night are of equal length, occurring at September 21$^{\text{th}}$ and March 21$^{\text{th}}$. The declination angle varies seasonally due to the tilt of the earth and the rotation around the Sun.

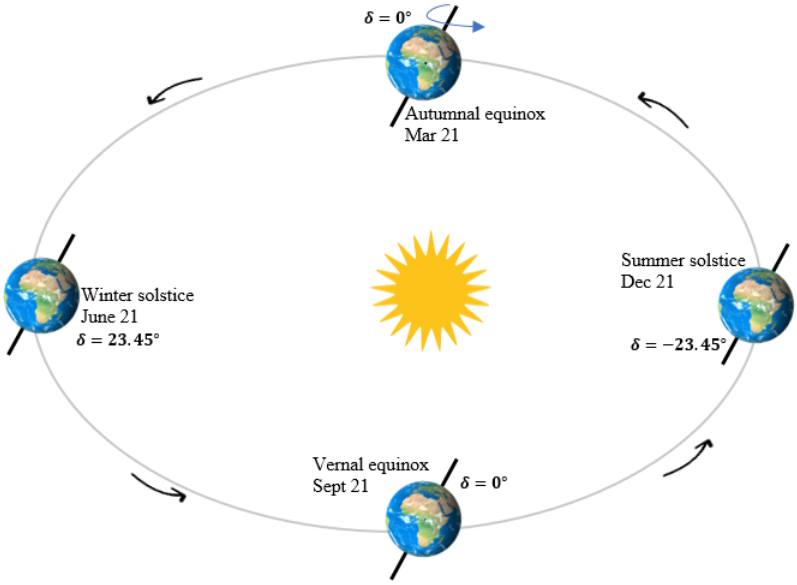

Figure 2.3: The tilt of the Earth and its path around the Sun. The seasons marked on the illustration are for the Southern Hemisphere. The declination angle varies from -23.45° $\leq \delta \leq$ 23.45° through the year.

2.1.4 Position of the Sun and PV module

Knowledge of the Sun's path relative to the PV modules is important for calculating irradiance values and the yield of a PV system. The Sun's position depends on the time of day, the time of year and the location on Earth. It can be expressed in terms of a solar altitude angle, α, describing the angular height of the Sun in the sky relative to the horizontal plane, and a solar azimuth angle, γ_s, describing the direction the sunlight is coming from. The azimuth angle is defined as -180° $\leq \gamma_s \leq$ 180°, with zero due north. East angles are positive (east = 90°) and west angles are negative (west = -90°).

The position of a PV module is defined by its tilt angle from the horizontal plane, β_m,

and orientation, expressed as the azimuth angle γ_m. The angle of incidence θ in figure 2.4b is the angle between the surface normal and the incident direction of the sunlight.

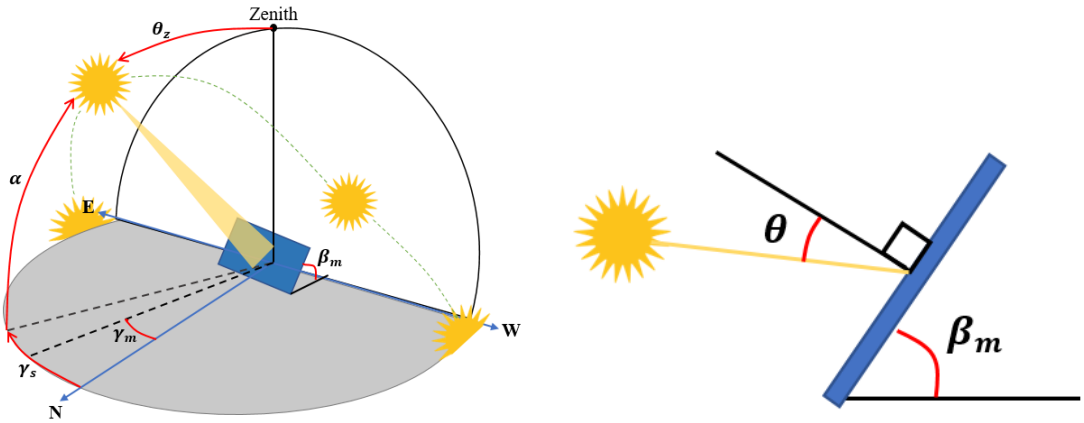

(a) Sun and PV module position angles. (b) Incidence angle.

Figure 2.4: Illustrates all relevant angles for describing the position of the Sun relative to the PV module.

The Sun's path throughout the year for a specific location can be portrayed graphically by plotting its altitude angles against azimuth angles, as shown in figure 2.5. This illustration is called a sun path diagram.

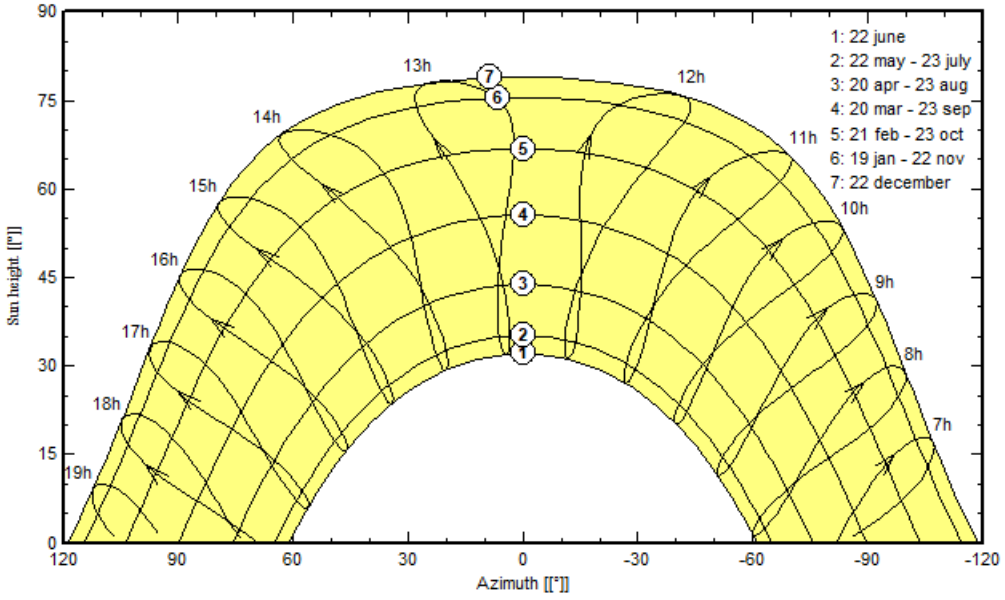

Figure 2.5: Illustration of a sun path diagram for the location -34.46°S, 19.53°E. The solar altitude angle is on the y-axis and the solar azimuth angle is on the x-axis.

2.1.5 Solar irradiance on a tilted PV module

The total irradiance, G_t, on a tilted PV module at a given location on Earth consists of direct irradiance, G_{dir}, diffuse irradiance, G_{dif}, and reflected irradiance, G_{ref}, as illustrated

in figure 2.6, and is given by

$$G_t = G_{dir} + G_{dif} + G_{ref}, \tag{2.3}$$

where all irradiance components are expressed in [W/m^2]. G_t is also called the global tilted irradiance (GTI).

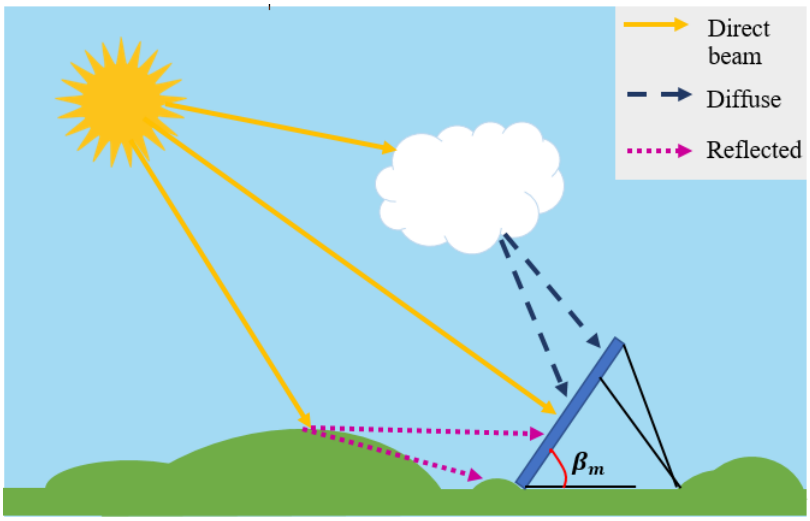

Figure 2.6: Solar radiation is reflected, absorbed and scattered when it travels through the atmosphere. The figure shows the three component the irradiance on a tilted PV module consists of: direct beam irradiance, diffuse irradiance and reflected irradiance. β_m is the tilt angle of the PV module.

2.2 PV system technology

A PV system is designed to supply electricity to a consumer by using photovoltaics and can be categorized as a stand-alone system or a grid-connected system. A standalone system relies only on solar power, while a grid-connected system relies on both solar power and the local grid. The main PV system component is the PV module. Other components required for a working PV system are called the balance of system (BoS). The most important BoS components are inverters, charge controllers, energy storage, AC and DC cables, and a mounting system.

2.2.1 The photovoltaic cell

A photovoltaic cell converts solar energy to electricity due to the photovoltaic effect. Most solar cells are made of semiconducting material, with crystalline silicon (c-Si) being the most commonly used in solar cells today [11]. The solar cell can absorb a wide spectrum of photons from the incident solar radiation, depending on the optical and electrical features of the semiconductor material used in the solar cell.

The physics of a semiconductor can be explained through the bonding model and the energy band model. In this section the bonding model is only used to visualize the

atomic structure of a semiconductor and doping.

Crystalline silicon and doping

Silicon has atomic number 14 and is tetravalent, i.e. has four valence electrons. In an ideal c-Si structure, at 0 K, each Si atom forms covalent bonds with four neighboring Si atoms. No electrons are free to move and the semiconductor behaves like an insulator. At temperatures above 0 K covalent bonds begin to break, resulting in mobile electrons called free electrons. Each hole left behind by a free electron can accept a neighboring valence electron, creating a current of holes in the opposite direction of electrons. Free electrons are negative charge carriers, while holes are positive charge carriers. This is illustrated by the bonding model in figure 2.7a.

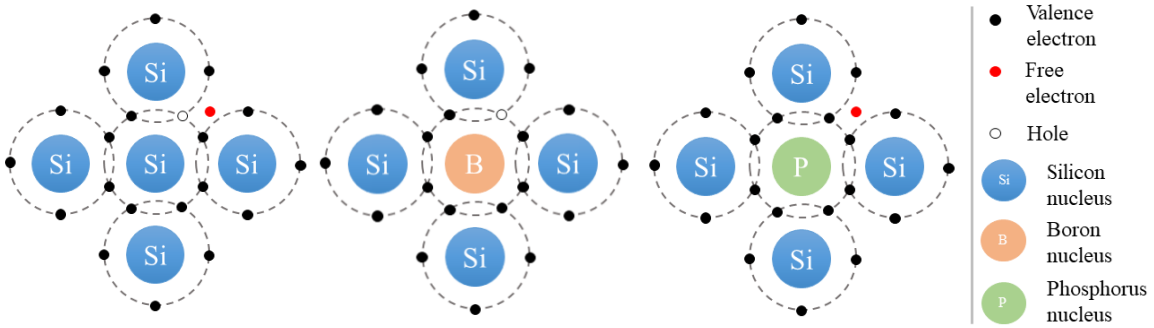

(a) (b) (c)

Figure 2.7: Bonding model illustrating (a) silicon above 0 K, (b) p-doping and (c) n-doping.

The conductivity of a semiconductor at room temperature is low, because there are few thermally generated electron-hole pairs [16]. To increase conductivity, a semiconductor can be doped with a pentavalent or a trivalent element, as illustrated in figure 2.7b and 2.7c. A pentavalent substance, such as Phosphorus, donates excess electrons to the crystal lattice, creating a n–type semiconductor. A trivalent substance, such as Boron, donates excess holes to the crystal lattice, creating a p–type semiconductor.

Working principle of the solar cell

Most solar cells are made by connecting a p-type and n-type semiconductor, forming a pn-junction, as illustrated in figure 2.8. The pn-junction create an internal electric field which may separate the generated electron-hole pair before they recombine. The difference in electron and hole concentration between the p- and n-type material causes a diffusion of electrons to the p-side and holes to the n-side, leaving behind space charges. The space charges set up an internal electric field, which balances the diffusion when steady state is reached. A net current is first produced when the solar cell is illuminated.

When a solar cell is illuminated, charge carriers are generated in the material by photons with energies higher than the band gap energy E_g. Only an energy of E_g will be utilized, even though the photon has a larger energy. Photons with an energy less than E_g will be

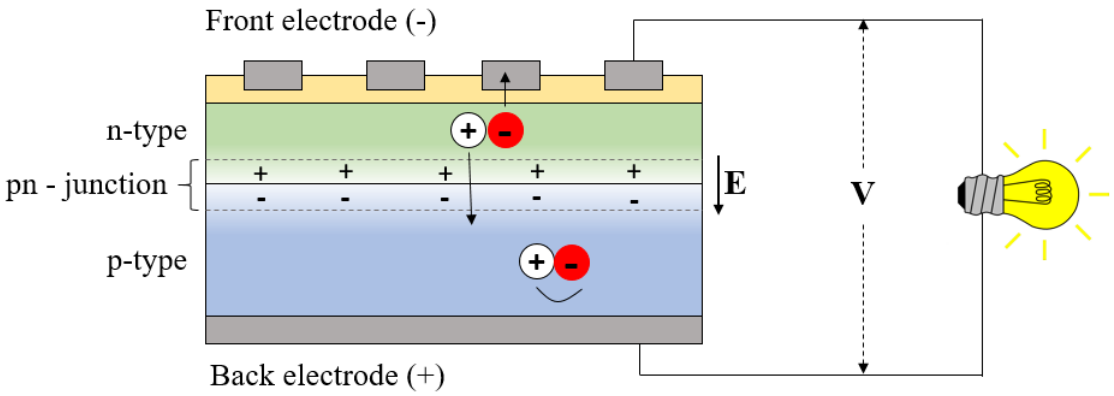

Figure 2.8: Illustrates the working principle of a solar cell. The n- and p-type semiconductor material are connected together, forming a pn-junction. E is the internal electrical field created at the pn-junction.

transmitted through the solar cell. The band gap energy is the energy difference between the top edge of the valence band, E_v, and the bottom edge of the conduction band, E_c. E_g represents the minimum energy required for an electron to break free from its bound state in the valence band. For silicon, the band gap energy is about 1.1 eV [16].

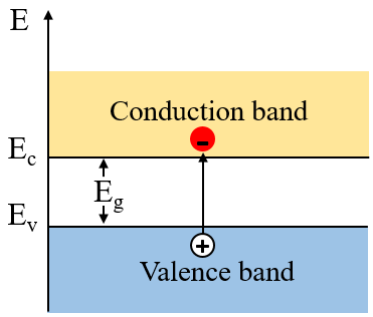

Figure 2.9: The band gap model for a semiconductor with the excitation of an electron by absorption of light. An energy equal to or greater than the band gap energy (E_g) is needed to excite an electron from the valence band to the conduction band.

Performance of a solar cell

The performance of a solar cell is mainly characterized by the peak power (P_{max}), the short circuit current (I_{SC}), the open circuit voltage (V_{OC}) and the fill factor (FF) [11]. These parameters can be determined by looking at the IV-curve of an illuminated solar cell, as illustrated in figure 2.10.

The short circuit current is the maximal current through the solar cell, obtained when the terminals are short circuited. If the solar cell is operated as an open circuit, no current will flow through the circuit i.e. there is infinite resistance between the terminals. Even though I_{SC} and V_{OC} are the maximal current and voltage, the power from the solar cell is zero at both points. The maximum power point (MPP) in figure 2.10 gives the maximal power output and is the ideal operating point. The power output at MPP is given by

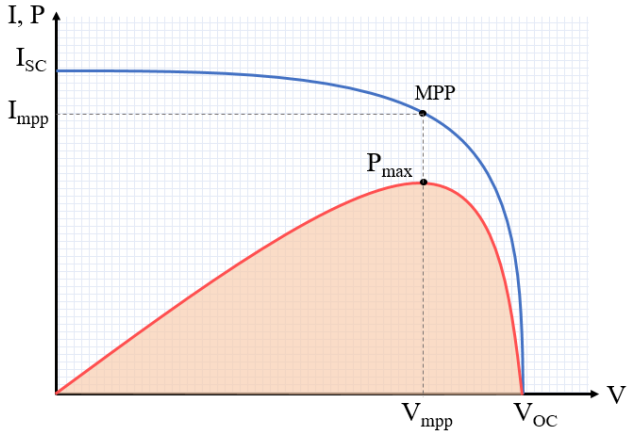

Figure 2.10: I-V curve and power curve for a solar cell. The blue line is the I-V curve and the red line is the power curve. MPP is the maximal power point, and P_{max} is the power at MPP.

$$P_{max} = I_{mpp} \cdot V_{mpp}, \tag{2.4}$$

where I_{mpp} is the current at MPP [A] and V_{mpp} is the voltage at MPP [V].

The fill factor describes the quality of a solar cell. FF is calculated by comparing the maximum power to the theoretical power at I_{SC} and V_{OC}. It is given by

$$FF = \frac{P_{max}}{V_{OC} \cdot I_{SC}}. \tag{2.5}$$

The conversion efficiency η of a solar cell is determined as the fraction of incident power which is converted to electricity and is a measure of its performance. In order to compare different solar cell technologies it is measured under standard test conditions (STC). STC are characterized by an irradiance of 1000 W/m^2, an AM1.5 spectrum and a cell temperature of 25°C. The module efficiency changes as the operation conditions deviate from STC and is idealistically defined as

$$\eta = \frac{P_{max}}{P_{in}} = \frac{V_{OC} \cdot I_{SC} \cdot FF}{P_{in}}, \tag{2.6}$$

where P_{in} is the incident power [W].

For a realistic, non-ideal, single-junction solar cell, several loss factors should be accounted for in the efficiency equation. The most important losses are due to [11]:

- non-absorption of long wavelengths
- thermalization of the excess energy of photons
- reflection
- incomplete absorption due to the finite thickness
- recombination
- metal electrode coverage, shading losses
- voltage factor
- fill factor.

Electrical properties of a solar cell

To schematically represent the behavior of a real, illuminated solar cell, the one-diode model in figure 2.11 can be used. The solar cell is represented by an equivalent circuit with a current source connected in parallel with a diode, representing the pn-junction. Internal resistance in the solar cell is represented by a shunt resistance R_{sh} and a series resistance R_s. The shunt resistance represents the leakage current and the series resistance represents the voltage drop when charge carriers migrate from the solar cell to the load, due to resistance in the metal contacts and the semiconductor itself.

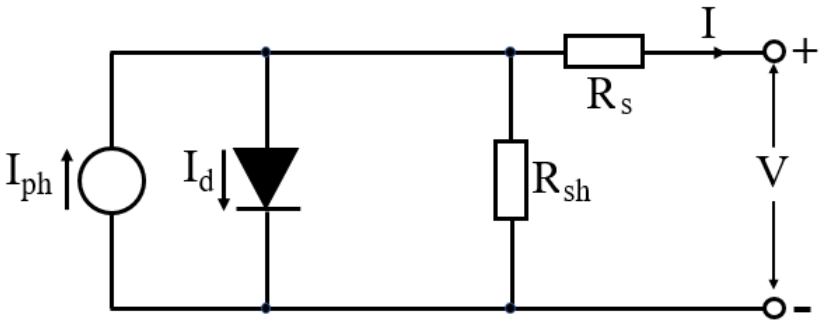

Figure 2.11: One-diode model for a solar cell. I_{ph} is the photogenerated current, I_d is the diode current, R_{sh} is the shunt resistance, R_s is the series resistance, I is the current out of the solar cell and V is the voltage of the solar cell.

The internal resistance in the solar cell affects the operating point and thus the power produced as illustrated in figure 2.12. To minimize this effect, a low value of R_s and high value of R_{sh} is optimal. The impact of R_{sh} is large at low light levels, because less current is generated. A larger part of the current will therefore escape an alternative path.

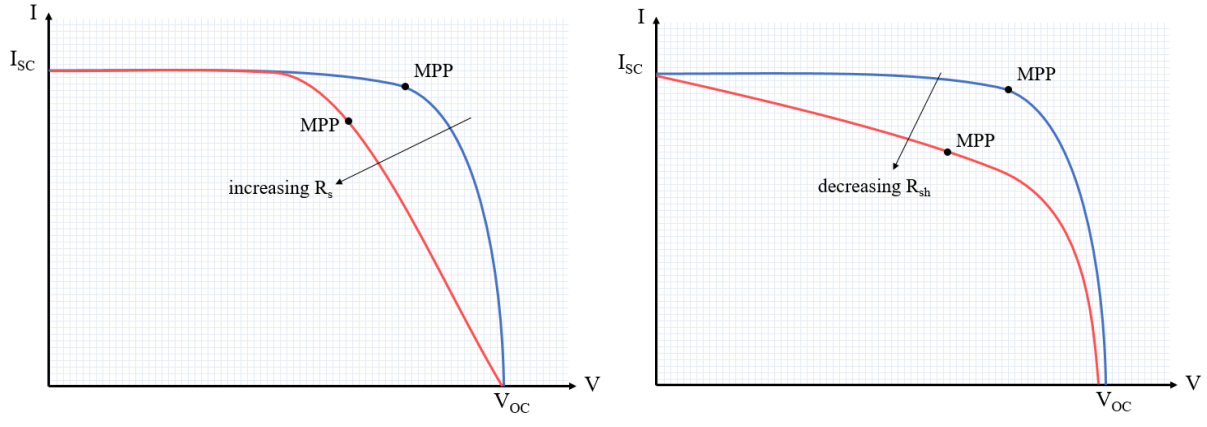

Figure 2.12: Effect of the (a) series and (b) shunt resistance on the IV curve of a solar cell. When the series resistance increases, the resistance in the solar cell increases and the power produced decreases. When the shunt resistance decreases, the leakage current increases and thus decreasing the produced power.

Effect of temperature and irradiance level

The IV-curve of a solar cell changes with temperature and irradiance level. An increase in temperature reduces the band gap of a semiconductor, resulting in a slight increase in current and a large decrease in the open circuit voltage as illustrated in figure 2.13a. The overall effect is a reduction in output power. The amount of photo-generated current in a solar cell is proportional to the irradiance level, as illustrated in figure 2.13b.

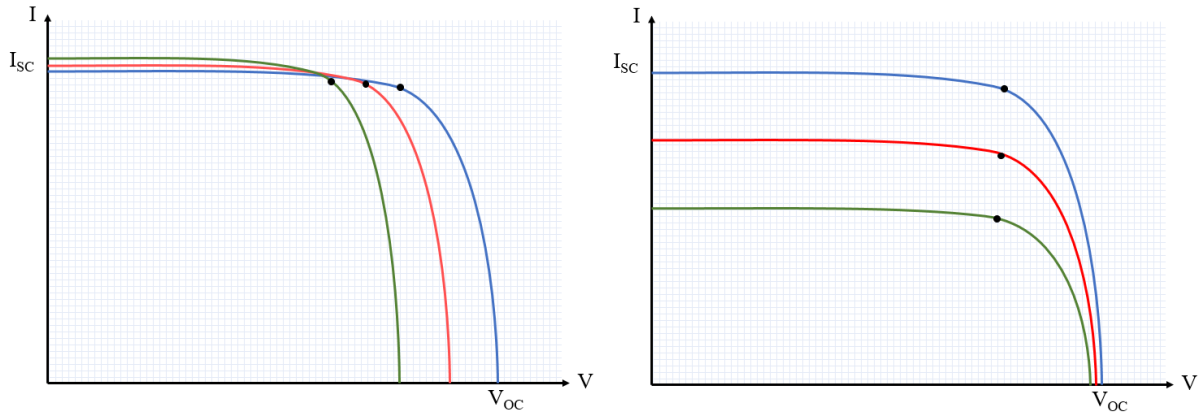

Figure 2.13: IV - curve for a solar cell under different (a) temperature and (b) irradiance conditions. For figure (a), the red and green curve indicates the resulting decrease in available power when the temperature increases. For figure (b), the red and green curve indicates the resulting decrease in available power when the irradiance decreases. The figure is inspired by [17].

2.2.2 The PV module

A solar cell typically has an open circuit voltage ranging from 0.55 - 0.72 V [17]. To generate a usable voltage and current, several solar cells can be interconnected to form a PV module. PV modules often contain 36, 60 or 72 solar cells, usually connected in series to minimize resistive losses and enable high voltages [11]. The efficiency of a module is lower than a solar cell due to i.a. mismatch losses and resistive losses in the interconnections between the cells.

Module structure and materials

The typical components of a crystalline silicon PV module are illustrated in figure 2.14. The front surface is a low iron, tempered glass with a high transmissivity which provides mechanical stability. The solar cells are sandwiched between two layers of encapsulants to protect them against the environment. The encapsulant needs to be transparent, have low thermal resistance and withstand high temperature and UV - radiation. A backsheet protects the cells from water, is electrically insulating and helps dissipate heat. The most common backsheet is a combination of Tedlar and polyester [11]. The surrounding frame enhances the mechanical stability and the junction box contains all the electrical connections to the solar cells.

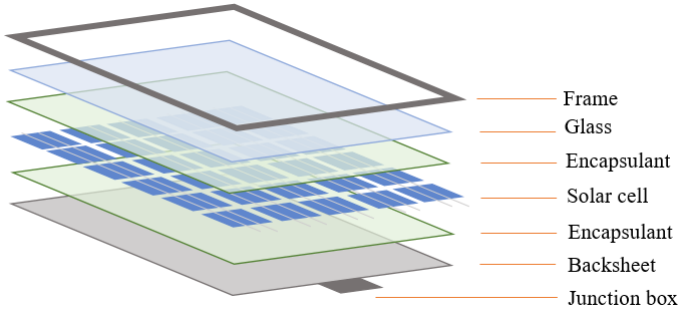

Figure 2.14: Structure of a crystalline silicon PV module. Illustration inspired by [11].

Shading

Shaded solar cells reduces the power output of the module and can under certain operating conditions lead to a hot spot formation. The solar cell output declines proportionally to the amount of shading. A string of solar cells in a PV module is limited by the solar cell producing the lowest current. When a solar cell is shaded, the current in the string falls to the level of the shaded cell.

Under normal operating conditions, each solar cell is forward biased and conducts current. When a solar cell is shaded the produced current reduces and it starts operating as a load, as the current from the non-shaded solar cells is driven through it. The forward bias across the non-shaded solar cells reverse biases the shaded cell, leading to large dissipation of power in the cell in the form of heat. A hot spot is created, which damages the solar cell. Bypass diodes prevents a hot spot from developing by diverting the current. A bypass diode is connected in parallel to a string of 18 to 20 solar cells and reverse biased under normal operating conditions. If a solar cell is reverse biased due to shading, the bypass diode reverses its polarity, allowing the current from the non-shaded solar cells to flow through it. The bypass diode protects solar cells from hot spot heating.

The IV-curve of a module is affected by shading. A PV module with three bypass diodes loses about 1/3 of the power output when one solar cell is 100% shaded, and 2/3 when two solar cells in different strings are 100% shaded, as illustrated in figure 2.15. Figure 2.15 also illustrates the effect on the IV curve when one cell in a string is partially shaded. Without bypass diodes the current of the module is determined by the shaded cell and the power output is significantly reduced.

PV module technologies

There are a range of different PV module technologies available today. Table 2.1 lists some key characteristics of different technologies to compare them.

Thin-film modules are generally able to absorb diffuse and low irradiation better than crystalline modules, achieving higher efficiencies in low irradiation conditions [14]. They tend to have a lower temperature coefficient, meaning the performance decreases less with increasing operating temperatures. Thin-film modules generally have lower efficien-

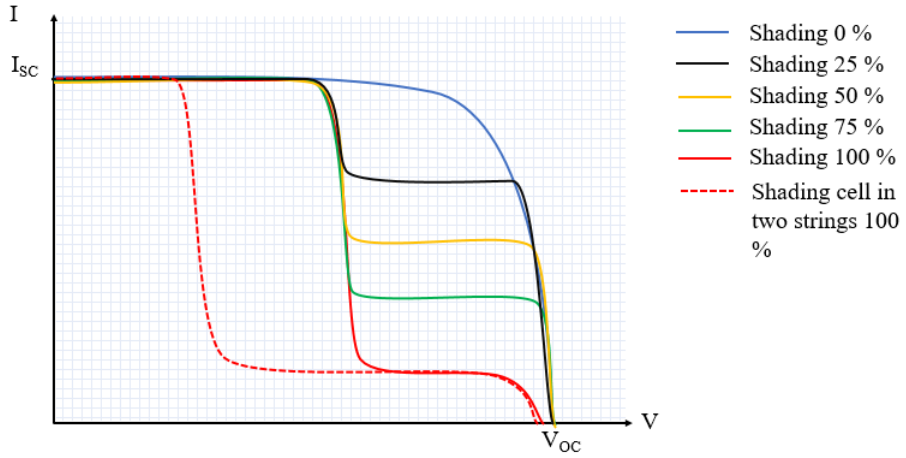

Figure 2.15: Shading effect on the IV-curve of a module with three bypass diodes. Figure inspired by [14].

Table 2.1: Comparison of different PV module technologies. Information from [18].

Technology	Crystalline		Thin-film	
	Mono	Poly	CdTe	CIS
Efficiency [%]	18	17	16	14
Market share [%]	24.5	69.5	3.8	1.6

cies than crystalline modules and a larger area is required to achieve the desired power. The market share for thin-film modules is smaller than for crystalline modules, but the prices for thin-film modules are lower. CIS modules observe an increase in performance when exposed to solar radiation, called the light soaking effect. The effect takes place progressively with sunlight exposure and becomes fully effective after several accumulated hours of exposure to the Sun [19].

Thin-film modules have a greater shading tolerance than crystalline modules. Crystalline modules typically consists of individual square cells connected in series, as illustrated in figure 2.16a. When a cell is shaded, the current flowing through all other cells in the string is limited. Thin-film modules are typically made up of long, narrow cell strips connected in series, as shown in figure 2.16b. If the thin-film module is oriented correctly, only the cells affected by shading will not contribute to energy production. When the shading is perpendicular to the module cells, all cells remain partially illuminated and the power loss reduces proportionally to the shaded area, minimizing the power loss due to shading. When shading runs parallel to cells in the module, the shaded cells limits the current and power produced by the module. The relationship is not linear and the power is initially significantly reduced, reaching zero when more than 50% of the module is shaded [14].

2.2.3 Inverters

The main task of an inverter is to convert direct current (DC) to alternating current (AC). It also performs maximum power point tracking to ensure a maximum output power.

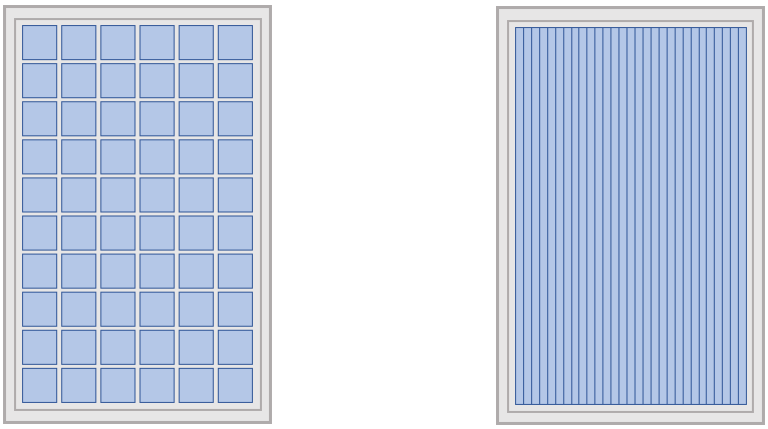

(a) Crystalline module. (b) Thin-film module.

Figure 2.16: Typical structure of (a) a crystalline module and (b) a thin-film module.

The inverter should also provide a safe operation and high efficiency. The efficiency of an inverter varies with input power and voltage.

Inverters are also classified as single-phased or three-phased inverters. Single-phased inverters are used for low power systems such as small residential PV systems, while three-phase inverters are used for higher power systems.

Inverters have different configurations depending on their size and if they are connected to the grid or not. In a stand-alone system the inverter creates a power grid for the PV system, while in a grid-connected system the inverter has to follow the voltage and phase of the grid. A grid-connected system has three main inverter configurations: central inverters for a PV array, string inverters for a PV string and module inverters for a module. A power optimizer can also be used alongside the inverter to increase energy output.

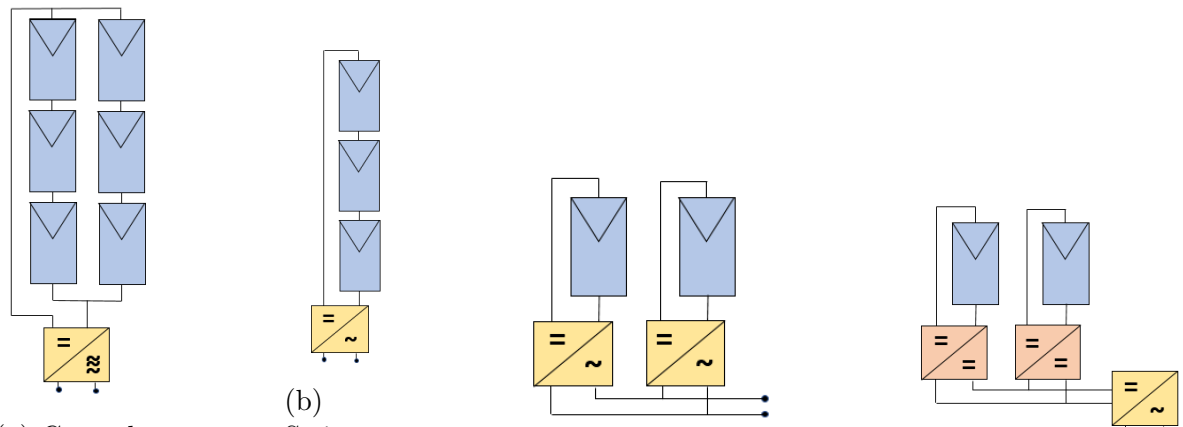

(a) Central inverter (b) String inverter (c) Module inverter (d) Optimizer

Figure 2.17: Main inverter configurations for a grid-connected PV system. The blue rectangles are PV modules, the yellow squares are inverters and the red squares are power optimizers. Inspired by [11].

Central inverter

In a central inverter configuration, as illustrated in figure 2.17a, several strings of PV modules are connected to a central inverter. This configuration leads to a high current and voltage and is mainly used in large-scale PV power plants. Central inverters have a low specific cost and are reliable, because they only uses a few components. However, they have the disadvantages of increased losses due to large amounts of DC cabling and mismatch losses, low system flexibility and sensitivity to partial shading.

String inverter

In a string inverter configuration, as illustrated in figure 2.17b, a string of PV modules is connected to an inverter. This reduces the cabling, shading and mismatch losses, increases the flexibility of the system and reduces the effect of inverter failure. However, it is less cost efficient and the high DC voltage needs special consideration because these inverters are often installed in households.

Module inverter

In a module inverter configuration, as illustrated in figure 2.17c, the inverter operates directly at one or several PV modules. This concept minimizes mismatch and partial shading losses, significantly reduces the amount of DC cabling and has a high system flexibility and expandability. It reduces the impact of the power production due to inverter failure and the failure is identifiable to a single point. However, the inverter has to operate in a harsh outdoor environment, leading to unfavorable ageing behavior [14]. It also has a high specific cost and a lower efficiency due to a need for boosting the low voltage of the PV module to a higher DC voltage. Module inverters are most suited for a PV system with considerable partial shading [14].

Power optimizer

A power optimizer contains a MPP tracker and a DC-DC converter and is attached to a single or two modules to minimize the overall mismatch losses, as illustrated in figure 2.17d. The optimizers are connected in series and communicate with each other to regulate the individual voltages [14]. The conversion to AC is carried out by a central or string inverter which operates in a voltage range. If the voltage falls outside the range, the current it adjusted so the voltage falls within the range again. The DC-DC conversion increases the efficiency losses, but optimizers does not heat up during operation as seen with module inverters [11].

2.2.4 Mounting system

There are a variety of mounting systems and configurations available today depending on if the PV system is ground mounted, integrated in the building (BIPV) or mounted on the building (BAPV). The mounting system must be designed to withstand the expected loads at the location without causing the PV array to lift or slip down, and to provide ventilation

for the modules [14]. The load include both PV modules and weather conditions such as wind and snow.

On inclined roofs the most common mounting system is an additive system with the same tilt angle as the roof. The modules are assembled on the existing roof by using mounting rails that are either attached directly to the roof covering or anchored to the roof structure [14]. The modules are fixed on the rails by using fasteners. Depending on the roof material, there are different methods to fasten the rails on the roof. For wave corrugated metal roofs the most commonly used fastening system is drilling mounting bolts through the roof waves. A typical roof mounting system is illustrated in figure 2.18a.

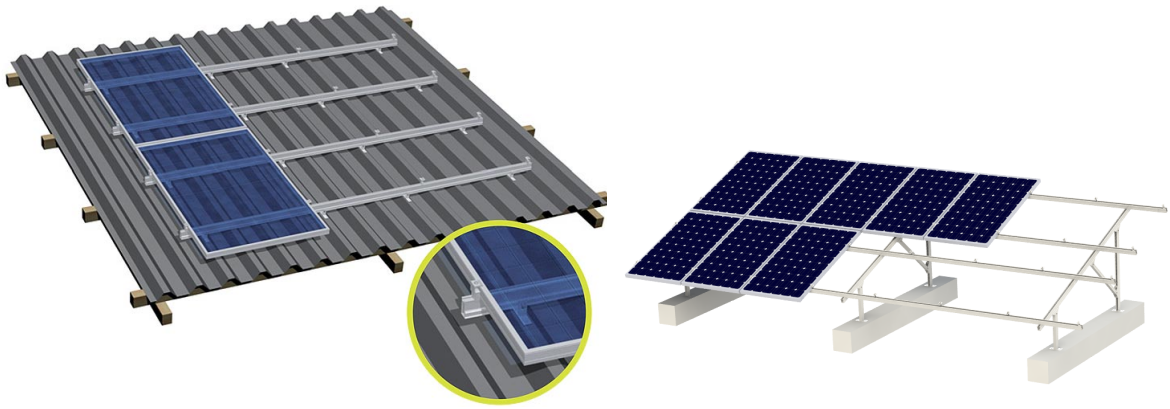

(a) Tilted roof [20]. (b) Ground mounted [21].

Figure 2.18: Mounting system for (a) tilted wave corrugated roof and (b) ground mounted with concrete piles.

The mounting system on a flat roof can either be inclined or aligned with the roof. Special care should be taken to avoid damaging the roof skin when installing the mounting system. If the modules are installed at an angle the extra wind load should be taken into account.

There is a wide selection of foundation and frames available for a ground mounted PV system, depending on the quality, load and pH value of the ground, and the topography of the site [14]. The foundation can be concrete slabs put on top of the ground or steel screws drilled into the ground. The frame is made of timber or metal and arranged in a rail system as illustrated in figure 2.18b.

2.2.5 Other BoS components

Other BoS components in a grid-connected PV system includes AC and DC cabling, a monitoring system, metering and protection and disconnection switches.

AC and DC cabling

The cabling of a PV system is divided into module or string cables, the DC main cable and the AC connection cable. Module cables are DC cables connecting individual modules

together at the junction box. The cable is used outdoors and needs to be UV and weather resistant, as well as earth fault and short circuit proof. These cables typically have a cross-section between 1.5 mm^2 and 6 mm^2 and uses plug connectors. The DC main cable connects the array or string of modules to the inverter.

The AC cable connects the inverter to the grid injection point and losses should be taken into account if the length is significant. When choosing the cable it is important to follow national codes and regulations.

Monitoring system

A monitoring system registers system parameters such as voltage, energy production, frequency, current and temperature. It monitors, diagnoses and performs validations of the PV system to give the user information about the the operating condition of the system. A monitoring system provides the owner with a learning tool to further understand how the system functions, and the installer with a system insight for remote troubleshooting. The monitoring system is usually a part of the inverter.

Inverter manufacturers also provides their own monitoring platforms, often available through both web browser and app, to give the customer an easy way to view production and consumption. Each manufacturer has their own available features in the monitoring platforms.

Protection, disconnection and metering

Protection and disconnection switches are installed to protect the system from faults and to carry out maintenance and repair work. A metering system registers the energy produced, energy fed to the grid and the energy consumed from the grid. A protection, disconnection and metering scheme for a grid-connected PV system is illustrated in figure 2.19.

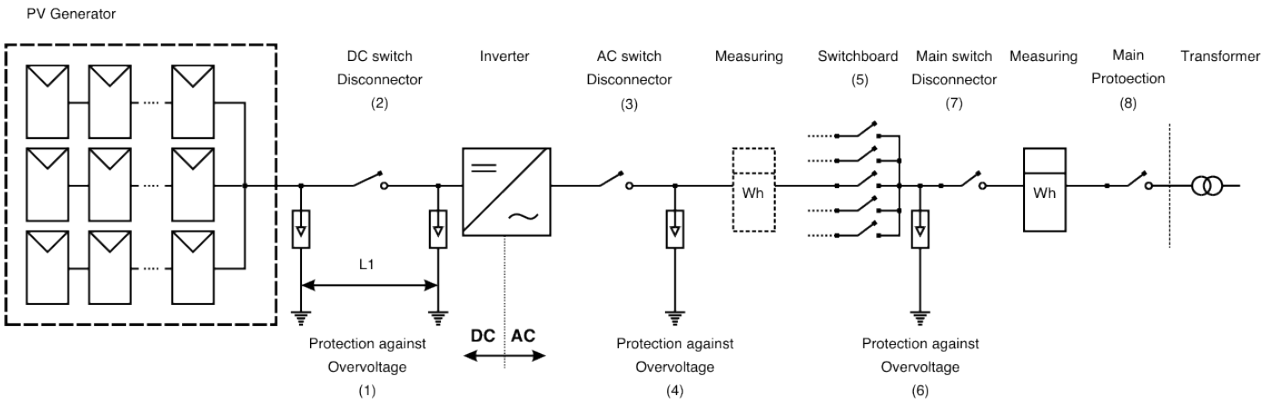

Figure 2.19: Grid-connected PV system and over-voltage protection scheme. Figure from [22].

A disconnector or disconnection switch cuts all the power in a circuit. It is installed on both the AC and DC side of the inverter and should be rated for the maximum open-

circuit voltage and generated current. An isolation disconnector is also installed on the AC side to protect the grid and isolate the PV system from the electricity grid in case of faults [14].

The electric switchboard divides electricity from the supply source to smaller circuits in the house. It contains a circuit breaker or fuse for each circuit, designed to protect the circuit against overcurrent. The circuit breaker interrupts the current flow after a fault is detected and can be reset to resume normal operation. A fuse operates once and must be replaced afterwards.

An overvoltage occurs when the voltage in a circuit is raised above the maximum design limit and can be caused by lightning. Protection against overvoltage prevents damage to the electric components by either cutting off excess voltage or shutting down the power supply. They are used on both the AC and DC side of the inverter.

2.3 Grid-connected PV system design and evaluation

This section describes important factors to consider when designing a grid-connected PV system. The theory is mainly from the book *Planning and installing Photovoltaic systems* [14] and *PVsyst contextual help* [19]. Other sources are specified.

2.3.1 Site assessment

A site assessment is essential before planning a PV system in order to design the PV system for the specific location. It gives the designer an opportunity to identify the condition and limiting factors of the site. For available roof surfaces, it is important to establish whether the building is suitable for installing a PV system. It is also important to consult with the customer regarding expectations and requirements for the PV system. The following points forms a basis for a good site assessment:

- customer consultation regarding desired energy yield and financial framework
- usable roof and ground area for installing the PV array
- orientation and tilt angle
- roof shape, structure and type of roofing
- shading items
- locations for BoS components
- cable lengths, wiring routes and routing method.

Information about local electricity consumption is also important in order to design a site specific PV system and avoid oversizing. Consumption data is used to design a system that produces the same amount or less than the site consumption is.

2.3.2 Shading analysis

As stated in subsection 2.2.2, shading on a PV module reduces the power output and can cause heating in a solar cell. The shading scenario of the installation site is therefore important to survey. Shading can be classified as temporary, resulting from location or caused by the PV system.

Temporary shading includes snow, leaves, dust, bird droppings and other types of soiling. These factors are strongly dependent on the location of the PV system and can be managed by having a good cleaning scheme. Shading from the location includes shading by objects in the PV array's surroundings such as trees, buildings and chimneys. Self shading is caused by components in the PV system, such as bolts on the mounting system or a neighbouring row of modules. The effect of shading on a PV system depends on the following factors:

- number of modules that are shaded
- module configuration of cells and bypass diodes
- degree of shading
- interconnection of the modules
- horizontal - or vertical module arrangement
- inverter design
- distance between rows of modules.

Particularly direct shading by objects causes high energy losses. The smaller the distance to the shadow casting object, the darker the shadow is, resulting in increased shading losses. Direct shading fluctuates during the time of day and season and should be reduced to a minimum. The shading fluctuation and the resulting losses may be calculated by modeling the PV system in a simulation program.

A shading analysis can be performed by using a site plan and sun path diagram to calculate the distance and dimensions of shadow-casting objects, and then calculating their azimuth and altitude angle. Alternatively, the elevation and azimuth angle of shadow-casting objects can be measured using a shading analyzer such as a special digital camera with software or a simulation program.

2.3.3 Climatic data acquisition

An important aspect of designing a PV system is to collect and assess meteorological data. The solar resource at the location affects power production, and accurate data of solar irradiance is important to acquire. Other meteorological data that affects the performance of the PV system are ambient temperature, wind speed and periodical rain.

Meteorological data can be collected from ground-based weather stations or from databases, often based on satellite data. Data from both ground-based weather stations and satellites can be obtained for hourly, daily, monthly and yearly time periods, depending on what

is available for the PV system location. Satellite data offer a wide geographical coverage and can be obtained for a long time period. The data is not susceptible to maintenance and calibration discontinuities. Weather station data, on the other hand, captures the micro scale features that affect a site better than satellite data. The climatic distance, D_{clim}, between a weather station and a location says something about how representative the weather station is for the location [19]. It is defined as

$$D_{clim} = \sqrt{D_{hor}^2 + (100 \cdot D_{alt\ diff})^2}, \tag{2.7}$$

where D_{hor} is their horizontal distance [m] and $D_{alt\ diff}$ is the difference in altitude between the weather station and location [m].

A comparison between different databases and ground-based weather stations can be made to achieve a better understanding of the actual local weather conditions at the PV system location.

2.3.4 Module orientation and inter-row spacing

To maximize energy production for a PV system, the azimuth and tilt angle of the modules should be optimized. An optimal azimuth is normally achieved by orienting the module towards the incoming sunlight at solar noon. In the Southern Hemisphere, the optimal orientation is therefore directly north. If energy production is to be optimized for hours of peak demand, the module may be oriented to achieve this.

The optimal tilt angle for a fixed PV module depends on if the power production is optimized for year-around performance, a specific period or a specific load. As a rule of thumb, to optimize for year-round performance, the tilt angle should be equal to the latitude of the location. Larger tilt angles are required to optimize for winter loads, while smaller tilt angles are required to optimize for summer loads. Other factors to consider when choosing the tilt angle are soiling losses, near shading objects, albedo and inter-row spacing between rows of tilted PV modules.

When designing a free standing PV system, mutual shading between different rows of PV modules should be considered. To optimize the power production of a PV system, an optimal point between module tilt angle and inter-row spacing should be found. The optimal tilt angle and inter-row spacing is chosen by considering factors such as optimizing power production, reducing shading and good area utilization. The configuration of the modules will also affect the inter-row spacing.

Inter-row spacing

A common approach is to decide the inter-row spacing under the condition that no mutual shading should occur for a given number of hours on the winter solstice [11]. The winter solstice is the day when the Sun is at its lowest and the range of azimuth angles is the smallest. An acceptable row spacing gives less than 1% annual shading loss. The inter-row spacing, d_{row}, is illustrated in figure **??** and calculated using the following equation

$$d_{row} = w_m \cdot cos\beta_z + w_m(\frac{sin\beta_m \cdot cos(\gamma_s - \gamma_m)}{tan\alpha}), \tag{2.8}$$

where w_m, β_m and γ_m is respectively the width, tilt angle and azimuth angle of the module, and γ_s and α is respectively the azimuth angle and the altitude angle of the Sun.

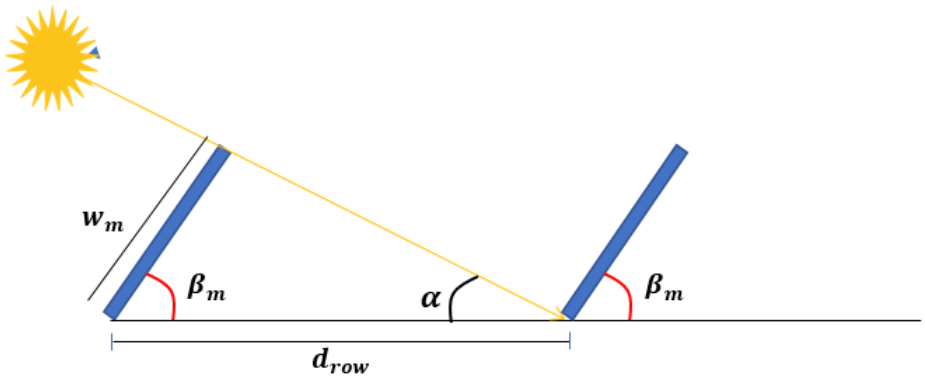

Figure 2.20: Inter-row spacing for a ground mounted PV system.

2.3.5 Module and inverter selection

Selecting a module to use may be challenging as there are numerous modules available in sizes, power, types, prices and efficiency from multiple manufacturers. It is important to make sure that the module complies with IEC standards for module design and quality and investigate the module warranty. Another factor to consider is which modules are available in the country and which modules installers are familiar with.

When choosing a module, site specific factors such as available area, local weather conditions, temperature and near shading objects should be taken into consideration, as well as price. For a limited available area, a module with high efficiency and power may be chosen to maximize the power production per area. If the available area is unlimited, cheaper, lower quality models may be chosen to reduce costs. Thin-film modules have a greater tolerance for shading than crystalline modules [14] and are more flexible in terms of their geometric dimensions. Thin-film modules have a lower efficiency than crystalline modules, but can absorb visible light with short and medium wavelengths more effectively. The power loss due to temperature is also lower for thin film modules.

When selecting the inverter, consideration should be made of the size of the system, cost, flexibility of the system, partial shading, number of sub-strings or strings and their orientation. Care should be taken to ensure that only modules with the same orientation, angle and shading conditions are connected together in strings.

As mentioned in subsection 2.2.3 there are several configurations of inverters for grid-connected PV systems. For areas with large amounts of shading or continuous diurnal shading, module inverters or a string inverter with optimizers may be a good alternative to maximize the power output. For areas with less shading, a string inverter may be

sufficient. A consideration should be made between maximum power output, price and availability in the country.

When choosing the installation site for the inverter it is important to comply with the environmental conditions specified by the manufacturer to ensure optimal performance. The ideal installation site is cool, dry and indoors [14]. String inverters have IP 54 protections and can withstand outdoor weather conditions [14], but should be protected from direct sunlight and rain to improve their lifetime. It is also important to consider accessibility when installing the inverter.

2.3.6 Array to inverter matching

Matching array output to inverter input ensures that the inverter captures as much as possible of the array power during all environmental conditions anticipated at the site. The inverter should operate at or near full power during normal operating conditions. In a well-designed system, the array's operating voltage, current and power output will be within the inverter's operating range at all times.

The number of modules in each string and strings in each array depends on the electrical characteristics of the module, the input voltage and current range of the inverter, and the expected high and low ambient temperatures of the site. The technical specifications from the manufacturer of the inverter provides information on sizing and installation. The system and connection concepts determines the number, voltage level and power class of the inverters [14].

DC and AC power matching

The sizing ratio between the nominal PV array power at STC and the nominal AC inverter power is called the $P_{nom\ ratio}$, and describes the capacity utilization of the inverter [14]. It is given by

$$P_{nom\ ratio} = \frac{P_{nom\ array}}{P_{inv\ AC}}, \tag{2.9}$$

where $P_{nom\ array}$ is the nominal PV array power at STC [W] and $P_{inv\ AC}$ is the nominal AC inverter power [W].

If $P_{nom\ ratio}$ is 1 the systems DC and AC capacity matches, if $P_{nom\ ratio}$ is lower than 1 the inverter is oversized and if $P_{nom\ ratio}$ is larger than 1 the inverter is undersized.

The AC nominal power is the power that the inverter can continuously feed into the grid without cutting out at an ambient temperature of 25°C [14]. The nominal power of inverters can be within ± 20% of the PV array power at STC, depending on the inverter and module technology, and the environmental conditions [14]. This gives the following power range for optimizing the performance [14]

$$0.8P_{nom\ array} < P_{inv\ AC} < 1.2P_{nom\ array}, \tag{2.10}$$

which results in the following $P_{nom\ ratio}$,

$$0.83 < P_{nom\ ratio} < 1.25. \tag{2.11}$$

Inverters installed on the roof or outside may need to be undersized, due to exposure to high ambient temperatures [14]. Systems without optimal alignment or partial shading can have a smaller inverter, taking into account the overload characteristics of inverters. Frequent, continuous overloading decreases the life of the inverter.

A system is undersized when the PV module capacity is greater than the inverter capacity. By undersizing a system, slightly more energy is produced in mornings and afternoons, as the inverter reaches its nominal AC power earlier in the day and continue to operate at that point until later in the afternoon. Slightly less energy is produced during the mid-day, as the power output is cut-off at the inverter's nominal capacity. Undersizing also lowers the specific cost of energy delivered and the inverter cost. Undersizing the PV inverter is also endorsed by inverter manufacturer SMA, one of the largest manufacturers in the industry [23]. When undersizing the inverter it is important to consider the inverter input conditions and inverter operating efficiency and heat generation [23]. NEC and IEC standards recommends a $P_{nom\ ratio}$ of 1.25 [24].

Voltage sizing

Module temperature and irradiance affects the IV curve of a module and the optimal operating point. Temperature affects the generated voltage, while irradiance affects the generated current. Module voltage increases at low temperatures and decreases at high temperatures. The operating range of the inverter should be matched with the IV curve of the PV array, with MPP of the array found within the MPP voltage range of the inverter. It is not possible to keep the array voltage within the MPP voltage range of the inverter at all operating temperatures.

The voltage of the PV array depends on the temperature, so the extreme cases of winter and summer operation are used when sizing the system [14]. When sizing a PV system, the following design criteria should be met [14, 19].

- The minimum and maximum array operating voltages (MPP voltages) should be within the inverter MPP voltage range, which is the range in which the inverter can search for the MPP.
- The absolute maximum array voltage should stay below the absolute maximum inverter input voltage and the maximum system voltage specified for the PV module.

If the array voltage falls below the minimum MPP inverter voltage, the inverter may not be able to find the MPP of the array and, in worst case, switch off.

The maximum and minimum number of modules in a string can be calculated based on these design criteria. The maximum number of modules in a string, n_{max}, is given by

$$n_{max} = \frac{V_{inv\ max}}{V_{module\ max}}, \tag{2.12}$$

where $V_{inv\ max}$ is the maximum DC input voltage of the inverter [V] and $V_{module\ max}$ is the maximum array voltage i.e. the open-circuit voltage at minimum module operating temperature [V].

The minimum number of modules in a string, n_{min}, is given by

$$n_{min} = \frac{V_{inv\ mpp\ min}}{V_{module\ mpp\ min}}, \tag{2.13}$$

where $V_{inv\ mpp\ min}$ is the minimum MPP voltage at which the inverter can search for the MPP [V] and $V_{module\ mpp\ min}$ is the minimum MPP voltage of the module [V].

The maximum module voltage is calculated by

$$V_{module\ max} = V_{OC\ STC} + \frac{\beta}{100\%} \cdot V_{OC\ STC} \cdot (T_{module} - T_{STC}), \tag{2.14}$$

where $V_{OC\ STC}$ is the open circuit voltage of the module when operating at STC [V], β is the voltage temperature coefficient of the module [%/°C], T_{STC} is the operating temperature at STC [°C] and T_{module} is the module operating temperature [°C]. This equation can also be used to find maximum and minimum array operating voltages by replacing $V_{OC\ STC}$ with $V_{mpp\ STC}$.

The operating temperature of a module with the nominal operating cell temperature (NOCT) as a reference point can be calculated by [11]

$$T_{module} = T_{amb} + (NOCT - 20°C) \cdot \frac{G_{inc}}{G_{NOCT}}, \tag{2.15}$$

where T_{amb} is the ambient temperature [°C], $NOCT$ is the nominal operating cell temperature [°C], G_{inc} is the solar irradiance [W/m^2] and G_{NOCT} is the irradiance at NOCT which is 800 W/m^2. The equation assumes a linear relationship between the solar irradiance and the difference between the module and ambient temperatures.

When considering a string inverter, the number of strings has to match the number of "string" inputs found in the inverter datasheet.

Current sizing

The maximum PV array current should not exceed the maximum inverter input current [14]. The maximum number of strings in an array, n_{string}, is limited by the maximum input current and can be calculated by

$$n_{string} \leq \frac{I_{inv\ max}}{I_{string\ max}}, \tag{2.16}$$

where $I_{inv\ max}$ is the maximum inverter input current [A] and $I_{string\ max}$ is the maximum

string current [A]. In most cases, the maximum string current is the short-circuit current at STC [14].

2.3.7 PV system performance

In order to compare the performance of different PV systems, parameters related to their performance are compared, as they indicate how well the system is designed. Yields are the specific energy production of the system and losses are the differences between these yields. In order to compare several PV systems, the performance parameters in PVsyst are normalized indicators with respect to the nominal power of the system. This means that they do not depend on the array size, geographical situation or field orientation. The normalized yield and loss factors can therefore be used to compare different configured and located PV systems.

- *Specific yield Y_f [kWh/kWp]*, also called final system yield, is the energy produced by the system, E, with respect to its nominal power. It is an indicator of the potential of the system and is given by

$$Y_f = \frac{E}{P_{nom\ array}}. \tag{2.17}$$

- *Performance ratio (PR)* represents the system efficiency with respect to the nominal power and the incident energy. It is defined as the ratio of the produced energy, with respect to the reference yield, Y_r (kWh/kWp). The reference yield is the theoretical energy produced by the system at STC conditions, with respect to its nominal power [19]. *PR* includes array and system losses and is an indicator of the quality of the system. It is given by

$$PR = \frac{Y_f}{Y_r}. \tag{2.18}$$

2.3.8 PV system losses

The total PV system losses can be divided into optical losses, array losses and system losses, as illustrated in figure 2.21. The *optical losses* decreases the amount of irradiation reaching the PV array and include horizon, near shading, reflection and soiling losses. *Array losses* are losses in the PV array caused by increased temperature, low irradiance, electrical shading, quality, mismatch and DC cable resistance. They are defined as $Y_r - Y_a$, where Y_a is the array yield, i.e. the energy produced by the array, with respect to the nominal power. Inverter losses, unavailability and AC cabling losses are *system losses*. System losses are defined as $Y_a - Y_f$. Thermal losses and ohmic losses are further explained in the following sections.

Thermal losses

The module temperature determines the operating voltage of a module. All modules have a defined nominal operating cell temperature (NOCT). The actual operating temperature

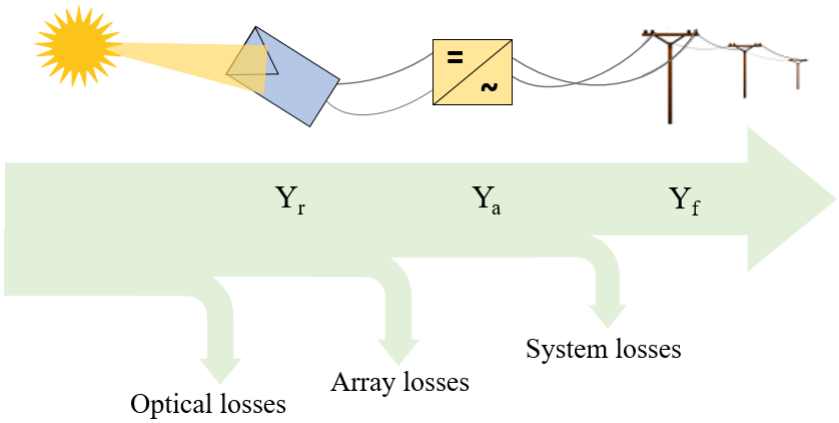

Figure 2.21: PV system loss diagram.

of a solar cell, under the given conditions, can be calculated by equation 2.15.

The thermal behavior of the PV system strongly influences the electrical performance, because the module temperature determines the operating voltage of a module. Thermal losses due to the operating temperature of a solar cell depends on the thermal balance of the cell.

To account for derivation from the given wind speed and ventilation, the thermal balance of the module can be used to calculate a more accurate module temperature. The thermal balance is given by [19]

$$U \cdot (T_{module} - T_{amb}) = \alpha_a \cdot G_{inc} \cdot (1 - n_M), \tag{2.19}$$

where U is the thermal loss factor [W/m^{2}K], T_{module} is the operating temperature of the module [°C], T_{amb} is the ambient temperature [°C], α_a is the solar irradiation absorption coefficient, G_{inc} is the incident solar irradiance on the module [W/m^2] and n_M is the module efficiency [%].

The thermal behavior is characterized by the thermal loss factor, also called a U-value, which is given by [19]

$$U = U_c + U_v \cdot v, \tag{2.20}$$

where U_c is a constant component [W/m^{2}K], U_v is a factor proportional to the wind velocity [W/m^{2}K/m/s] and v is the wind velocity [m/s].

The thermal loss factor depends on the mounting of the modules and the wind velocity. For a free-standing system with circulation all around the module, the U-value will be higher than for a system with a fully insulated backside.

Ohmic losses

Wiring resistance in both AC and DC cables causes ohmic losses when electricity is transported through the cables. Ohmic losses can be specified as a fraction of the PV array output of at STC, called an ohmic loss ratio. An ohmic loss ratio is the ratio of the wiring ohmic loss, P_w, compared to the nominal array power. The ohmic loss ratio is given by [19]

$$\frac{P_w}{P_{nom\,array}} = \frac{R_w \cdot I_{SC}^2}{R_{array} \cdot I_{SC}^2} = \frac{R_w}{R_{array}}, \tag{2.21}$$

where R_w is the global wiring resistance of the system [Ω] and R_{array} is the array cabling resistance at STC [Ω], given by

$$R_{array} = \frac{V_{mpp}}{I_{mpp}}. \tag{2.22}$$

The resistance in the cables can alternatively be calculated by

$$R_{array} = \rho_{cable}\frac{l}{A}, \tag{2.23}$$

where ρ_{cable} is the specific resistance of the cable material [Ω mm^2/m], l is the cable length [m] and A is the cross section of the cable [mm].

2.4 Economical evaluation of a PV system

When investing in a PV system, the investor is interested in a system that gives a reasonable profit. An economical evaluation should be made to evaluate the cost-benefit of different configured PV systems. Some economical terms to consider are payback time, return on investment (ROI), net present value (NPV) and levelized cost of electricity (LCoE).

2.4.1 Payback time

The *payback time* is defined as the amount of time it takes to recover the cost of an investment. It is defined as [11]

$$payback\ time = \frac{total\ investment}{annual\ income}. \tag{2.24}$$

The payback time is influenced by factors such as annual solar radiation, investment cost of the PV system and the electricity grid price. Return on investment (ROI) is the ratio of annual income to total investment and indicates how profitable an investment is.

2.4.2 Net Present Value (NPV)

The Net Present Value (NPV) method is used to calculate the present value of the future cash flows and is a common way of evaluating a PV system. A project is considered

profitable if the NPV > 0 [25]. The payback time shows how long it will take to make the invested money back, while NPV shows the profit one can expect at the end of the investment period.

The yearly cash flows of the project are calculated and discounted using the discount factor $\frac{1}{(1+r)}$, were r is the discount rate [25]. The discount rate is specific to the investment and set based on the risk level of the project. The present value of the lifecycle costs is calculated by [26]

$$NPV = \sum_{t=0}^{T} \frac{C_t}{(1+r)^t} = \sum_{t=0}^{T} \frac{Revenue_t - Costs_t}{(1+r)^t}, \tag{2.25}$$

where t is the year of operation , C_t is the net cash flow, T is the lifetime of the system, r is the discount rate, $Revenue_t$ is the cash inflow and $Costs_t$ is the cash outflow.

2.4.3 Levelized cost of electricity

Levelized Cost of Electricity (LCoE) is used method to evaluate the economic feasibility of an electricity generation project and makes it possible to compare the lifetime costs of different energy producing technologies [11].

As the LCoE calculates the life-cycle costs and energy production, the future expenses and revenues have to be accounted for in the present time value of money. This is done by calculating the present value of the cash flows with a discount rate r. The LCoE is determined when [27]

$$\sum_{t=0}^{T} \frac{Revenue_t}{(1+r)^t} = \sum_{t=0}^{T} \frac{Costs_t}{(1+r)^t}, \tag{2.26}$$

which occurs when the NPV of the project is zero, i.e. $NPV = \sum_{t=0}^{T} \frac{Revenue_t - Costs_t}{(1+r)^t} = 0$.

The LCoE is therefore the average electricity price needed for a project to break even. The revenue for year t is the LCoE multiplied with the generated electricity. By rearranging equation 2.26 and assuming a constant annual value for the LCoE, the following expression for LCoE can be used [27]

$$LCoE = \frac{I_0 + \sum_{t=1}^{T} \frac{Costs_t}{(1+r)^t}}{\sum_{t=1}^{T} \frac{E_{t=0}}{(1+r)^t}}, \tag{2.27}$$

where I_0 is the initial investment cost and $E_{t=0}$ is the initial yearly energy production of the system. Note that as the investment costs occur at the beginning of the first year, it should not be discounted and is therefore put outside the summation. It may also look like energy is being discounted for, but it is just a result of rearranging the equation.

The total costs for a PV system consists of cash outflows like the initial investment, interest payments if debt financed, operation and maintenance costs and decommissioning costs. A residual value of the system at the end of its lifetime may also be included. The residual

value is the scrape value of the PV system components. The LCoE model used in this thesis considers the mentioned cash flows, residual value and also takes into account PV system degradation. It is expressed as

$$LCoE = \frac{I_0 + \sum_{t=1}^{T} \frac{O_t + M_t + D_t}{(1+r)^t} - \frac{RV}{(1+r)^t}}{\sum_{t=1}^{T} \frac{E_{t=0}(1-d)^t}{(1+r)^t}}, \tag{2.28}$$

where O_t is the operation and maintenance cost, M_t are the interest payments, D_t is the decommissioning cost, RV is the residual value, and d is the system degradation rate.

Decommissioning and waste management costs occur at the end of a PV systems lifetime. For solar panels, rather than decommissioning, what takes place in practice at the end of their lifetime is a replacement of equipment [28].

Operation and maintenance costs include the replacement of components, such as inverters, cleaning and general system repairs. The cost can be set as a percentage of the investment cost recurring each year or as a rate per kW of the system. Smaller PV systems can often be more expensive to maintain than utility-scale systems, and the operation and maintenance cost tends to be underestimates [29]. Operation and maintenance costs tend to decrease on a R/kW basis as system size increases, because the costs can be spread across a greater number of project components [29].

LCoE varies between projects, depending on the location and the initial investment required for the PV system. The discount rate r also strongly influences the LCoE. The LCoE used in this thesis does not take into account inflation.

2.4.4 Funding and compensation schemes

There are a number of different support schemes to accelerate the development of renewable energy, such as:

- feed-in-tariffs
- green certificates
- tax exemption or reductions
- investment subsidy, grant or rebate
- net metering scheme

The South African government has made available a variety of incentives in the form of tax incentives and grants to increase the renewable energy production [10]. There are also created an increasing number of funding solutions from the private sector and governmental organizations [10].

Tax incentives

The South African Revenue Service (SARS) allows for a tax deduction on assets acquired by the taxpayer to generate electricity from photovoltaic solar energy solutions not exceeding 1 MW [30]. The allowance is for business owners who pay a 28% commercial

tax. The value of the PV systems can be deducted as a depreciation expense from their business income tax in the first year. As businesses pays a commercial tax of 28%, the depreciation tax of the system is 28% of the capital value.

The government is also introducing a carbon tax for businesses, which means they have to pay more for electricity and fuel. Solar power is a low carbon source of energy and can help businesses avoid carbon tax.

Feed-in-tariffs

When using *feed-in-tariffs (FITs)*, electricity generated by the PV system can be sold to the grid utility for a fixed price. A smart meter or two analogue electricity meters are required for this system. In a *net* feed-in-tariff only the surplus electricity is sold to the grid.

Some municipalities in South Africa buy surplus energy at a given feed-in-rate. However, the tariff is structured in a way that makes it more financially beneficial for the consumer to consume the generated electricity compared to selling it to the grid.

Green certificates

The Excellence in Design for Greater Efficiencies (EDGE) is a green building certification system recently introduced in South Africa to increase efficiency in buildings and empower the real estate market to build sustainably [10]. The certification requires a performance improvement over and above regulatory compliance, with a minimum improvement of 20% on energy, water and materials.

2.5 Policies and regulations

There are several governmental departments involved in developing the rules and regulations for the energy service sector in South Africa. The main departments are [10]:

- *Department of energy (DoE)* is responsible for energy policies and is the custodian department for energy.
- *Department of Public Enterprise (DPE)* is responsible for the country's energy infrastructure through state-owned entities, such as Eskom.
- *Eskom* is the state-owned energy utility.
- *National Energy Regulator of South Africa (NERSA)* sets and approves the annual Eskom tariff increases. It is also responsible for regulating the electricity sector.
- *Municipalities* are closest to the end user and responsible for a large portion of the electricity distribution.

Small Scale Embedded Generation (SSEG) is a new and growing concept in South Africa. It refers to power generation under 1MWp which are located on residential, commercial or industrial sites where electricity is also consumed [9]. The DoE is in the process of

drafting licensing regulations for SSEG which will provide the policy framework within which the regulatory rules will be formulated and applied. NERSA is in the process of drafting regulatory rules for SSEG. The current policies and regulations a SSEG customer must follow are:

- *Electricity licensing regulations*: Facilities meeting the following criteria will not require a generating licence, but must register with NERSA [10]:
  - facilities connected to the load side of the national grid and exports into the grid from the same point that the load imports from the national grid
  - facilities that serve to supply an end user or "related end user"
  - facilities under 1 MWp size
- *Local municipal guidelines for SSEG of 2016*: The only existing SSEG rules and regulations are developed by South African provinces and local municipalities. The purpose of the guidelines is to give each stakeholder relevant guidance regarding the draft municipal SSEG rules, regulations, tariffs and application process [9].

Overstrand Municipality, in which Panthera Africa is located, made available their guidelines for SSEG in 2016. The following rules and regulations are an excerpt of the main points in the guideline [9]:

- *Illegal connections*: Generation equipment may only be connected to the municipal electrical grid with consent from the Manager of the Electricity Department. This may be obtained through the application process.
- *Generation Curtailment*: If operating conditions result in municipal electrical grid parameters not meeting statutory minimum quality-of-support standards, peak generation limits on embedded generator installations may be imposed.
- *Tax clearance certificate requirements*: A valid Tax clearance certificate is required annually to conduct business in Overstrand municipality if the customer is VAT registered.
- *Right to deny access*: Written approval from the municipality should be obtained before purchasing equipment, as approval from the municipality after the application process is not guaranteed.
- *Registered professional sign off*: All SSEG project shall be signed off by a registered professional engineer and a certificate of compliance shall be issued.
- *Testing inverters*: The municipality require proof in the form of test certificates, of type tests having been successfully carried out by a third party testing authority.
- *Net consumer*: All SSEG customers shall purchase more electricity from the utility than they feed back onto the utility grid on a consecutive financial 12 month period.

- *Eskom grid connection*: Customers residing within the municipal boundaries, but located in Eskom's area of supply, need to apply to Eskom for consent to connect SSEG to the Eskom electrical grid.
- *Load management profile*: The SSEG tariff has been structured in such a way that customers shall find it most beneficial from a financial point of view, to utilize as much of the generated electricity as possible, to avoid or minimize reverse power flow.

Chapter 3
Methodology

In this chapter the simulation software PVsyst, which is used in this thesis, is presented. Parameters and settings for simulating a PV system at Panthera Africa are discussed and set in this chapter. The methodology for designing a grid-connected PV system in PVsyst is presented and the simulation factors changed the sensitivity analysis are presented. An economical evaluation of the PV systems is also performed.

3.1 Simulation Software: PVsyst

PVsyst was selected as the simulation software, because it is a powerful tool for studying, sizing and analyzing data of a PV system. It contains databases of both meteorological data and PV system components from several manufacturers. For this thesis version 6.63 of PVsyst is used. The information in this section is based on the *PVsyst contextual help* [19]. Other sources are specified.

Figure 3.1 shows an outline of the different steps in performing a PV system design and simulation in PVsyst. Each step will explained in this section, as it is the methodology used in this thesis.

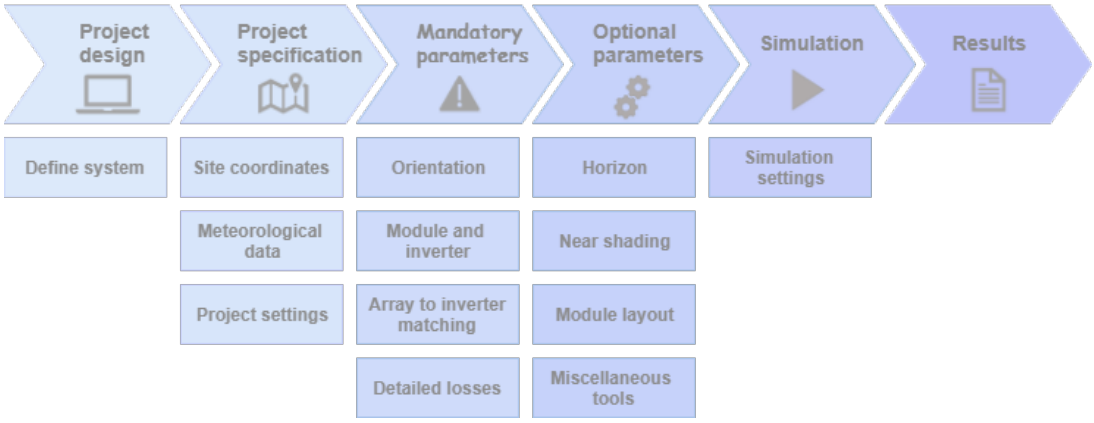

Figure 3.1: Project design steps in PVsyst [19].

3.1.1 Project design

Project design is the main part of the software and used to give a complete study of a PV system project. It includes selection of the parameters specified in figure 3.1. PVsyst perform a through design and performance analysis using a detailed simulation performed over a full year in hourly steps. The output is a detailed system performance report.

Optimization and parameter analysis can be performed through different simulation runs, also called simulation variants. Figure 3.2 shows screen dialogue for a project design.

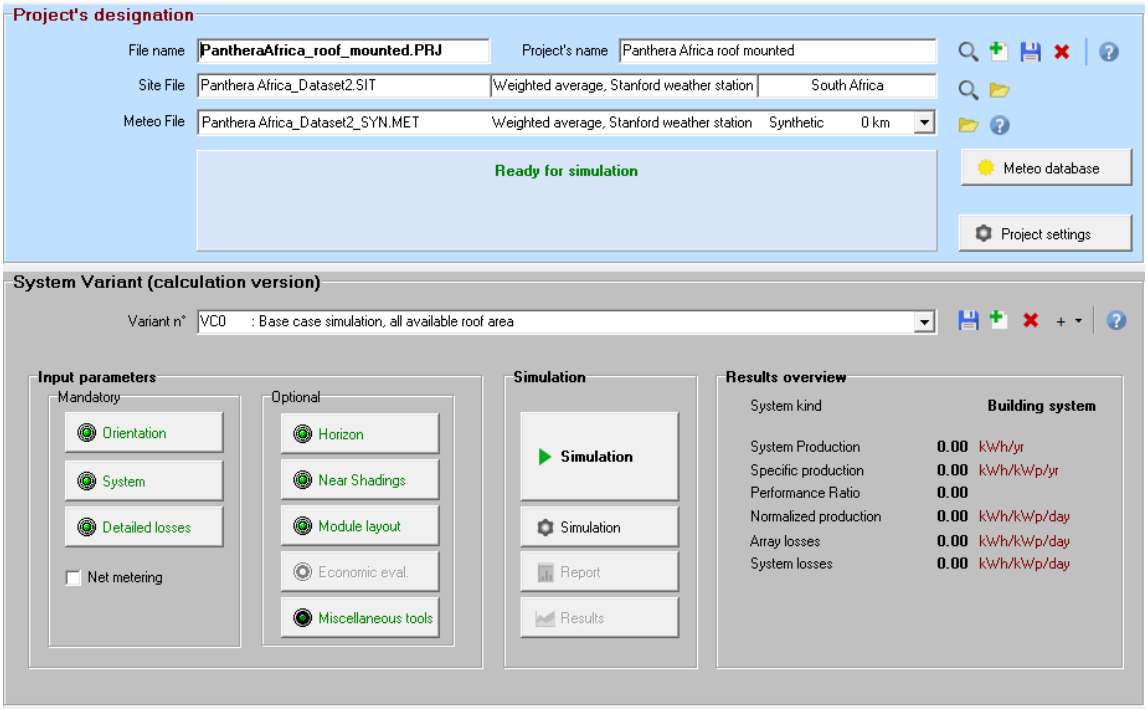

Figure 3.2: Screen dialogue of *Project design* in PVsyst.

System type

In *Project design* it is possible to select grid-connected, stand-alone, pumping and DC Grid systems. In this thesis a grid-connected system is selected.

3.1.2 Project specification

A *Project* in PVsyst is the central object for which to construct different system configurations, called variants. The *Project specification* section is a definition of site specific parameters such as geographical location, local meteorological data and albedo.

Project site

The project site can either be chosen from a built-in database or a new site can be created. When defining a new site, the location and site coordinates in latitudinal and longitudinal degrees must be specified. The site coordinates are used to calculate the sun's position throughout the year. An hourly or monthly meteorological datafile for the site must also be specified. Subsection 3.2.1 specifies the coordinates for the project site considered in this master thesis.

Meteorological data

The meteorological datafile can be chosen from one of the databases included in PVsyst, which are NASA-SSE and Meteonorm7.1, imported from another database that PVsyst supports or created based on measured data from e.g. weather stations. The required parameters in the meteorological file are horizontal global irradiance and ambient temperature. Horizontal diffuse irradiance and wind velocity are optional parameters, but the result will be more accurate if they are included.

Since the simulation in PVsyst is operated at hourly intervals, hourly meteorological data are required to perform a simulation. For the meteorological data sources only containing monthly data, synthetic hourly data are constructed from the monthly values. The synthetic hourly generation is performed using the Meteonorm7.1 algorithm [31]. For irradiance, the algorithm is based on the stochastic model of Collares-Pereira [32]. It uses Markov transition matrices to first generate daily values, giving an average daily irradiance profile. Then the intermittent hourly variations are simulated using an autoregressive procedure, resulting in 24 hourly values per day. This model tries to reproduce irradiance time series, with a statistical behaviour analogous to measured values in several sites in the world.

Table 3.3 in subsection 3.3.2 lists the considered databases in this thesis. The acquired meteorological data was from the specified project site. Hourly meteorological data was synthetically generated for the databases that only had monthly values.

Project settings

Access to monthly albedo values, design conditions and other limitations are available in the *Project settings* tab. Design temperatures, used to properly match a PV array to an inverter, can be modified in the *Design conditions* tab. The temperatures are only used for sizing and not involved in the simulation. The design temperatures to be chosen for the PV system are the following [19]:

- *Absolute minimum operating temperature* for determining the absolute maximum PV array voltage, as this must stay below the maximum inverter input voltage. This is the lowest temperature the array will experience and should ideally be the lowest temperatures ever measured on-site.
- *Winter minimum operating temperature* to ensure that the PV string voltage does not exceed the maximum inverter MPP voltage. This is used to calculate the maximum number of modules in series for the inverter.
- *Summer usual operating temperature under 1000 W/m^2* to calculate the common operating voltage of the array. This temperature is not used for sizing constraints.
- *Summer maximum operating temperature* to ensure that the string voltage does not fall below the minimum inverter MPP voltage. This is used to calculate the minimum number of modules in series for the inverter.

The choice of reference temperatures are given in subsection 3.7.2 and the chosen albedo values are given in subsection 3.3.4.

3.1.3 System variant management

Each system variant specifies a detailed PV system, by a set of input parameters, and simulates the system. There are mandatory and optional input parameters. The optional parameters can make the simulation more accurate.

Mandatory parameters

In *Orientation*, module tilt and azimuth angle is defined as well as field type. The azimuth is defined as the angle between the south direction and the direction the modules are facing. Angles to the west are counted positive and angles to the east are counted negative. PVsyst proposes an optimal tilt and azimuth angle for the geographical location and a percentage loss factor with respect to optimum when other tilt and azimuth angles are chosen. A choice is also available for optimizing energy production with respect to a yearly, summer or winter yield. The field type of a PV surface can be chosen as a fixed tilted plane, several orientations, seasonally adjusted plane or a tracking system.

In the *System* tab the module and inverter type of the PV system are selected and the number of sub-arrays and strings are chosen to match the inverter. The PV system is designed in this section.

Loss parameters related to the PV system can be set according to system specifications, in the *Detailed losses* tab. The loss parameters are initially set to default values. In PVsyst the following system loss factors can be defined:

- *Thermal parameter*: The thermal behaviour of a module is calculated in PVsyst by the thermal balance shown in equation 2.19. This establishes the instantaneous operating temperatures to be used by the PV modules. The thermal balance is characterized by the *Thermal loss factor*, called the U-value, shown in equation 2.20. U_c is a constant component of the thermal loss factor and U_v is a factor proportional to the wind speed v. The value of these factors depends on the mounting of the modules, which determines how well the modules are ventilated. PVsyst advices to not use the wind dependency factor, as the wind speed is usually not well defined in the meteorological data and the parameter U_v is now well known.

- *DC ohmic wiring loss*: The wiring ohmic resistance induces DC losses in the cable between the modules and the input of the inverter. These losses are characterized by a global wiring resistance parameter R defined for the global array. The global wiring resistance can be calculated by specifying average length and cross section of the cables in the *Detailed computation* tab, or specified explicitly if details about cross section and length are not known. If the global wiring resistance is unknown, an ohmic loss ratio at STC can be defined and the global wiring resistance will be

calculated from this value. The ohmic loss ratio is a percentage showing the order of magnitude of the ohmic losses, as defined in equation 2.21.

- *AC ohmic loss*: The wiring ohmic resistance induces AC losses between the output of the inverter and the injection point. AC losses are only accounted for if the cable length is significant. The loss will be calculated by entering the length and cross section of the cable or by specifying an ohmic loss ratio at STC.

- *Module quality loss*: The module efficiency loss specifies the deviation of the module's performance in the simulation, compared to the manufacturer's technical specification. A negative value indicates an under-performance, while a positive value indicates an over-performance. This is called the power tolerance of the module. The default value in PVsyst is half the lower tolerance of the modules.

- *Light Induced Degradation (LID)*: LID is a loss of performance for crystalline modules arising in the first hours of exposition to the sun. The loss depends on the quality of the wafer manufacturing.

- *Module array mismatch loss*: Differences in IV-characteristics for modules in an array results in loss, due to the lowest module current limiting the current of the string. The mismatch loss can be set as a percentage power loss at MPP or calculated by specifying parameters in the *Detailed computation* tab.

- *Soiling loss*: Soiling losses include everything that covers a PV module and reduces the transmission through the front glass, resulting in an efficiency drop over time. Soiling types include dust and particles, bird droppings, snow and leafs. The loss depends on the environmental conditions, precipitation frequency and on the cleaning strategy of the PV modules. Soiling losses in PVsyst can be specified as a percentage for each month or as a yearly factor. When specifying the soiling loss periodical cleaning and rainy periods should be taken into account.

- *Incidence Angle Modifier (IAM)*: Reflection of the module surface increases with increasing irradiation incidence angle, resulting in an irradiation loss. IAM losses are sufficiently well defined in PVsyst by a parametrization proposed by "Ashrae", which depends on a parameter b_0. It is also possible to define points for a custom curve according to the module manufacturer's specification.

- *Auxiliary loss*: Auxiliary losses accounts for loss due to components such as inverters, light, fans that draw power, resulting in reduced output power of a PV plant. Auxiliary loss is not relevant for this study and will not be accounted for.

- *Ageing loss*: Simulates the growth of mismatch loss and degradation loss of individual modules over time. The mismatch loss will grow over time due to the un-even rate of degradation between modules in a string. The *Global degradation factor* is the cumulated average degradation factor for individual modules, and is set by specifying the *average degradation factor*. This gives the *basic degradation* line in

the graph. The *Mismatch degradation factor* is the cumulated mismatch loss, defined by specifying the I_{SC} *dispersion RMS* and V_{OC} *dispersion RMS*. PVsyst uses the Monte Carlo (MC) model to compute these values, which is a stochastic model, resulting in different values at each execution. To keep the same MC values within the variant, the *Keep these MC values* can be checked at the *Mismatch calculation* page. The MC values can also be saved and used in different projects. The combination of mismatch loss and degradation loss gives an *annual increasing mismatch* curve in the graph. The *Module warranty* page defines the maximum degradation rate, as specified by the PV module manufacturer. This degradation rate should be taken as an extreme value and considered an absolute maximum rate.

- *System unavailability*: Unavailability loss is downtime of the PV system due to system failure, maintenance or downtime of the grid. This loss can be defined in PVsyst as a fraction of time or a number of days. The actual energy losses depend on the season and the weather during unavailability periods.

Optional parameters

The *Horizon* describes far shading objects located sufficiently far from the PV system. The horizon is a horizontal curve defined by a set of height and azimuth points. The curve can be defined manually based on measured angles or imported from e.g. Meteonorm.

Objects close to the PV array causing shading on the array can be defined in the *Near shading* tab. This is implemented in the simulation by making a 3D model of the PV array and its surroundings. Objects, trees and building dimensions can be obtained from architect drawing, topological information and by measuring. There are three options for taking the shading into account:

- *Linear shading*: Accounts for the deficit of irradiance on the PV array. The losses are due to near shading objects reducing the direct and diffuse irradiance reaching the module. This represents a lower limit of the full shading loss.

- *According to module strings*: Accounts for electrical losses in addition to the deficit of irradiance on the PV array. The electrical losses results from the mismatch of electrical response of the modules in series and strings in parallel. The current in a string of modules is determined by the current of the most shaded module. This represents a upper limit of the full shading loss.

- *Detailed, according to Module layout*: A more realistic calculation of shading effects. In addition to the *Linear shading*, this accounts for the energy lost due to the electrical effect of shading. Shading losses are calculated according to a specified *Module layout* configuration, where each module is positioned on the PV surface.

The *Module layout* tab lets the user specify the geometrical arrangements of modules and their interconnections as strings in the 3D scene defined in the near shading tab. These specifications helps with the accurate calculation of the electrical effects of partial shading

of near objects. It is not suited for electrical shading calculation for thin film modules. The module layout is defined based on the 3D shading scene.

3.1.4 Accuracy of PVsyst

The accuracy of the simulation result from PVsyst depends on the meteorological data and defined simulation parameters. The model accuracy can be evaluated by comparing simulation results with measured data. According to PVsyst [33], it is often difficult to obtain high quality measured data for this validation. The accuracy evaluation consists of a measurement and modelling accuracy. Correct irradiance measurements requires well calibrated instruments and are often hard to obtain. In comparison, PVsyst states that the measurement of electrical data are usually more accurate. However, system malfunctions are often not well documented and may affect the measurements. The main uncertainty in the modelling accuracy is the PV module performance. It is based on STC values provided by the manufacturer, temperature coefficients, the internal resistance (R_{shunt} and R_{series}) parameters, module quality, light induced degradation and Potential Induced Degradation (PID). According to PVsyst, the shading losses are evaluated by a complex model, with inaccuracies of less than 1-2%. Other losses are specified by user defined parameters and are not significant for the accuracy of the simulation.

Of the user defined loss values, the model for calculating the *Thermal loss factor* is simplified. Both U_c and U_v are assumed to be constant, but the wind velocity varies and the U-value varies over the module. The PV array temperature is inhomogeneous. Air has a low heat capacity, so the air flowing under a PV module can equilibrate with the module temperature before the outlet, leading to no further heat exchange.

According to PVsyst [19], the simulation results with default loss values have an accuracy of $\pm$ 5%. This is based on rough analysis of several PV plants.

The calculative accuracy of five simulation software, including PVsyst, were evaluated and tested in an article [34]. The article states that all the software packages generally overestimates the incident irradiation while underestimating the generated electricity. The main source of error in the simulation is the PV cell model the software packages uses.

3.2 Site assessment

A site assessment was carried out during a field trip from the 23$^{\text{rd}}$ of September to the 30$^{\text{th}}$ of September. During the site assessment, available area for installation, building orientation and dimensions, far and near shading objects, electricity consumption pattern and roof materials were investigated.

3.2.1 Geographical location

Panthera Africa is located outside of Stanford in the Western Cape, South Africa. The geographical location is listed in table 3.1. These coordinates were used for all weather

data and site specific data throughout the thesis.

Table 3.1: Geographical location of Panthera Africa.

Latitude	Longitude	Altitude	Time Zone
-34.458942	19.532096	113 m	+2

3.2.2 Available area specifications and orientations

Panthera Africa has five buildings on their property. They have plans of building an educational center, which can be built to optimize energy production for roof mounted PV modules. In addition to roof surfaces, Panthera Africa has an available ground area, of which ground mounted PV modules can be placed. A map of Panthera Africa is illustrated in figure 3.3. Each available roof surface is coloured purple and the buildings used in this thesis are numbered. The blue area indicates available ground area and the red area indicates the placing of the future educational center. The current parking lot is located in the yellow area and the black lines and circles indicate electric fences. The main electricity consumption is within the green lines.

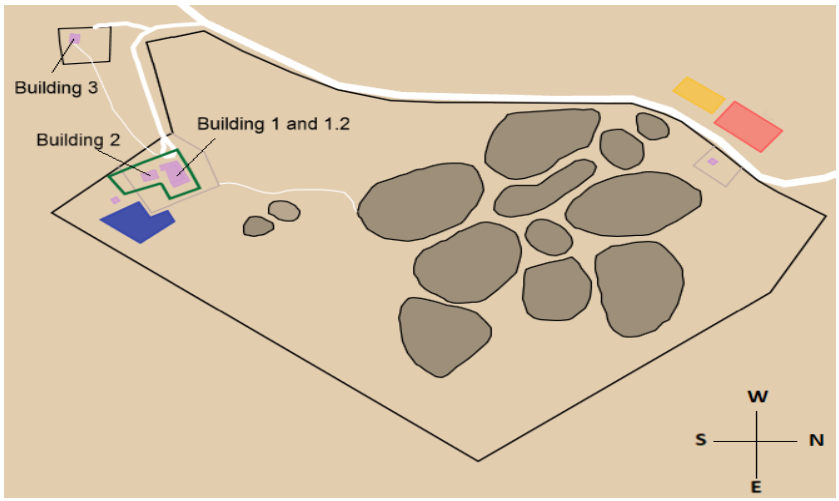

Figure 3.3: Site map of Panthera Africa.

Roof surfaces

Two buildings were excluded in this thesis, due to a small roof area and non-ideal orientation. The remaining three buildings are all orientated towards north, and their placing on the property is indicated in figure 3.3. Measurements and pictures of each building were taken during the field trip. The pictures were used to measure the roof tilt and building height, as this was difficult to do on-site. Distances on the pictures were measured using Sketchup. Real measurements of building dimensions in each picture were used to resize the image and control that the calculated distances were correct.

All roof tilt angles were calculated based on the building measurements and checked using a protractor. The angle of each building facade was measured using google earth, and the azimuth angle was then calculated based on this measurement. All azimuth angles are given with respect to the definition of an azimuth angle used by PVsyst.

Each building, with its specifications, is listed in table 3.2. The main house, building 1, has a surrounding porch roof, of which is indicated as building 1.2 in table 3.2. Figure 3.4 shows the considered roof area for each building in blue. The roofs of all buildings are made of corrugated iron sheets.

Table 3.2: Building specifications for Panthera Africa.

Building	Description	Azimuth angle [°]	Roof tilt angle [°]	Total roof area [m^2]
1	Main house	20	34.7	30
1.2	Porch roof	20	4.7	42.9
2	Apartment and garage	18	0	125
3	Cottage	-7	22.9	37

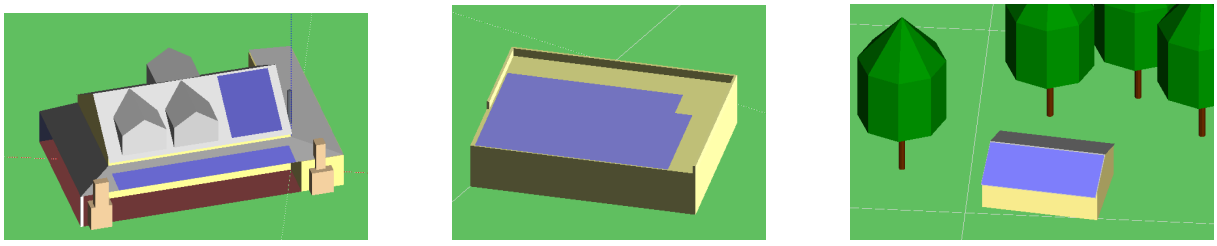

(a) Building 1 and 1.2 (b) Building 2 (c) Building 3

Figure 3.4: Available roof area for installing PV modules.

Ground area

The available ground area with measurements is illustrated in figure 3.5a and the ground condition is shown in figure 3.5b. The ground consists of dry sand, with some low green bushes and plants. The ground area has an azimuth angle of 18° and a total area of 1069 m^2.

3.2.3 Near shading items

Building 1 has a small aluminium chimney on the front west side and two wall dormers on the front east side with the potential to cast shadows during morning and afternoon. Building 1.2 has a white chimney on both the east and west side. These will also cast shadows during morning and afternoon. All shading items are shown in figure 3.6a.

Building 2 has a raised concrete edge along the north, west and half the south side of the building, as shown in figure 3.6b. Building 1 is also located 6 meters north of the building, and has the potential to cast shade.

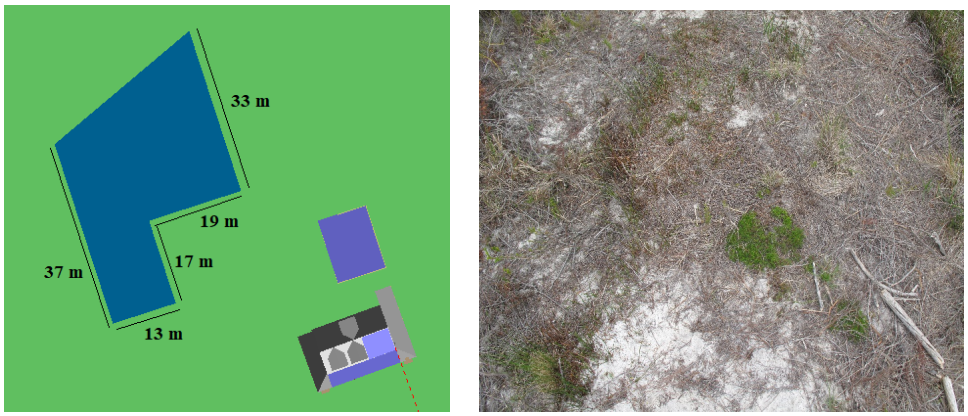

(a) Ground area (b) Ground coverage

Figure 3.5: Available ground area for installing PV modules.

Building 3 is located about 150 meters south west of building 1 and 2. As shown in figure 3.6c, the surrounding trees have the potential to cast shade. The trees on the west side cast shadows during the afternoon.

(a) Building 1 and 1.2 (b) Building 2 (c) Building 3

Figure 3.6: Near shading objects for each building.

Near shading objects for the available ground area are building 1 and 2, as shown in figure 3.7. Other shading items, such as bushes and trees, will be removed if building the ground mounted PV system.

Figure 3.7: Near shading objects for the available ground area.

3.2.4 Location of BoS components

Building 1 has a storeroom on the second floor, where the water heaters are located. This room could be suitable to install an inverter, but the space is limited. Building 2 has a storage room which can be accessed from the outside and is an ideal location for inverters. The white doors in figure 3.6b lead in to this storage room. Building 3 has indoor space for a small inverter.

3.2.5 Electricity consumption and grid connection

Panthera Africa has a three-phase grid-connection, with Eskom as their electricity supplier. Eskom is a South African electricity utility and the largest producer of electricity in Africa. Panthera Africa has a tariff named Landrate 123, which is an electricity tariff for rural costumers.

Monthly energy consumption data was received from Panthera Africa for the period March 2013 - September 2017. Monthly consumption data from 2013, 2014 and 2015 were excluded, as the consumption was much smaller than the current consumption. Figure 3.8 shows the electricity consumption from January 2016 to September 2017. Note that October 2016 has a zero energy consumption and August 2017 has a very low consumption listed. This is because the consumptions were estimated by Eskom and not read from the electricity meter. The result of the estimates is a higher energy consumption the following month. All other dates, excluding the two dips and peaks, are actual monthly energy consumptions.

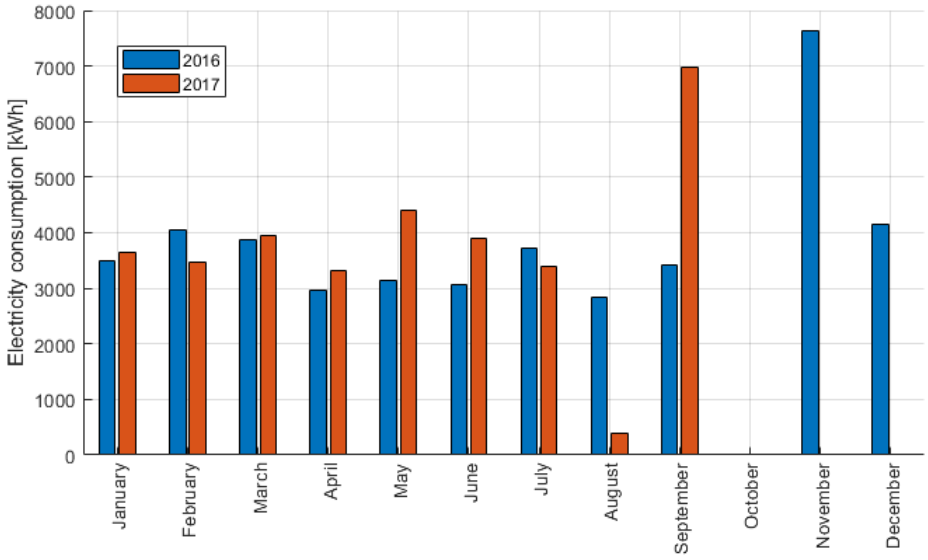

Figure 3.8: Monthly energy consumption for Panthera Africa from jan. 2016 to sep. 2017.

The total energy consumption in 2016 was 42.34 MWh, with an average monthly consumption of 3528 kWh. The total energy consumption per 01.10.2017 was 33.423 MWh, which is 2864 kWh more than per 01.10.2016. The average monthly consumption in 2017 was 3714 kWh.

An energy audit of Panthera Africa was conducted by Sustainable Technologies in February 2016 where the hourly energy consumption was measured for 14 days. The measured consumption data was received from Sustainable Technologies and used to create the average daily load profile illustrated in figure 3.9. The two components using the largest amount of energy is a container freezer and water heaters. The container freezer and water heaters used an average of, respectively, 72.3% and 9.2% of the daily energy consumption. Panthera Africa has a base load of 5.3 kW, as illustrated by the dotted line in figure 3.9.

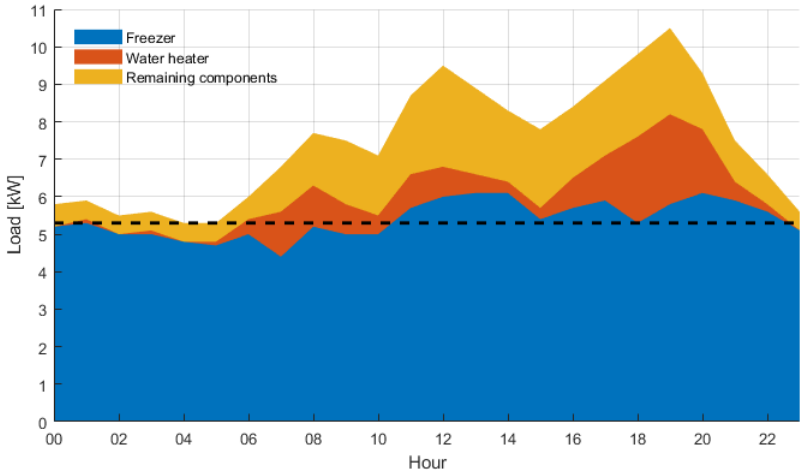

Figure 3.9: Daily load profile for Panthera Africa. The dotted line represents the base load.

As seen in figure 3.9, the consumption pattern for Panthera Africa consists of three consumptions tops, the largest in the afternoon. The consumption tops corresponds to breakfast, lunch break and after work hours, when workers at Panthera Africa have their breaks.

The container freezer is three-phased and used to store meat for the animals living on Panthera Africa. It is a Carrier Transicold freezer with a model number of 69NT40 – 511 – 112 and parts ID number of NT0289.

3.3 Climatic data acquisition

The power output from a PV system depends on the amount of irradiation at the site. Other important meteorological data are ambient temperature, wind speed and rainfall. Meteorological data from both databases and local weather stations were assessed to get an overview of the solar resource potential, local weather conditions and extreme weather occurrence.

3.3.1 Local weather stations

Inquiries were made to the Agricultural Research Council (ARC) and the South African Weather Service (SAWS) for meteorological data. Available meteorological data for each weather station are listed in table 3.3 and their location are displayed in figure 3.10.

Stanford weather station is located closest to Panthera Africa and operated by ARC. It has been in operation since 2002. Hourly data from 2002 – 2017 of the indicated variables were received by email from ARC and average values were calculated using MATLAB.

Hourly data from the weather station at Stellenbosch University from 2013 – 2017 of the indicated values were downloaded from *The South African Universities Radiometric Network* (SAURAN) [35] website [36]. Monthly average values were calculated using MATLAB.

The remaining weather stations are operated by SAWS. Radiation data from Cape Town Airport weather station from 1957 - 1986 was received, due to the radiation data from Cape Point station not yet being available. Hourly data for the indicated time periods was received from all SAWS stations by email. Monthly average values were calculated using MATLAB.

Table 3.3: Weather station information. The meteorological data temperature (T), wind speed (WS), rainfall (RF), global horizontal radiation (GHI), diffuse horizontal radiation (DHI) and direct normal radiation (DNI) are listed for nine different locations close to Panthera Africa. There are variations in the amount of meteorological data collected at the different weather stations.

Location	Distance to site [km]	Altitude [m]	Climatic distance [km]	Operator	Values	Period	Meteorological data
Cape point	96.6	152	96.7	SAWS	Hourly	1950 - 2017	T, WS
Cape Town Airport	102	48	102.2	SAWS	Hourly	1957 - 1986	GHI, DHI, DNI
Elgin Exp Farm	59	311	62.2	SAWS	Hourly	2004 - 2014	T, WS
Tygerhoek	48.2	157	42.4	SAWS	Hourly	1965 - 2017	T, WS
Hermanus	28.6	15	30.2	SAWS	Hourly	1996 - 2017	T, WS
Stanford	12.5	51	13.9	ARC	Hourly	2002 - 2017	T, WS, GHI, RF
Cape Agulhas	60	10	60.9	SAWS	Hourly	1950 - 2017	T, WS
Struisbaai	61	5	61.9	SAWS	Hourly	1996 - 2017	T, WS
Stellenbosch	85	113	85.7	SAURAN	Hourly	2013 - 2017	T, WS, GHI, DHI, DNI

The climatic distance for each weather station was calculated using equation 2.7, and are presented in table 3.3. For a weather station to be representative of the climatic conditions at a given site, their climatic distance should not exceed around 20 km according to Meteonorm [19]. Based on this definition, only Stanford weather station represents the climatic conditions of Panthera Africa.

Average, maximum and minimum temperature and wind speed values from Stanford weather station are listed, respectively, in table 3.4. Figure 3.11 illustrates the average daily precipitation in Stanford and the average number of days with precipitation each month.

Figure 3.10: Map showing the location of all the weather stations listed in table 3.3.

Table 3.4: Average, maximum and minimum temperature and wind speed values from Stanford weather station.

	Average		Max		Min	
	T [°C]	Wind [m/s]	T [°C]	Wind [m/s]	T [°C]	Wind [m/s]
Jan	21.3	3.1	39.7	10.8	8.6	0.2
Feb	21.2	2.9	38.2	9.6	10.2	0.2
Mar	19.8	2.8	38.9	9.5	5.4	0.2
Apr	17.6	2.7	37.6	9.6	5.3	0.2
May	15.5	2.6	32.7	11.0	4.7	0.2
Jun	13.3	2.8	32.5	12.8	3.0	0.2
Jul	12.8	2.8	30.9	12.0	2.6	0.2
Aug	12.9	3.1	30.7	13.0	2.7	0.2
Sep	14.3	3.2	33.5	11.6	2.3	0.2
Oct	16.1	3.3	34.5	11.4	3.6	0.2
Nov	17.7	3.2	35.4	11.9	5.4	0.2
Dec	20.0	3.1	35.7	11.6	7.7	0.2
Average	16.9	3.0	35.0	11.2	5.1	0.2

According to table 3.4, temperatures in Stanford range from a maximum at 39.7 °C during summer to a minimum of 2.3 °C during winter. Wind speeds range from 13 m/s to 0.2 m/s. Temperatures does not drop below zero during winter.

3.3.2 Databases

In this study, six databases with meteorological data were used. Selected information about each database is listed in table 3.5. Databases with monthly values are monthly average values.

Meteonorm collect data by interpolating values from the three closest meteorological stations and using satellite data when weather records are not available or the location is

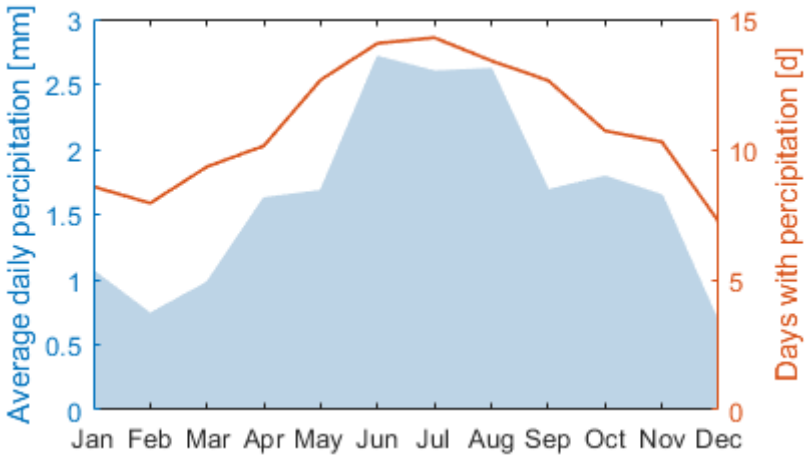

Figure 3.11: Average daily precipitation and number of days with precipitation for each month in e year. The graph is made based on data from Stanford weather station.

Table 3.5: Information about the climatic databases used in this thesis.

Database	Data inputs	Spatial resolution	Time resolution	Period	Meteorological data available
3Tier Vaisala	Satellites	3 x 3 km	Hourly	1999 - 2016	GHI, DHI, T, WS
NASA-SSE	Satellites	110 x 110 km	Monthly	1983 - 2005	GHI, DHI, T
PVgis Helioclim1	Meteosat	30 x 30 km	Monthly	1985 - 2004	GHI, DHI
PVgis Climate-SAF	Meteosat	3 x 3 km	Monthly	1998 - 2011	GHI, DHI
Solargis	Meteosat	3 x 3 km	Monthly	1994 - 2011	GHI, DHI, T
Meteonorm7.1	Meteo stations, satellite data	Interpolation, 8 x 8 km	Monthly	1953 - 1976	GHI, DHI, T, WS

between 30 and 200 km away from the weather station. In South Africa, Meteonorm has twelve meteorological stations, with the three closest to the site being Cape Town (113 km), Port Elizabeth (560 km) and Middelburg (612 km).

The remaining databases collect data from various satellite records. The climate data from both PVgis databases were downloaded online [37], the data from Solargis and 3Tier-Vaisala were received by email from Scatec Solar and data from Meteonorm7.1 and NASA-SSE are both included in PVsyst.

3.3.3 Data comparison and analysis

The location has meteorological data from both ground based weather stations and databases. The various meteorological databases differ in input data, methodology, covered area, time intervals and spatial resolution, as shown in table 3.5. These factors result in differences in global horizontal radiation, ambient temperature and wind velocity.

Yearly and monthly GHI comparison

The annual GHI values from the listed weather stations and databases are shown in table 3.6. Figure 3.12 shows a comparison of monthly GHI values for all databases.

Table 3.6: Annual GHI values from databases and weather stations.

Data from	Source	GHI [kWh/m^2]
Stanford	Measured	1561
Stellenbosch	Measured	1967
Cape Town Airport	Measured	1952
Solargis	Database	1709
PVgis Climate-SAF	Database	1854
PVgis Helioclim1	Database	1782
3Tier Vaisala	Database	1814
NASA-SSE	Database	1855
Meteonorm7.1	Database	1794

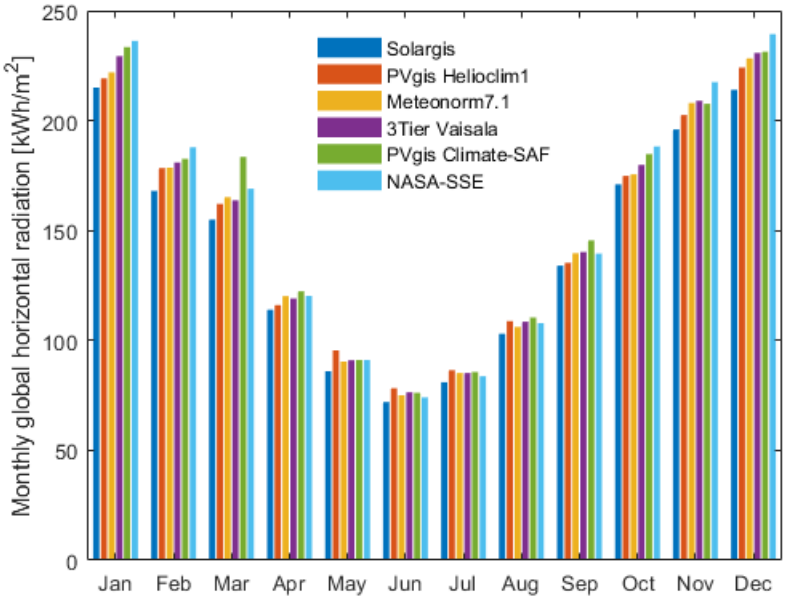

Figure 3.12: Comparison of monthly GHI values for the databases.

As shown in table 3.6, the radiation data measured at Stanford is significantly lower than the radiation data measured in Stellenbosch and Cape Town Airport. Even though the weather stations in Stellenbosch and Cape Town Airport are not representative of the local climate at Panthera Africa, they still give an indicator to which range the annual global radiation data should be in. The radiation data from Stanford is also significantly lower than all the databases.

The monthly GHI values differ most in summer months and least in winter months. NASA-SSE has the highest values during summer months, while PVgis Helioclim1 and PVgis SAF has the highest values during winter months. Of the databases, Solargis has the lowest monthly value during the whole year. When comparing the databases to the measured value in Stanford, it has similar values to Solargis from January to June, but differ increasingly from July to December.

Temperature and wind speed comparison

Table 3.7 shows a comparison of ambient temperature and wind speed data between Stanford weather station and the listed databases. When comparing the temperature measurements from Stanford to the temperatures calculated by the databases, 3Tier-Vaisala closely resembles the monthly temperatures recorded at Stanford weather station. Solargis has a lower temperature estimate each month, while both NASA-SSE and Meteonorm7.1 has a higher temperature estimate.

Table 3.7: Comparison of ambient temperature and wind speed data for Stanford and the listed databases.

	Temperature [°C]					Wind speed [m/s]		
	Stanford	Solargis	3Tier Vaisala	NASA-SSE	Meteonorm 7.1	Stanford	3Tier Vaisala	Meteonorm 7.1
Jan	21.3	20.4	21.1	20.5	22.1	3.1	5.7	5.2
Feb	21.2	20.8	21.3	21.0	22.3	2.9	5.5	4.9
Mar	19.8	19.6	20.0	20.0	20.5	2.8	5.2	4.4
Apr	17.6	17.4	17.5	18.3	17.7	2.7	4.9	3.7
May	15.5	15.0	15.4	16.4	15.1	2.6	4.8	3.9
Jun	13.3	12.9	13.3	14.4	12.4	2.8	4.9	3.7
Jul	12.8	12.1	12.6	13.8	12.1	2.8	5.0	3.8
Aug	12.9	12.4	12.9	13.9	12.6	3.1	5.3	4.3
Sep	14.3	13.9	14.0	14.8	14.2	3.2	5.4	4.4
Oct	16.1	15.8	16.2	16.4	17.2	3.3	5.5	4.6
Nov	17.7	17.6	17.8	17.9	19.0	3.2	5.6	5.0
Dec	20.0	19.5	20.0	19.4	21.1	3.1	5.6	5.1
Average	16.9	16.4	16.8	17.2	17.2	3.0	5.3	4.4

When comparing the wind speeds, both 3Tier Vaisala and Meteonorm7.1 overestimates compared to measured values at Stanford. Meteonorm7.1 is closest to the measured values.

3.3.4 Choosing meteorological datasets and albedo values

It is difficult to determine which datasets give the most realistic picture of the climatic situation at the site. As shown in table 3.5, the databases have different time period, source, available meteorological data variables and spatial resolution. Due to uncertainties, three datasets of climate data were used in the simulation; one giving the highest yield, one giving an average yield, and one giving the most conservative yield. In all three datasets, temperature and wind speed measured at Stanford weather station were used.

Dataset 1 is considered the best-case scenario and gives the best annual system yield. NASA-SSE and PVgis SAF has the highest yearly irradiation values, which are respectively 1855 kWh/m^2 and 1854 kWh/m^2. Of these two, the global and diffuse irradiation data from PVgis SAF is chosen for the best-case scenario, because it has a better spatial resolution and a more current time period. Dataset 1 is given in appendix A table A.1.

Which of the datasets provides the true irradiation value is not known, but an average irradiation value to approximate a true value can be calculated. To further reduce uncertainties, a weighted average can be built using indicators like time interval and spatial resolution.

Dataset 2 is constructed by using a weighted average, where each database is weighted based on the time period of the dataset (50%) and the inverse spatial resolution (50%). The weighing of each database is presented in table 3.8. This dataset will be used in the

main simulation. Dataset 2 is given in appendix A table A.2.

Table 3.8: Weighting of each database for time period and spatial resolution.

Database	Time period	Spatial resolution
3Tier Vaisala	0.153	0.286
NASA-SSE	0.198	0.008
PVgis Helioclim1	0.171	0.028
PVgis Climate-SAF	0.117	0.286
Solargis	0.153	0.286
Meteonorm7.1	0.207	0.107

Table 3.9: Albedo values [38].

Surface	Albedo
Grass covered ground	0.2 - 0.3
Green forest	0.1 - 0.2
Wet ground	0.1 - 0.2
Dry ground	0.15 - 0.3
Sand	0.3 - 0.4

Dataset 3 is considered the worst-case scenario, and gives the most conservative system yield. The weather station at Stanford does not measure diffuse radiation, which is a required input value in PVsyst, and is therefore not used in this dataset. This dataset consists of global and diffuse values from Solargis, which is the database giving the lowest yearly irradiation values. Dataset 3 is given in appendix A table A.3.

Soil albedo depends on the surface color and moisture content. The albedo will be slightly lower when the ground is wet. Albedo values for different natural surfaces are given in table 3.9 [38].

The albedo value of 0.2 is set as default value in PVsyst, but it is possible to change the value according to physical conditions of the project location. The project is located in a rural area, with the ground consisting of light sand and partly covered by low, green vegetation. There is no snow during winter months, but June, July and August are months with high precipitation, as shown in figure 3.11. The albedo is therefore set to 0.2 during these months, and slightly higher the rest of the year, at 0.25.

3.4 Module orientation and inter-row spacing

The chosen field type, azimuth angle and tilt angle for both the ground mounted and roof mounted system, in addition to inter-row spacing, are presented in this section.

3.4.1 Roof mounted PV system

A several orientations plane and fixed tilted plane are chosen for the roof surfaces, with energy production optimized for a yearly irradiation yield. The tilt- and azimuth angle of a roof mounted module was assumed to be equal to the tilt- and azimuth angle of the roof. Both tilt angles and azimuth angles for each building are listed in table 3.2.

Optimal tilt- and azimuth angle

The optimal tilt- and azimuth angle for the site is 32° and directly North, according to PVsyst. Radiation losses with respect to optimal tilt- and azimuth angle for each building are given in table 3.10.

Table 3.10: Percentage radiation loss with respect to optimum for buildings located at Panthera Africa. The listed tilt and azimuth angles are the actual and the radiation loss is the percentage loss as these angles are not the optimal angles.

	Azimuth angle [°]	Tilt angle [°]	Radiation loss [%]
Building 1	20	34.7	1
Building 1.2	20	4.7	10.4
Building 2	18	0	13.7
Building 3	-7	22.9	1.6

3.4.2 Ground mounted PV system

The field type of a ground mounted PV system can be chosen as either a fixed tilted plane or unlimited sheds in PVsyst. A shed in PVsyst is a row of modules. When using a fixed tilted plane, the module rows are constructed in the near shading scene. Both mutual shading and near shading items are therefore accounted for. A fixed tilted plane is recommended for smaller ground systems, and will be used in this thesis. The energy production will be optimized for a yearly irradiation yield.

When choosing the tilt angle and azimuth angle for a ground mounted PV system, the inter-row spacing must be considered together with the orientation.

Inter-row spacing

An optimization between tilt angle, azimuth angle, area utilization and maximum energy production is ideal when choosing the inter-row spacing. In this study, the condition of no mutual shading from 9.00 – 15.00 during the winter solstice was used. Six module configurations were considered; 1-, 2- and 3 x Portrait module configuration and 2-, 3- and 5 x Landscape module configuration. The inter-row spacing was then calculated for all six configurations by using equation 2.8. Azimuth angles from -38° to 38° and tilt angles from 0° to 44° were used. The inter-row spacing is affected by module size, and was calculated for four module sizes using MATLAB.

Based on the calculated inter-row spacings, two tilt and azimuth scenarios were considered. For a good area utilization, an azimuth angle of 18° was chosen. To minimize radiation losses while optimizing spacing, a tilt angle of 28° was chosen. For maximum power production, an azimuth angle of 0° and tilt angle of 32° was chosen. The inter-row spacing for each scenario is listed in table 3.11.

Table 3.11: Inter-row spacing for a module when considering good area utilization and maximum power production. *Pitch 1*, *Pitch 2*, *Pitch 3* and *Pitch 4* are, respectively, for modules of sizes 1.96 m x 0.992 m, 1.2 m x 0.6 m, 1.257 m x 0.977 m and 1.65 x 0.992 m.

	Good area utilization					Maximal power production				
	Tilt, azimuth [°]	Pitch 1 [m]	Pitch 2 [m]	Pitch 3 [m]	Pitch 4 [m]	Tilt, azimuth [°]	Pitch 1 [m]	Pitch 2 [m]	Pitch 3 [m]	Pitch 4 [m]
1 x Portrait	28, 18	3.7	2.3	2.4	3.1	32, 0	4.7	2.9	3.0	4.0
2 x Portrait	28, 18	7.4	4.5	4.8	6.3	32, 0	9.5	5.8	6.1	8.0
3 x Portrait	28, 18	11.1	6.8	7.1	9.4	32, 0	14.2	8.7	9.1	12.0
2 x Landscape	28, 18	3.8	2.3	3.7	3.8	32, 0	4.8	2.9	4.7	4.8
3 x Landscape	28, 18	5.6	3.4	5.6	5.6	32, 0	7.2	4.3	7.1	7.2
5 x Landscape	28, 18	9.4	5.7	9.3	9.4	32, 0	12.0	7.2	11.8	12.0

A tilt angle of 32° and azimuth angle of 0° were chosen for the ground mounted system, to maximize power production. Two rows of modules were used in the simulation and a Landscape configuration for the modules were chosen. A 3 x Landscape configuration was chosen for modules of sizes 1.96 m x 0.992 m, 1.257 m x 0.997 m and 1.65 m x 0.992 m. A 5 x Landscape configuration was chosen for the module of size 1.2 m x 0.6 m. This was done to achieve an almost equal inter-row spacing for all module sizes.

3.5 Shading

PVsyst distinguishes between near shading and far shading. Near shading is shading produced by objects close to the PV module while far shading is shading from objects sufficiently far from the PV field, also called a horizon.

3.5.1 Near shading on buildings

An analysis of the effect of near shading objects on the PV system was made for the roof of building 1, 1.2, 2 and 3. Each building has near shading objects as listed in subsection 3.2.3. The percentage irradiation losses (beam linear losses) due to shading were determined at the 21^{th} of each month. All losses were calculated for a clear day.

An initial shading analysis, using the total available roof area for each building listed in table 3.2, was done. To minimize shading losses, an adjustment was made to the available area of all buildings. The shading analysis was performed on the area shown in figure 3.4 for each building. The percentage irradiation loss due to shading is shown in table 3.12.

As seen in table 3.12, building 1 has the largest amount of shading losses and building 1 has the smallest amount. Building 3 has the highest percentage shading, which occurs during summer months.

In addition to giving the percentage loss of direct irradiation, PVsyst also creates iso-shading diagrams. An iso-shading diagram shows the percentage direct irradiation losses for a surface at different sun angles. It indicates when shading occurs during the year.

Table 3.12: Percentage losses of direct irradiation due to shading for each building.

	Building 1 [%]	Building 1.2 [%]	Building 2 [%]	Building 3 [%]	All roofs [%]
Jan	1.0	4.0	0.2	7.4	1.9
Feb	1.4	2.2	0.1	4.6	1.8
Mar	2.0	0.7	0.1	1.7	1.3
Apr	2.3	0.8	0.1	0.0	0.6
May	2.3	1.3	0.2	0.0	0.7
Jun	2.3	1.5	0.2	0.0	0.9
Jul	2.4	1.5	0.2	0.0	0.8
Aug	2.3	0.7	0.1	0.1	0.7
Sep	1.9	0.7	0.1	1.8	1.3
Oct	1.4	2.4	0.2	4.9	1.9
Nov	1.0	4.0	0.2	7.5	1.9
Dec	1.0	4.6	0.3	8.1	1.8

Each curve on the diagram represents a percentage shading loss. Figure 3.13 shows the iso-shading diagram for building 1.

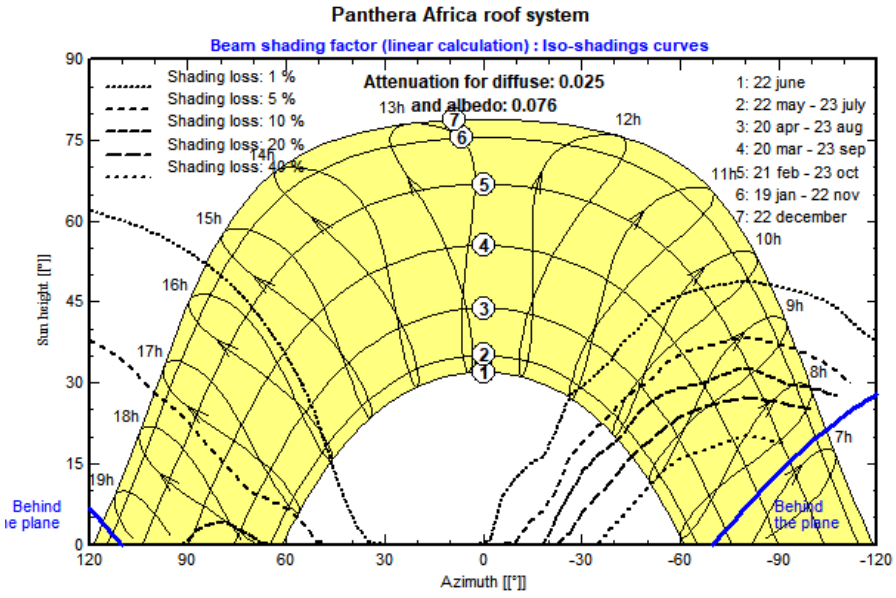

Figure 3.13: Iso-shading diagram for building 1.

As seen in figure 3.13, shading on roof 1 mainly occurs before 9 in the morning during summer months and 11 in the morning during winter months. This is due to the dormer on the second floor. In the evening there is some shading from the aluminium chimney.

Shading on roof 1.2 mainly occurs before 10 in the morning, due to shading from building 1. The larger shading component in the summer months are due to shading from the eaves on building 1. There is some shading from the chimney in the evening. Roof 2 has the lowest amount of shading. The shading loss mainly occur in the afternoon due to the edges surrounding the roof. The afternoon shading loss is higher during winter months,

as the Sun's position is lower in the sky. Shading on roof 3 mainly occur in the summer months before 10 in the morning and after 16 in the afternoon. The shading is mainly due to surrounding trees. Roof 3 has no shading during winter months.

3.5.2 Near shading on ground area

An analysis of the effect of near shading objects on the PV system was made for the available ground area. Near shading objects for the area are listed in subchapter 3.2.3. The percentage irradiation losses due to shading was determined at the 21^{th} of each month and is shown in table 3.13. All losses are calculated for a clear day.

The shading analysis was done for a ground system with two rows of modules, having an inter-row spacing of 7.2 m, a tilt angle of 32° and an azimuth angle of 0°. This corresponds to the ground system configuration specified in subsection 3.4.2. The shading analysis was done for the area illustrated in figure 3.14, which is equal to the total area of all buildings. The percentage irradiation losses due to shading of the ground area are given in table 3.13.

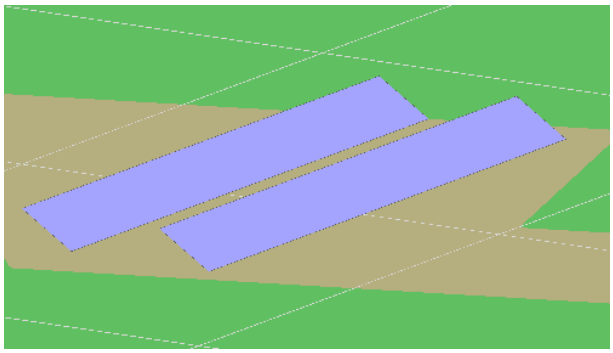

Figure 3.14: Area that was used in the shading analysis for the ground mounted system. The area is 180 m^2.

Table 3.13: Percentage irradiation losses due to shading for ground area.

	Jan	Feb	Mar	Apr	May	Jun	Jul	Aug	Sep	Oct	Nov	Dec
Ground area [%]	0.0	0.0	0.0	0.1	0.4	0.8	0.5	0.1	0.0	0.0	0.0	0.0

Shading on the ground area mainly occur during winter months, as the Sun's position in the sky is lower. Due to the chosen inter-row spacing, no mutual shading occur from 9.00 to 15.00 during the winter months. The shading is mainly due to mutual shading between the module rows in mornings and afternoons. Building 1 also casts shades on the modules during the afternoon.

3.5.3 Far shading

As illustrated in figure 3.15, there is a mountain located north of Panthera Africa. This is the only object contributing to the far shading scheme of the location.

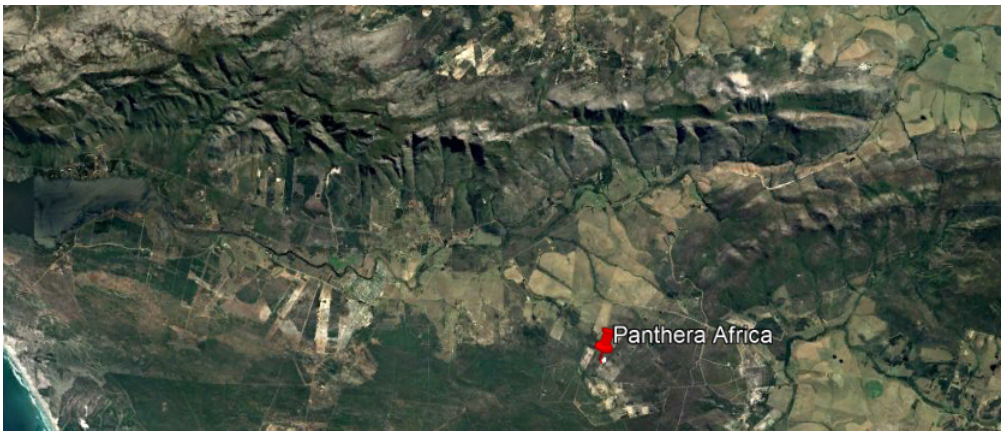

Figure 3.15: Illustrates the mountain contributing to far shading for Panthera Africa.

The horizon profile of Panthera Africa has been found from both Meteonorm and PVGis, and then compared with on-site measurements. Meteonorm and PVGis have very similar altitude values for the mountain, but Meteonorm has some higher values and will therefore be used in the simulation. The horizon profile with height and azimuth values from Meteonorm is shown in figure 3.16. As seen from figure 3.16 the far shading due to the horizon occur in the morning and evening and have a small effect on the overall radiation.

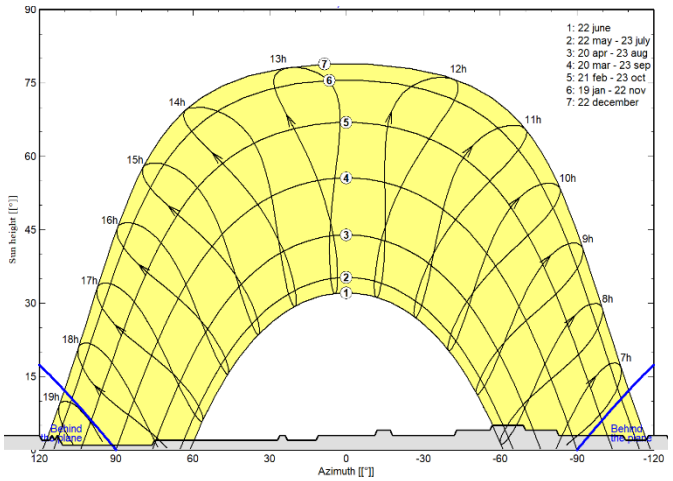

Height [°]	3.0	3.0	2.0	2.0	3.0	3.0	2.0	2.0	3.0	3.0	4.0	4.0
Azimuth [°]	-180	-147	-146	-126	-125	-118	-117	-109	-108	-83	-82	-70
Height [°]	5.0	5.0	4.0	4.0	3.0	3.0	4.0	4.0	3.0	3.0	2.0	2.0
Azimuth [°]	-69	-57	-56	-43	-42	-18	-17	-12	-11	11	12	23
Height [°]	3.0	3.0	2.0	2.0	1.0	1.0	3.0	2.0	3.0	2.0	2.0	3.0
Azimuth [°]	24	26	27	75	76	111	113	114	115	116	119	120
Height [°]	3.0	4.0	4.0	5.0	5.0	4.0	4.0	3.0	3.0			
Azimuth [°]	146	147	150	151	154	155	163	164	180			

Figure 3.16: The horizon profile used for this thesis with height and azimuth values stated. Each point on the horizon profile corresponds to a height and azimuth angle listed below the figure. The azimuth angle is defined along the x-axis, with negative values being due east, zero due north and positive values due west. The height angles are defined along the y-axis and corresponds to the heigh of the horizon in degrees.

3.6 Selection of modules and inverters

There is a wide selection of modules and inverters in today's PV market. To make the simulation as realistic as possible, several solar PV companies in South Africa were contacted regarding modules and inverters that are available and often used. One of the contacted companies, called Solareff, replied and gave information about PV system component pricing and recommendations.

3.6.1 Selecting modules

PVsyst has a wide selection of PV modules in the database, with different nominal power, technology, size and manufacturer. Jinko Solar, Canadian Solar, Trina Solar and First Solar were among the top 10 PV module manufacturers of 2016 [39], and are also available in South Africa.

Modules with high efficiency and rated power were required due to limited available roof area. As modules have different sizes, modules with a high rated power per square meter were preferred. The chosen modules also had to comply with the following International Standards:

- IEC 61215: design qualification and type approval for crystalline modules
- IEC 61646: design qualification and type approval for thin film modules
- IEC 61730: module safety qualification

To compare the performance and pricing of different system configurations, four different module technologies were selected. The selected modules are listed in table 3.14 with the datasheets given in appendix B. The same modules were used in both the ground mounted and the roof mounted PV system configurations.

Table 3.14: Information about selected modules. β is the voltage temperature coefficient for and γ is the power temperature coefficient.

Manufacturer Model	Technology	Nominal power [W]	Efficiency [%]	β [%/°C]	γ [%/°C]	NOCT [°C]	Area required for 1 kWp [m^2]
CanadianSolar CS6U-330P	Poly-crystalline	330	16.97	-0.31	-0.41	43/47	5.9
CanadianSolar CS6K-305MS	Mono-crystalline	305	18.63	-0.29	-0.39	40/44	5.4
First Solar FS-4120-3	Thin-film CdTe	120	16.7	-0.28	-0.28	45	6.0
Solar Frontier SF170-S	Thin-film CIS	170	13.8	-0.30	-0.31	47	7.2

Canadian Solar was listed as the top preferred module brand in South Africa as of February 2017 [40], and is also recommended by Solareff. Both a 72-cell and 60-cell module were chosen, as they have different sizes. The chosen poly-crystalline module was a 72-cell module from the MaxPower series, used by Solareff on their PV system installations. The chosen mono-crystalline module was a 60-cell module with the largest rated power from the SuperPower series.

Both First Solar and Solar Frontier were listed among the top 10 preferred module brands in South Africa as of February 2017 [40] and were chosen as brands for the thin-film modules. The CIS module from Solar Frontier with the highest power per area was chosen. The Series 4 CdTe module from First Solar with the highest power per area is the FS-4122-3 module, but as this was not available in the PVsyst database, the FS-4120-3 modules was chosen. When installing First Solar modules in a ground mounted system, the modules have to be oriented in a Landscape configuration according to First Solar. This is due to avoid the effect of parallel shading on the module cells, as explained in subsection 2.2.2.

3.6.2 Selecting inverters

There is a wide selection of inverters to choose from in South Africa and the most used inverter brand for PV systems in the 11 - 99 kWp range is SMA [41]. The selected inverters must handle 72-cell modules, be available in South Africa and manufactured during recent years. In this thesis, the selected string inverter is a three-phase inverter, as the container freezer requires three-phase AC current.

When selecting inverters for the simulation, the inverters should be on the list of approved inverters in Overstrand municipality, where Panthera Africa is located. As the list does not contain any module inverters, the module inverters used in the simulation does not comply with this requirement. It is worth noting that the list was published in 2016 and has not been updated since.

As listed in subsection 2.2.3, different inverter configurations handle shading differently. To compare the effect of shading on energy production, the roofs were simulated with string inverters, string inverters with optimizers and module inverters. As the shading analysis in subsection 3.5.2 showed a low shading loss, the ground systems were only simulated with string inverters.

The selected inverters are listed in table 3.15, with datasheets given in appendix B. The selected string inverter for the thesis was chosen based on a recommendation from Solareff, as well as the availability and popularity of SMA inverters in South Africa. Tigo optimizers are compatible with SMA inverters, and were therefore chosen as the optimizer manufacturer. The largest module inverter producer is Enphase, which was chosen as the module inverter brand.

Table 3.15: List of inverters with selected information about each.

Manufacturer	Model	Configuration	Maximum efficiency [%]	Min./max. input voltage [V]
SMA	Sunny Tripower series	String inverter	98	150/1000
Tigo	TS4-R-O	Optimizer	99.6	12/90
Enphase	IQ6+, IQ6	Module inverter	97, 97	22/62 , 22/48

The Enphase module inverters are not three-phase inverters, but can be connected in three-phase. Enphase has published a technical brief on how to connect and wire the module inverter as both single-phased and three-phased. When modelling Enphase inverters in PVsyst, an adjustments to the following *Hidden parameters* are recommended by Enphase [42]:

- *Lower limit power treshold*, as the inverters can convert energy at very low power levels with high conversion efficiency. The default value in PVsyst is 0.5%, but Enphase recommends a value of 0.01%.
- *Maximum P_{nom} ratio* for inverter sizing. The default value in PVsyst is 1.3, but Enphase recommends a value of 1.5.

The SMA Sunny Tripower series are inverters with two unbalanced MPPT inputs, meaning the two inputs can have strings of different lengths. Each MPPT input must be designed as a sub-array, with the choice between *Main* and *Secondary* MPPT input. This increases the design flexibility, and strings can be designed to minimize the impact of shading. SMA offers TS4 Tigo optimizers that are compatible with their inverters. The optimizers only need to be mounted on modules that are affected by e.g. partial shading. The TS4-R-O optimizers offers module level monitoring, shutdown and optimization. The optimizer can be mounted on a module frame.

3.7 System design

PVsyst calculates the lower and upper voltage limit for a module and suggests a minimum and maximum amount of modules in a string for a given inverter. To estimate the minimum and maximum number of modules in a string, the module operating temperatures and module voltages were calculated.

3.7.1 Matching energy production and consumption

As noted in subsection 3.2.5 the total energy consumption in 2016 was 42.34 MWh. Based on the monthly average energy consumption in 2017 of 3714 kWh, the total energy consumption in 2017 was expected to be 44.57 MWh. Panthera Africa has a vision to be a zero net energy project, meaning that the annual consumed energy is less than or equal to the on-site generated energy. South Africa is in the beginning phases regarding residential solar PV and the current tariffs are structured to make it most beneficial for customers to consume the generated electricity. All customers that generate electricity must also be net customers, meaning that they have to buy more electricity than they sell to the grid utility on a consecutive 12 month period.

For the project to be economical and comply with the restrictions mentioned above, an annual energy target of about 30 - 35 MWh is set for both roof and ground mounted system design.

3.7.2 Design temperatures

To properly size a PV system in PVsyst, the two design criteria mentioned under *Voltage sizing* in subsection 2.3.6 have to be met. These conditions involve the design temperatures mentioned under *Project settings* in subsection 3.1.2. The design temperatures may be changed according to the climatic conditions at the project site.

The *absolute minimum operating temperature* is the lowest temperature a PV array will experience and should be the lowest temperature ever measured on-site. The lowest measured temperature at Stanford weather station is 2.3°C. PVsyst uses a default value of -10°C, which is a universal common practice and not recommended to change [43].

The *winter minimum operating temperature* was found by calculating the module temperatures during winter at different irradiance level. The lowest NOCT listed in table 2.1 and the average minimum ambient winter temperature of 8.8°C were used. The *summer maximum operating temperature* was found by calculating the module temperatures during summer at different irradiance levels. The highest NOCT listed in table 2.1 and the average maximum ambient summer temperature of 26.2°C were used. The module temperatures were calculated using equation 2.15 and are listed in table 3.16. The NOCT and ambient temperature were kept constant, while the irradiance was varied.

Table 3.16: Module temperatures for summer and winter operation at different irradiance levels, G_{inc}. The irradiance during winter months vary from 0 W/m^2 to 550 W/m^2, while the irradiance during summer months vary from 0 W/m^2 to 1100 W/m^2.

Winter operation		Summer operation	
G_{inc} [W/m^2]	Module temp. [°C]	G_{inc} [W/m^2]	Module temp. [°C]
0	8.8	800	53.2
200	13.8	1000	60
400	18.8	1200	66.7

Based on table 3.16, a *winter minimum operating temperature* of 10°C and *summer maximum operating temperature* of 70°C are used. The default PVsyst values of 50°C for the *summer usual operating temperature* and -10°C for the *absolute minimum operating temperature* are used.

3.7.3 Array to inverter matching

The module voltages were then calculated using equation 2.14 and the design temperatures found in subsection 3.7.2. The resulting voltages are given in table 3.17.

By using equation 2.12 and 2.13 together with the calculated voltages in table 3.17 and the inverter specifications, the minimum and maximum number of modules in a string were calculated for different SMA Sunny Tripower inverters. These numbers are listed in table 3.18.

Table 3.17: Module voltages for the selected modules at the design temperatures. The voltage temperature coefficients from table 3.14 were used.

	V_{OC} [V]	$V_{mpp\ max}$ [V]	V_{mpp} [V]	$V_{mpp\ min}$ [V]
CS6U-330P	49.8	38.9	34.3	32.0
CS6K-305MS	43.4	34.1	30.3	28.4
FS-4120-3	96.2	73.8	65.8	61.9
SF170-S	122.1	91.4	80.9	75.7

Table 3.18: Minimum and maximum number of modules in a string for the inverter SMA Sunny Tripower.

	SMA Sunny Tripower					
	5 kW		6 kW		7 kW	
	n_{min}	n_{max}	n_{min}	n_{max}	n_{min}	n_{max}
CS6U-330P	8	20	10	20	10	20
CS6K-305MS	9	23	11	23	11	23
FS-4120-3	4	10	5	10	5	10
SF170-S	4	8	4	8	4	8

3.7.4 System design configuration

When designing and simulating the PV system, both a ground mounted PV system and a roof mounted PV system scenario were considered.

Roof mounted system configurations

The four roofs used in the roof mounted system all have different tilt, size, shading and orientation. Table 3.19 lists the simulated configuration for each building. The systems with thin-film modules were not simulated with module inverters or optimizers. Each roof is simulated with a maximum number of modules, while considering the shading losses. All systems have a similar layout as the blue area in figure 3.4, thus having similar shading losses as listed in subsection 3.5.1.

The first number in the system name indicates the building, the second number indicates the inverter type and the last number indicates the module type. Systems marked R1.x.x are systems on building 1 and 1.2. Building 1 and 1.2 were simulated together, due to a small amount of modules fitting onto both roofs. R2.x.x are systems on building 2 and R3.x.x are systems on building 3.

Systems Rx.1.x were simulated with SMA string inverters, systems Rx.2.x have SMA string inverters with optimizers and Rx.3.x systems uses Enphase module inverters. For the different modules, systems Rx.x.1. Rx.x.2, Rx.x.3 and Rx.x.4 were simulated with, respectively, Canadian Solar CS6U-330P modules, Canadian Solar CS6K-305MS modules, First Solar FS-4120-3 modules and Solar Frontier FS170-S modules.

Table 3.19: Roof mounted system configurations used in the simulation. SMA is a Sunny Tripower inverter, Tigo is an optimizer and IQ6 and IQ6+ are Enphase inverters. Systems marked with an r are the same as the system above, only with reduced amounts of modules.

System	Module	# modules	# strings	modules per string	Inverter	# inverters	P_{nom} ratio
Building 1 and 1.2							
R1.1.1	CS6U-330P	24	1,1	10,14	SMA: 7kW	1	1.18,1.1
R1.2.1	CS6U-330P	24	1,1	10,14	SMA: 7kW + Tigo	1	1.18,1.1
R1.3.1	CS6U-330P	24	10,14	1,1	IQ6+	24	1.18
R1.1.2	CS6K-305MS	26	1,1	12,14	SMA: 7kW	1	1.31,1.02
R1.2.2	CS6K-305MS	26	1,1	12,14	SMA: 7kW + Tigo	1	1.31,1.02
R1.3.2	CS6K-305MS	26	12,14	1,1	IQ6	26	1.09
R1.1.3	FS-4120-3	63	3,4	9,9	SMA: 7kW	1	1.16,1.03
R1.1.4	SF170-S	42	3,4	6	SMA: 7kW	1	1.09,0.97
Building 2							
R2.1.1	CS6U-330P	43	2,1,1	9,15,10	SMA: 5kW, 7kW	1, 1	1.13-1.25
R2.1.1r	CS6U-330P	25	1,1	15,10	SMA: 7kW	1	1.18
R2.2.1	CS6U-330P	43	2,1,1	9,15,10	SMA: 5kW, 7kW + Tigo	1, 1	1.13-1.25
R2.3.1	CS6U-330P	43	43	1	IQ6+	43	1.18
R2.1.2	CS6K-305MS	45	2,1,1	10,14,11	SMA: 5kW, 7kW	1, 1	1.02-1.28
R2.1.2r	CS6K-305MS	25	1,1	14,11	SMA: 7kW	1	1.02,1.2
R2.2.2	CS6K-305MS	45	2,1,1	10,14,11	SMA: 5kW, 7kW + Tigo	1, 1	1.02-1.28
R2.3.2	CS6K-305MS	45	45	1	IQ6	45	1.33
R2.1.3	FS-4120-3	112	3,3,4,3	7,8,10,9	SMA: 5kW, 7kW	1,1	1.06-1.16
R2.1.4	SF170-S	74	2,2,4,3	8,8,6,6	SMA: 5kW, 7kW	1,1	0.97-1.14
Building 3							
R3.1.1	CS6U-330P	18	2	9	SMA: 5kW	1	1.13,1.25
R3.2.1	CS6U-330P	18	2	9	SMA: 5kW + Tigo	1	1.13,1.25
R3.3.1	CS6U-330P	18	18	1	IQ6+	18	1.18
R3.1.2	CS6K-305MS	20	2	10	SMA: 5kW	1	1.16,1.28
R3.2.2	CS6K-305MS	20	2	10	SMA: 5kW + Tigo	1	1.16,1.28
R3.3.2	CS6K-305MS	20	20	1	IQ6	20	1.33
R3.1.3	FS-4120-3	42	2,3	9,8	SMA: 5kW	1	0.91,1.1
R3.1.4	SF170-S	28	2,2	7,7	SMA: 5kW	1	0.91,1.0

Ground mounted system configurations

The ground mounted PV systems have a low shading factor and the same module tilt, orientation and alignment. The ground mounted systems were therefore only simulated with string inverters. The SMA Sunny Tripower 9000TL-20 inverter was used in all ground mounted simulations. Table 3.20 presents the ground mounted system configurations with different PV modules.

The number in the system name indicates the module used in the simulation. Systems G1, G2, G3 and G4 were simulated with, respectively, Canadian Solar CS6U-330P modules, Canadian Solar CS6K-305MS modules, First Solar FS-4120-3 modules and Solar Frontier FS170-S modules.

Table 3.20: Ground mounted system configurations used in the simulation.

System	Module	# modules	# rows	strings per row	modules per string	# inverters	P_{nom} ratio
G1	CS6U-330P	60	2	1,1	13,17	2	1.19,1.04
G2	CS6K-305MS	66	2	1,1	14,19	2	1.19,1.07
G3	FS-4120-3	160	2	4,6	8,8	2	1.07,1.07
G4	SF170-S	108	2	3,5	8,6	2	1.13,0.94

3.8 System losses

The system loss factors used in this thesis are listed in table 3.21. Both Enphase inverters and Tigo optimizers have PVsyst user guides with recommended system loss values [42, 44]. Therefore when *Tigo* or *Enphase* appears in the table, the specified value is used in combination with the inverter.

Table 3.21: System loss factors.

Parameter	Value	Explanation
Thermal loss factor (U-value)	Ground mounted: $U_c = 29$ [W/m^{2}K] $U_v = 0$ [W/m^{2}K/m/s] Roof mounted: $U_c = 20$ [W/m^{2}K] $U_v = 0$ [W/m^{2}K/m/s]	A ground mounted system is assumed to be free-standing, while a roof mounted system is assumed to be semi- - integrated with air ducts behind the module. The default values in PVsyst were used for both cases.
DC ohmic wiring loss	1% Enphase: 0%	Defined as a percentage ohmic loss at STC. According to the planning and installation manual for PV systems [14], a DC voltage drop of 1% is recommended for systems with an inverter operating at a higher DC input voltage (V_{mpp} >120 V). For PV systems with inverters operating with lower DC input voltage (V_{mpp} <120 V), a 2% voltage drop is recommended [14]. The IEC standard for ohmic losses is also 1% [11]. For Enphase module inverters, a DC ohmic loss of 0% and global wiring resistance of 0 mOhm is used, as the current is converted from DC to AC at the module.
AC ohmic wiring loss	1% Enphase: 1.75%	Defined as a percentage ohmic loss at STC. According to the planning and installation manual for PV systems [14], PV arrays are recommended to minimize the AC cable loss to a maximum of 1%. Enphase recommends an AC ohmic wiring loss of maximum 1.75% when using their module inverters [42].
Module quality loss	Default value	The module efficiency loss varies according to manufacturer's specification. It is set to *Default value*, as PVsyst then initializes the loss according to the PV module manufacturer's tolerance specification.

Light induced degradation loss	Crystalline modules: 2% Thin-film modules: 0%	According to the *Solar Energy* book [11] light induced degradation can cause a loss of 2 - 3% for crystalline modules. PVsyst states that LID can cause a reduction of 1 - 3%. The default value in Pvsyst of 2% is therefore used.
Module array mismatch loss	1% Tigo, Enphase: 0%	The default value in PVsyst is used for string inverters. The module mismatch loss is 0% for Tigo optimizers and Enphase module inverters.
Soiling loss	Jan 6% Feb 6% Mar 3% Apr 3% May 2% Jun 2% Jul 2% Aug 2% Sep 3% Oct 3% Nov 6% Dec 6% Enphase: Jan 4% Feb 4% Mar 1% Apr 1% May 0% Jun 0% Jul 0% Aug 0% Sep 1% Oct 1% Nov 4% Dec 4%	The site is located in a rural environment with some agricultural activity and many wine farms. The site is not located in a bird migration area and does not experience problems with bird droppings. The ground consists of sand. Periodic precipitation occurs during the winter months May - August. Many studies have been conducted regarding soiling losses, but they are site-specific. Average annual energy loss due to soiling in a normal location with sufficient tilt angle are typically in the range of 2 - 5% [14]. Monthly soiling rates of up to 11.5% in heavy agricultural areas in California have been observed [45]. A study in Italy concluded that a plant built on a sandy site had soiling loss of 6.9%, while a plant built on more compact ground has soiling loss of 1.1% [46]. Soiling losses of residential and commercial PV sites in California were studied during dry periods and the study found that daily soiling losses averaged 0.051% and 26% of the sites had daily losses greater than 0.1% [47]. A master's thesis on soiling effects in Kalkbult, South Africa, concluded that during the period were soling losses were most distinct, a soiling loss of 1% for poly Si modules was found [48]. The effect of soiling is reduced if the module is washed by rainwater. To achieve this, the tilt angle should be at least 19°[14]. Lower tilt angles have higher accumulation of dust. If a system is heavily affected by soiling regular cleaning of the modules will increase the power yield. Summer months have less periodic rainfall and coincides with harvest season, but have higher wind speeds. Winter months have periodic rainfall, but lower wind speeds. Soiling losses are therefore assumed to be slightly higher in November - February. As module inverters maximizes the performance of each individual module independently, some of the soiling loss is mitigated, compared to a string inverter. Enphase recommends an adjusted soiling loss according to their table of soiling loss changes [42].
Incidence Angle Modifier	$b_0 = 0.05$	The default value in PVsyst is used.

Ageing loss	Avg. degradation: 0.4%/year I_{SC} dispersion RMS: 0.4%/year V_{OC} dispersion RMS: 0.4%/year	The default values in PVsyst are used.
	Tigo, Enphase: I_{SC} dispersion RMS: 0%/year V_{OC} dispersion RMS: 0%/year	When using Tigo optimizers and Enphase module inverters, the mismatch loss over the lifetime of the system is 0%. The I_{SC} dispersion RMS and V_{OC} dispersion RMS are therefore set to 0%. Only the ageing loss of the first production year is used in the simulation.
Unavailability	Fraction: 2% Duration: 7.3 days/yr Periods: 3	Difficult to predict. The South African power grid has been unreliable in the past, and Panthera Africa have experienced some yearly outages. There have been no outages during the last year. Due to uncertainty in the grid reliability and possible PV system failure, the default unavailability time fraction value in PVsyst is used. The unavailability periods are set at random by PVsyst, due to no knowledge of when they can occur.
Light soaking effect	2%	The default value in PVsyst is used.

3.9 Sensitivity analysis

Uncertainties in system loss factors and meteorological data may influence system performance. To investigate the actual performance impact, a sensitivity analysis on such factors may be performed. In this section a sensitivity analysis is performed on the meteorological data and soiling losses. All system values and settings, except for the sensitivity parameter, were kept the same as in the main simulation.

3.9.1 Irradiation data sensitivity

It is difficult to determine which meteorological dataset gives the most realistic picture of the climatic situation at the site. To investigate the impact of different irradiation values, simulations using the three datasets mentioned in subsection 3.3.4 were carried out.

The three datasets consists of the highest yield, and average yield and the most conservative yield. *Dataset 2* has the average yield and is used in the main simulation. *Dataset 1* has the highest yield and *Dataset 3* has the lowest yield. All datasets have irradiation data from databases and wind velocity and temperature data from Stanford weather station.

3.9.2 Soiling loss sensitivity

Soiling losses are site specific and difficult to correctly predict. The soiling losses used in the main simulation are based on the explanation listed in table 3.21. The actual losses

may differ from the stated soiling losses. To explore the PV system's sensitivity to soiling losses, the three cases listed in table 3.22 were used in the sensitivity analysis. *Soiling Case 1* is a minimum of 0% soiling loss each month and *Soiling Case 3* is a maximum of 6% soiling loss each month. *Soiling Case 2* has a monthly soiling loss 2% lower than the main simulation.

Table 3.22: Monthy soiling loss parameters used in the sensitivity analysis.

	Jan [%]	Feb [%]	Mar [%]	Apr [%]	May [%]	Jun [%]	Jul [%]	Aug [%]	Sep [%]	Oct [%]	Nov [%]	Dec [%]
Soiling Case 1	0	0	0	0	0	0	0	0	0	0	0	0
Soiling Case 2	4	4	1	1	0	0	0	0	1	1	4	4
Soiling Case 3	6	6	6	6	6	6	6	6	6	6	6	6

3.9.3 Thermal parameter sensitivity

As Panthera Africa is located in a warm climate, the effect of the thermal parameter on PV system performance may have a large impact. The thermal parameter used in the main simulation is the default parameter suggested by PVsyst. To analyze the PV system's sensitivity to changes in the U-value, the two cases listed in table 3.23 were used in the sensitivity analysis.

Table 3.23: Thermal parameters used in the sensitivity analysis.

	Roof mounted	Ground mounted
U-value Case 1	$U_c = 15$, $U_v = 0$	$U_c = 20$, $U_v = 0$
U-value Case 2	$U_c = 29$, $U_v = 0$	$U_c = 30.7$, $U_v = 0$

3.9.4 Ageing sensitivity

The main simulation only simulates the ageing loss for the first year. As the ageing loss is a progressive loss, a further analysis of the decrease in system performance over time due to ageing loss was carried out. The ageing losses used in the main simulation were used to explore the progressive losses from production year 1 to production year 20.

The impact of different degradation rates on the system and the resulting degradation losses were explored. The different degradation rates used in the analysis were 0.2%/year, 0.5%/year and 0.7%/year.

3.9.5 Ground mounted orientation sensitivity

When changing the inter-row spacing between rows of ground mounted modules, the mutual shading between the rows are changed. A change in mutual shading results in a change in near shading loss due to irradiance and electrical losses, thus affecting the

system performance. Inter-row spacings ranging from 7.2 m to 3.4 m were used in the sensitivity analysis. The effect of inter-row spacing on system performance was carreid out for system G1.1 and G2.1.

As the ground mounted systems were simulated with an azimuth angle of 0°, an exploration of the effect of changing the azimuth angle was done. The available ground area is oriented at 18°, so this azimuth angle was used in the sensitivity analysis.

3.10 Economical evaluation

An economical evaluation of the PV systems were performed, where the payback time, net present value and levelized cost of electricity were calculated for the PV systems. South Africa uses rand (R) as their currency. All prices in the economical evaluation are given in rand, and the exchange rates listed in appendix C table C.1 were used.

In order to calculate the investment cost for a PV system, information about component prices, application fees and installation cost are needed. Several PV system consultant companies in South Africa were contacted regarding component prices. Solareff, one of the contacted companies, provided information about the cost of a 13.2 kWp PV system and individual component costs.

South Africa has several internet based PV component suppliers. The following suppliers were consulted regarding component prices: *Sunflare Renewable Systems* [49], *Sustainable* [50] and *GW store* [51]. When comparing the component prices from Solareff and internet suppliers, the internet suppliers have about 20% - 25% higher component prices.

When calculating the LCoE, NPV and payback time, the following assumptions and simplifications were made:

- Costs for other BoS component costs were assumed to be equal for all systems, as they all are of similar sizes.
- The installation and cabling costs were assumed to be independent on inverter type and only dependent on the kWp of installed capacity.
- The inverter must be replaced once in the lifetime of the system. Inverter lifetime is in this thesis assumed to be 15 years [52].
- The investment cost is paid upfront, so no loan payments.
- No increase in electricity prices or prices for selling electricity to the utility.
- No increase in consumption.
- The cost of replacing the inverters is equal to the current cost of the inverter. The cost is divided equally over the first 15 years, as the inverter has to be replaced after 15 years.

The system component costs used in the economical evaluation are given in appendix C table C.2. All costs, except for invreters, modules and the roof mounted structure, are

from Solareff. All costs in the table that are given in R/kWp were assumed to be in R/kWp, as the costs from Solareff were given as unit prices in R.

The financial assumptions listed in table 3.25 were used when calculating the NPV, LCoE and payback time. Note that the investment support is not used when calculating the LCoE. As the calculation of the NPV and payback time includes electricity cost savings as a cash inflow, the utility prices for Panthera Africa are listed in table 3.24. Panthera Africa has Eskom as their utility company and is currently on the tariff *Landrate 1,2,3*. The prices are for 2017/2018 and they are excluding VAT. Note that the *standard connection charge*, *service and administration charge* and *network capacity carge* are costs for being connected to the grid. They will therefore not be included when calculating the electricity cost savings. Eskom does not have a feed-in-tariff at the moment, but Overstrand Municipality, which Panthera Africa is located in, has the feed-in-tariff listed in table 3.24. This feed-in-tariff will be used for calculating the utility value for the exported energy. The operation and maintenance values mentioned in table 3.25 are calculated from dollars to rand by use of the dollar exchange rate listed in table C.1.

Table 3.24: Utility prices at Landrate 1,2,3 and feed-in-tariff. Utility prices are from Eskom [53] and Panthera Africa's energy bills. The feed-in-tariff is from Overstrand Municipality [54].

Utility charge type	Charge unit	Charge rate
Standard Connection Charge	R/month	90
Service and Administration Charge	R/day	21.03
Network Capacity Charge	R/day	38.93
Network Demand Charge	R/kWh	0.2369
Ancillary Service Charge	R/kWh	0.0037
Energy Charge	R/kWh	0.9483
SSEG feed-in-tariff	R/kWh	0.5724

Table 3.25: Financial assumptions for the economical evaluation.

Input parameter	Symbol [unit]	Value	Explanation
System lifetime	T [years]	25	The key component of the PV system is the module, which has a warranty of 25 years. The system lifetime is assumed to be equal to the module lifetime. The International Energy Agency (IEA) also assumes a PV system lifetime of 25 years [28].
Discount rate	r [%]	7	The discount rate reflects the risk and uncertainty of the project and is assumed to not vary during the lifetime of the project. The International Energy Agency (IEA) assumes discount rates between 3% and 10% with an average of 7% [28]. A discount rate of 7% corresponds to the market rate in deregulated or restructured markets, while a rate of 10 % corresponds to investments in a high-risk market [28].
Degradation rate	d [%/year]	0.4	Several studies have explored the degradation rate for actual in-field PV systems, with values in the range of 0.2% - 0.75% [52, 55, 56]. The National Renewable Energy Laboratory (NREL) has published several articles regarding degradation rates for outdoor modules and systems [57, 58]. Both articles shows a median degradation value of 0.5% for both Si and thin-film technology. The study [58] also indicates that outdoor exposure length influences the degradation length. Modules exposed 10 years or longer has a lower degradation rate than modules exposed up to 10 years. A degradation rate of 0.4%/year was used in the main simulation, and is therefore used here as well.
Residual value	RV [%]	10	The residual value is the scrape value of the PV system components that needs to be replaces either during or after the lifetime of the system. There are few studies estimating the residual value of PV system components. In two different studies, IEA estimated a value of 10% and 20% of the investment cost [28, 59]. As there are few studies confirming this value, the most conservative value of 10 % was used.
Operation and maintenance	O_t [R/kW]	260	NREL estimated in 2016 an operation and maintenance cost of 248 $\pm$ 236 R/kW for systems less than 10 kW in size and 224 $\pm$ 212 R/kW for systems of sizes 10 - 100 kW [60]. In a solar PV system cost report published in 2017 by NREL, they used an operation and maintenance cost of 248 R/kW for residential systems and 177 R/kW for commercial systems [52]. A report by Stefan Reichelstein and Michael Yorston published operation and maintenance costs of 271 R/kW for Si modules and 354 R/kW for thin film modules [61]. The report was based on commercial PV systems. The Electric Power Research Institute (EPRI) assumes an annual operation and maintenance cost of 236 - 260 R/kW [29].
Decommissioning	D_t [R/kW]	0	Assumes that equipment will be replaced at the end of its lifetime, so the decommissioning cost is zero. This assumption was made based on a lack of information and articles regarding decommissioning costs for residential PV systems.
Investment support	[%/capital cost]	28	The South African revenue service (SARS) allows business owners to deduct the value of new PV systems as a depreciation expense from their business income tax in the first year. As businesses pays a commercial tax of 28%, the depreciation tax of the system is 28% of the capital value.

Chapter 4
Simulation results and discussion

This chapter presents and discusses the results from the base case simulation, the sensitivity analysis and the economical evaluation.

When performing a simulation, PVsyst produces a six page report containing the system configuration and simulation results. PVsyst calculates the losses mentioned in subsection 3.1.2, and shows them in a loss diagram as illustrated in figure 4.1. The upper part of the diagram are optical losses, the middle part are array losses, and lower part are system losses.

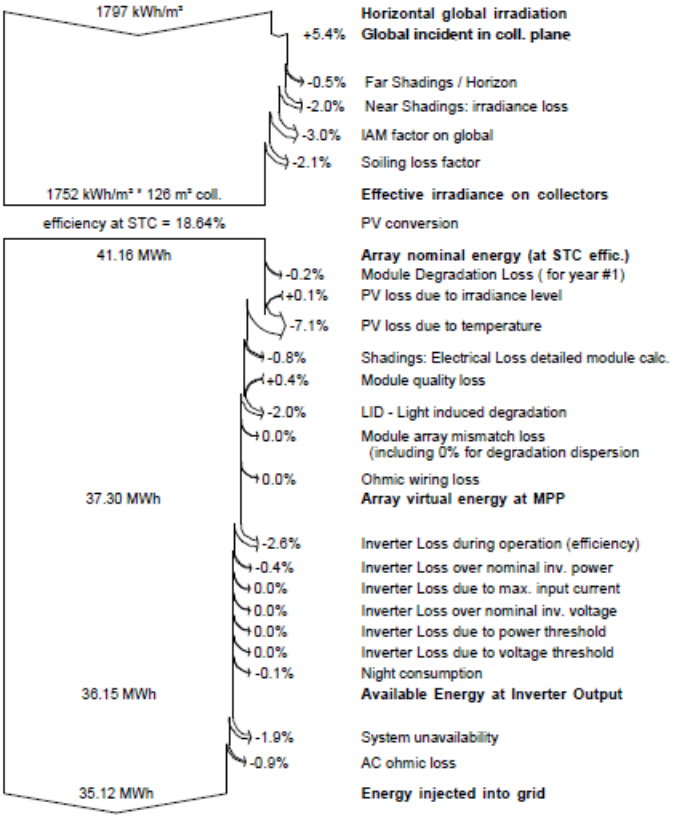

Figure 4.1: Loss diagram from a PVsyst report.

4.1 Base case simulation

This section presents the simulation results and discussion regarding the roof and ground mounted system configurations listed, respectively, in table 3.19 and table 3.20. The presented losses are the largest and those who varies the most between systems.

The optical losses are site specific and depend on the climate and building orientation. Table 4.1 present the optical losses for the buildings and ground systems. The presented horizon and near shading losses vary by 0.1% to 0.2% for building 1 and 1.2, as they are simulated together. Systems with Enphase inverters have a 2% lower soiling loss than the stated value, as they are simulated with a 2% lower soiling loss. The global incident irradiation (GIR) in the collector plane is the actual irradiation reaching the module and depends on the roof orientation.

Table 4.1: Optical losses for the buildings and ground systems. The losses are site specific.

	GIR [kWh/m^2]	Horizon loss [%]	Near shading loss [%]	IAM loss [%]	Soiling loss [%]
Building 1 and 1.2	1928	0.5	4.6	2.8	4.0
Building 2	1797	0.2	0.7	3.6	4.2
Building 3	2033	0.8	4.8	2.2	3.9
Ground systems	2057	1.0	1.2	2.6	3.9

4.1.1 Roof mounted system results

The simulation results for the roof systems presented in table 3.19 are given in table D.1 in appendix D. As the simulation results for the individual buildings did not yield the required energy amount of about 30-35 MWh, combinations of the individual systems were put together. When choosing the combinations only the same module type and inverter type were used in a system. Ideally it would be optimal to combine the best performing systems, regardless of inverter type. However, this was not done in this Master's thesis as it is currently not possible, in PVsyst, to simulate a complete system with different inverter types. For the combinations, either building 1, 1.2 or 3 were excluded, or the module area of building 2 was reduced. A number of scenarios were simulated, and the best performing system combinations for each module and inverter combination are presented in table 4.2. A "m" indicates that building 1.2 was excluded.

Table 4.2: Roof mounted system combinations and results. The first number in the system name indicates the building, the second number indicates the inverter type and the last number indicates the module type. An explanation of the numbers are given in subsection 3.7.4.

System combination			System yield [kWh]	Specific yield [kWh/kWp]	PR [%]	Efficiency loss temp. [%]	Electrical loss [%]	Inverter loss [%]	Unavailability loss [%]
R1.1.1	R2.1.1r	R3.1.1	31440	1422	74.6	7.5	1.6	3.0	1.3
R1.2.1	R2.2.1r	R3.2.1	31667	1432	75.1	7.5	1.0	3.0	1.6
R1.3.1m	R2.3.1	R3.3.1	34620	1478	78.2	7.6	0.8	3.3	1.3
R1.1.2	R2.1.2r	R3.1.2	31260	1444	75.4	6.9	1.6	3.2	1.3
R1.2.2	R2.2.2r	R3.2.2	31504	1455	76.0	6.9	1.0	3.2	1.5
R1.3.2m	R2.3.2	R3.3.2	35120	1496	79.0	7.1	0.8	3.1	1.9
R1.1.3	R2.1.3	R3.1.3	38401	1475	78.4	5.4	-	2.6	1.9
R1.1.4	R2.1.4	R3.1.4	37499	1532	81.4	5.9	-	2.6	1.3

The *Efficiency loss temp.* in table 4.2 is module loss due to reduced efficiency when operating at temperatures different than STC conditions. The loss depends on the chosen thermal parameter (U-value), meteorological data and module specifications. It was only possible to simulate thin-film modules with *Linear shading* for near shading objects, which is why they are listed without electrical losses in table 4.2.

The best performing crystalline and thin-film system were, respectively, system R1.3.2m R2.3.2 R3.3.2 and system R1.1.4 R2.1.4 R3.1.4. The monthly normalized production and PR for both systems are shown in figure 4.2. In the normalized production figures, the purple parts are array losses, the green parts are system losses and the red parts are the output energy of the system. The loss diagram for system R1.3.2m R2.3.2 R3.3.2 is shown in figure 4.1.

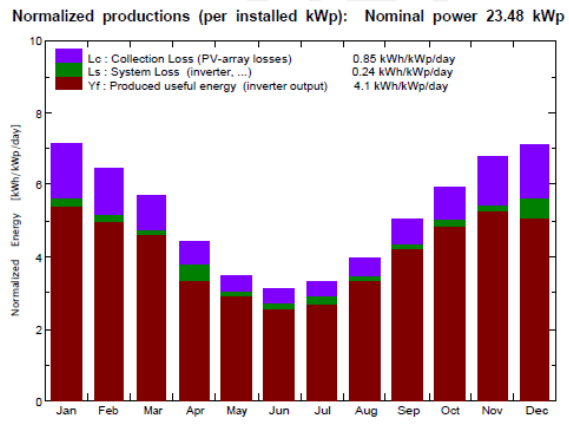

(a) System R1.3.2m R2.3.2 R3.3.2.

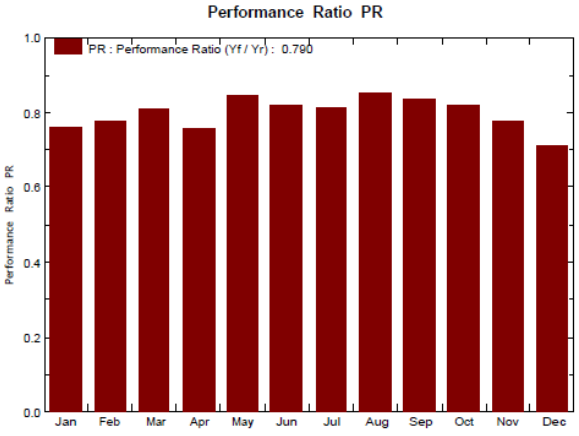

(b) System R1.3.2m R2.3.2 R3.3.2.

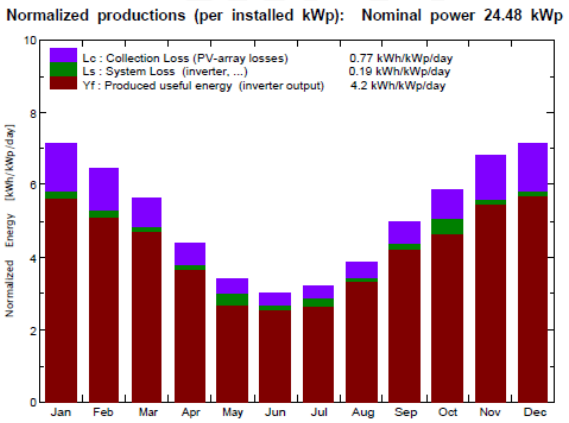

(c) System R1.1.4 R2.1.4 R3.1.4.

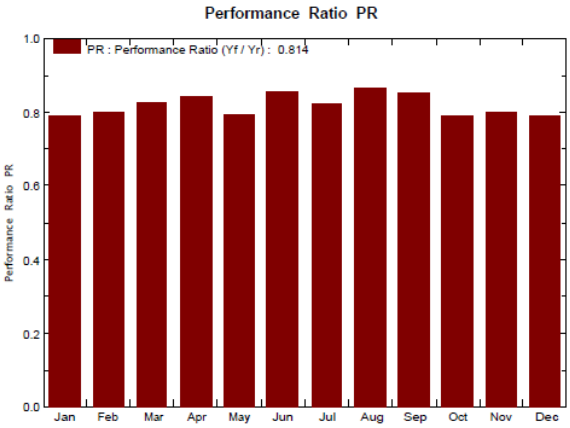

(d) System R1.1.4 R2.1.4 R3.1.4.

Figure 4.2: Normalized production (a), (c) and PR (b), (d) for system R1.3.2m R2.3.2 R3.3.2 and system R1.1.4 R2.1.4 R3.1.4.

Module layout

The module layout was only designed for crystalline modules, not for thin-film modules, since this implementation in the current version of PVsyst only were available for

crystalline modules. As the module types are of different sizes, the string design for each building is presented for each module type. Figure 4.3 shows the module layout for CS6U-330P modules, figure 4.4 shows the module layout for CS6K-305MS modules and figure 4.5 presents the suggested module layout for SF-170S modules. Each color in the figures represents a different string.

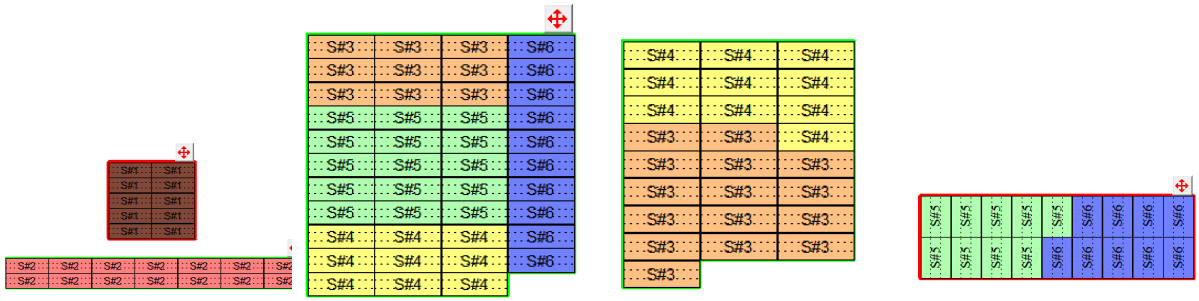

(a) Building 1 and 1.2 (b) Building 2 (c) Building 2r (d) Building 3

Figure 4.3: String configuration for each building when simulating with CS6U-330P modules.

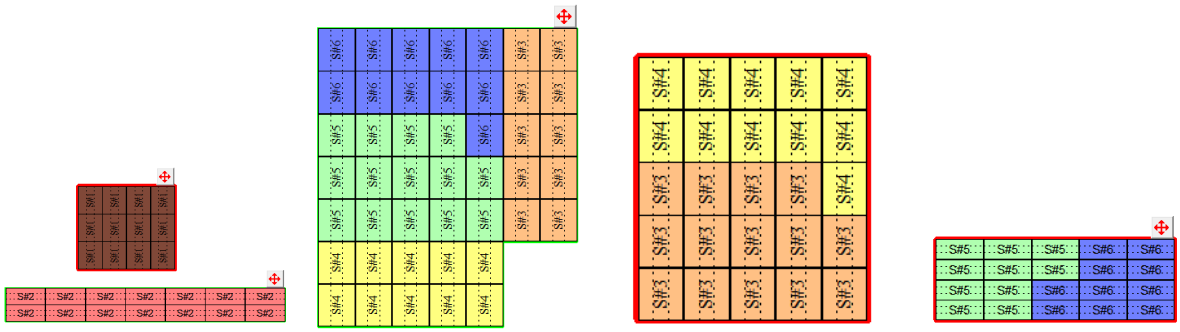

(a) Building 1 and 1.2 (b) Building 2 (c) Building 2r (d) Building 3

Figure 4.4: String configuration for each building when simulating with CS6K-305MS modules.

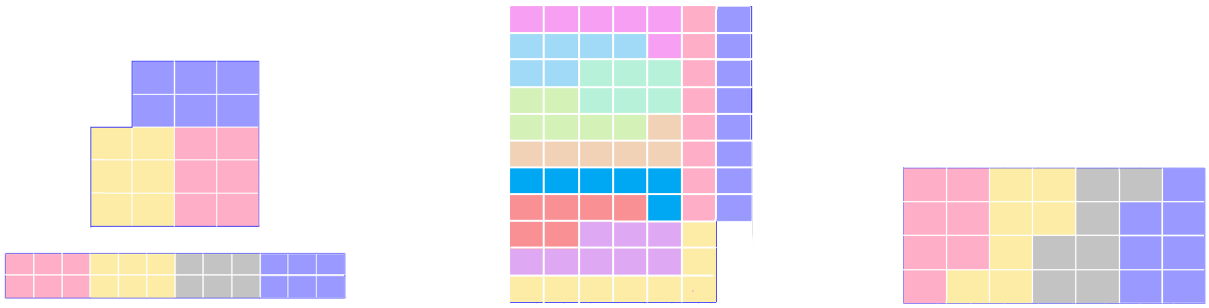

(a) Building 1 and 1.2 (b) Building 2 (c) Building 3

Figure 4.5: String configuration for each building when simulating with SF170-S modules.

4.1.2 Ground mounted system results

Table 4.3 shows the simulation results for the ground mounted systems. The best performing crystalline and thin-film system were, respectively, system G2 and system G4. The monthly normalized production and PR for both systems are shown in figure 4.6.

Table 4.3: Ground mounted system results. The number in the system name indicates the PV module used in the simulation. An explanation of the numbers are given in subsection 3.7.4.

System	System yield [kWh]	Specific yield [kWh/kWp]	PR [%]	Efficiency loss temp. [%]	Electrical loss [%]	Inverter loss [%]	Unavailability loss [%]
G1	32360	1634	79.5	4.8	0.1	2.6	1.9
G2	33230	1651	80.3	4.4	0.1	2.7	1.9
G3	32213	1678	81.6	3.5	-	2.5	1.7
G4	31797	1732	84.2	3.9	-	2.6	1.9

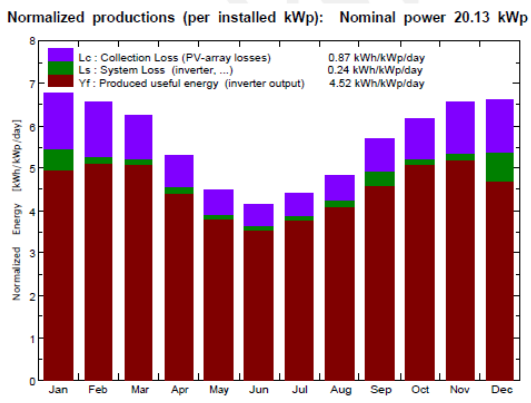

(a) System G2.

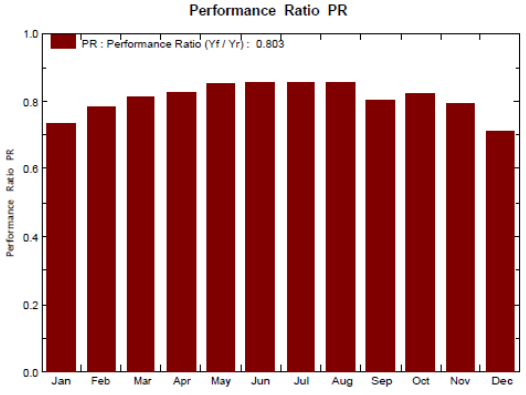

(b) System G2.

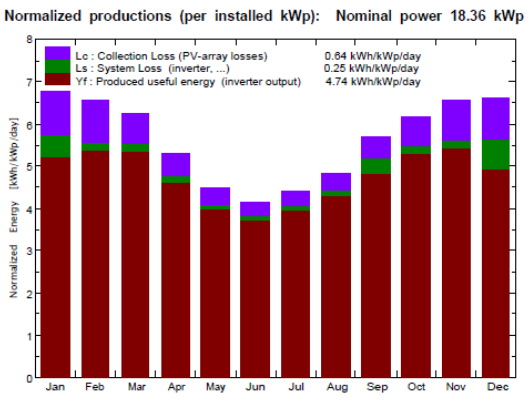

(c) System G4.

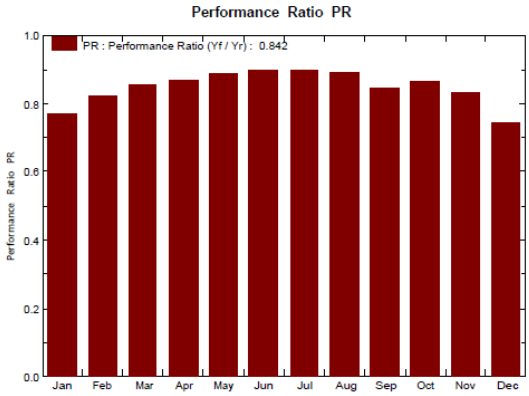

(d) System G4.

Figure 4.6: Normalized production (a), (c) and PR (b), (d) for system G2 and system G4.

Module layout

Each string was designed to minimize shading loss and optimize energy production. Figure 4.7a shows the module layout for Canadian Solar CS6U-330P modules and figure 4.7b shows the module layout for Canadian Solar CS6K-305MS modules. Figure 4.7c presents the suggested module layout for First Solar FS-4120-3 modules and figure 4.7d shows the suggested module layout for SF-170S modules.

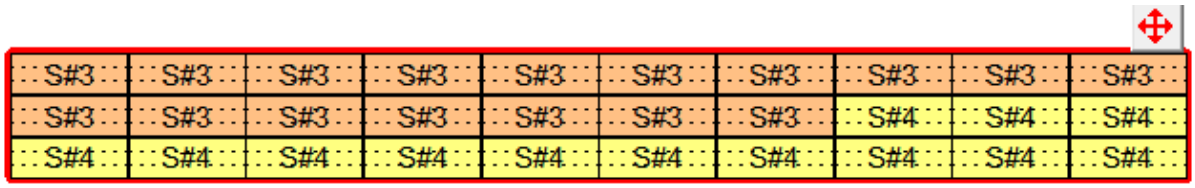

(a) CS6U-330P module.

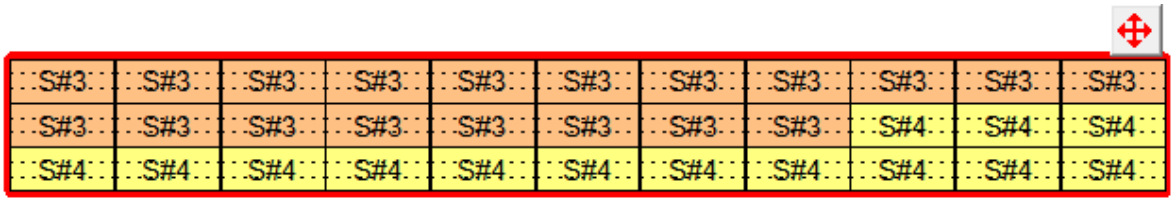

(b) CS6K-305MS module.

(c) FS-4120-3 module.

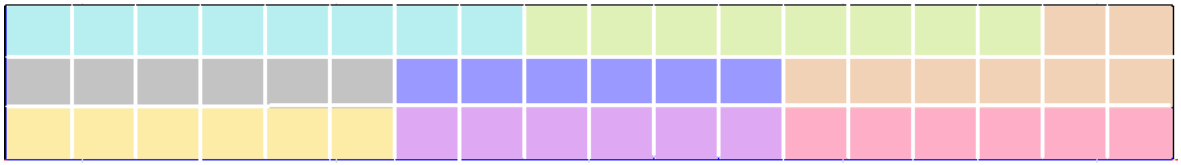

(d) SF170-S module.

Figure 4.7: String configuration for each row of a ground mounted system.

4.1.3 Discussion

Soiling loss and near shading irradiance loss were the largest optical losses, as shown in table 4.1. The array and system losses that had the greatest effect on system performance were inverter loss, efficiency loss due to temperatures different from STC and unavailability loss, as seen in table 4.2 and 4.3.

The module performance at high temperatures depends on the thermal loss factor (U-value) of the system and the temperature behavior of the PV module. Ground mounted,

free-standing systems, have a lower efficiency loss due to temperature than roof mounted systems. This is expected, as the specified U-value in table 3.21 for ground and roof mounted systems are different and reflects how well ventilated the system is. The module performance at high temperatures vary between the different module types, depending on the power temperature coefficient specified by the manufacturer. The thin-film modules perform better in high temperature conditions, which is expected, as they have lower power temperature coefficients than crystalline modules. The First Solar module shows the best performance regarding changes in temperature, having an efficiency loss of about 3.5% for the ground mounted system and 5.4% for the roof mounted system. The effect of the U-value on system performance was further analyzed in the sensitivity analysis.

The efficiency loss/gain due to irradiance levels different from STC depends on the module characteristics and the irradiance intensity. The efficiency behavior at different irradiance levels in PVsyst is an application of the one-diode model, with the specified shunt and series resistance (R_{sh} and R_s) of the module. R_{sh} increases exponentially with decreasing irradiance. A lower shunt resistance at STC, results in higher module efficiency at low irradiance levels. R_s increases with power. A higher R_s at STC, results in higher module efficiency at low irradiance levels. Thus, modules with low R_{sh} and high R_s performs better under low irradiance conditions, compared to STC. The Solar Frontier module showed a 0.2% gain in efficiency due to irradiance levels different than STC. This may be due to the combination of a lower shunt resistance and higher series resistance. The First Solar module, on the other hand, had a loss between 2.2% and 2.7% in efficiency. The higher loss of the First Solar module may be due to its high R_{sh} of 3500 Ω compared to the other modules, which ranged from 350 Ω to 630 Ω. The Canadian Solar mono-crystalline module had a gain of 0.1%, while the poly-crystalline module had a loss between 0.5% and 0.7%.

The inverter loss ranged from 2.5% to 3.2% for the different systems. Ground mounted systems had a slightly lower inverter loss than roof mounted systems. Of the total inverter loss listed in table 4.2 and 4.3, most of it was efficiency loss during normal operation. The module inverters had, in addition, a 0.4% inverter loss over nominal power and a 0.1% night consumption loss. All the systems with thin-film modules had a 0.1% inverter loss due to power threshold.

All the modules had a positive module quality loss ranging from 0.4% for the Canadian Solar modules to 1.1% for the First Solar module. A positive module quality loss result in a power gain, which can be explained by the modules positive tolerance. For string inverters the modules in a string is limited by the weakest module, regardless of the power gain. When using optimizers or module inverters, the power gain for each module results in a higher power.

Systems with string inverters were simulated with both a DC and AC ohmic wiring loss of 1%. The losses are applicable at STC conditions and the simulated output values were slightly lower than the pre-set values. As the current in the cables will normally be lower than at STC conditions, this is expected. DC losses varied marginally from 0.6% to 0.7%

and the AC ohmic losses varied marginally from 0.5% to 0.6%. The slight variation is likely due to minor rounding errors in the simulation. Systems with module inverters were simulated with a DC ohmic loss of 0% and an AC ohmic loss of 1.75%. The output AC losses were 0.9%.

Unavailability loss should reflect the expected time period of system downtime due to maintenance or system failure. The default value for system unavailability was used in the simulation and the unavailable days were chosen randomly by PVsyst. The energy loss due to unavailability is dependent on the season and the weather during the season [19]. System failure occurring during summer will result in higher unavailability loss compared to the same situation in the winter, due to higher irradiation in the summer. Thus, the unavailability loss varied from 1.2% to 1.9%.

The soiling loss was 3.9% for ground mounted systems and 4.1% for roof mounted systems. Systems with module inverters had a 2% lower soiling loss than the stated value, which was expected, as they were simulated with a 2% lower soiling loss. The lower soiling loss was specified based on a recommendation from Enphase (the module inverter manufacturer). A lower soiling loss for optimizers could also have been considered, as both module inverters and optimizers maximizes the power of each module, thus reducing the effect of uneven soiling on the string. One of the reasons why module inverters had a better performance ratio than optimizers, may be due to the fact that they were simulated with a lower soiling loss value. This will be further explored in the soiling loss sensitivity analysis.

The near shading loss is irradiance loss due to near shading objects. It varied from 2% to 3.3% for the roof mounted systems listed in table 4.2. As seen in table 4.1, the different buildings had different near shading losses. The irradiance loss therefore varied depending on the amount of modules placed each the building and the module size. The ground mounted systems had a near shading loss of 2.6%, mainly due to mutual shading between the rows.

The irradiance losses due to near shading objects were calculated according to the 3D near shading scene defined in PVsyst. The loss depends on the specific objects in the model and their placing. The object dimensions and placing were measured using Google Earth, a measuring tape and a phone app measuring objecy heights. As there are many uncertainties related to the measurement methods, the dimensions and placings may vary from real life. Trees are modeled as solid objects in the 3D scene, when in real life they have branches that sunlight can penetrate through. The shading on building 3 is mainly due to trees, so there are uncertainties connected to the amount this shading.

The ground mounted systems had the lowest electrical losses due to shading. This was expected, as the inter-row spacings and string designs were optimized to reduce the amount of electrical and near shading losses. The effect of inter-row spacing on electrical and irradiance losses were further analyzed in the sensitivity analysis.

The roof mounted systems were simulated with string inverters, optimizers and module

inverters to analyze the effect of shading the PV system. Electrical losses with string inverters were 1.6%, with optimizers 1.0% and with module inverters 0.8%. Systems with module inverters showed the highest increase in performance and the largest reduction in electrical losses. There was only a slight increase in performance when using optimizers. As mentioned above, one of the reasons why module inverters performed better than optimizers may be due to the fact that they were simulated with different soiling losses. The optimizers had an additional efficiency loss of 0.6% - 0.7%, which is equal to the reduction in electrical losses. The reason that optimizers, in spite of this, performed better than string inverters may be due to the fact that they were simulated with a 0% mismatch loss. In the simulations with optimizers, all modules had to have an optimizer in PVsyst. In real life, only the modules affected by shading need to have an optimizer. Therefore, compared to the simulations, it's possible to reduce the amount of optimizers and thus the efficiency loss of the optimizers.

Thin-film modules were simulated with linear shading losses in PVsyst, meaning only irradiance loss due to shading were considered. As mentioned under *PV module technology* in subsection 2.2.2, thin-film modules have a linear shading loss if oriented properly. If the shading is perpendicular to the module cells, the shading loss is linear. If, in addition, the shading on each module in a string is equal, there are no mismatch losses in the string. For the ground mounted systems, a linear shading loss may therefore be a correct assumption. For the roof mounted systems, it is difficult to orient the modules to reduce shading, as the shading varies during the day. The assumption of no electrical losses on the roof systems due to shading may therefore give a slightly better performance than in real life.

The yearly average PR ranges from 79.5% to 84.2% for ground mounted systems and from 74.6% to 81.4% for roof mounted systems. The greater variation in PR for roof mounted systems is mainly due to larger differences in efficiency loss due to temperatures different from STC, electrical losses and inverter losses. For ground mounted systems, the performance ratio is higher during winter months than during summer months, as can be observed in figure 4.6b and 4.6d. This is expected as winter months have lower temperatures and soiling, resulting in lower losses. The normalized production for each month seen in figure 4.6a and 4.6c shows the array and system losses. Both losses are lower during winter months and increase during summer months. The array losses increases significantly during summer months, as it includes the efficiency loss due to temperature. A marked increase in system losses can be observed in January, September and December, which corresponds to the unavailability periods. For the roof mounted systems, the PR varies more throughout the year. As seen in figure 4.2d, system R1.1.4 R2.1.4 R3.1.4 has a dip in performance ratio in May, June and October. These dips corresponds to months with unavailability periods. The same applies to the system R1.3.2m R2.3.2 R3.3.2, which has dips in PR in April, June and December.

All the best performing systems consists of thin-film modules. They have a lower efficiency loss due to temperature, a slightly lower inverter loss and does also not have a light induced degradation loss of 2%, as the crystalline modules have. Of the two thin-film modules,

the Solar Frontier module has the best performance ratio in all simulations. The First Solar module has a lower efficiency loss due to temperature, but a higher efficiency loss due to irradiance. The Solar Frontier module has an efficiency gain of 2% due to the light soaking effect. The light soaking effect is set as a default in PVsyst, which is according to the manufacturer's specification. According to PVsyst, the light soaking gain increases progressively with exposure to the sun; stabilizing at default value after several hundreds of hours of sun exposure [19]. This means that a simulation based on a default value of 2% gain, will have a certain time period with deviations from this value. Depending on this time period and the deviation from the default value, the effect on the simulations can be either of minor or major importance. Solar Frontier states on their website that the light soaking effect for their modules stabilizes after 50 hours of sunshine, meaning the 2% value is valid for the first year production [62]. Of the Canadian Solar modules, the mono-crystalline module performed slightly better than the poly-crystalline module.

It is worth noting that the best performing system may not be the best choice from a cost/benefit perspective. The cost of each system needs to be analyzed in an economical evaluation before deciding on the overall best alternative. When selecting a system it is a weighted optimization of both performance and cost.

4.2 Irradiation data sensitivity

Table 4.4 compares the performance of the systems for constant system parameters, only changing the meteorological dataset. Therefore, the yield difference is the difference in energy produced by the system when the meteorological dataset is changed. Dataset 1 had the highest yield and Dataset 3 has the most conservative yield.

Table 4.4: Simulation result from irradiance data sensitivity analysis. Dataset 2 was used in the main simulation.

System			Main dataset		Dataset 1			Dataset 3		
			Yield [kWh]	PR [%]	Yield [kWh]	PR [%]	Yield diff. [%]	Yield [kWh]	PR [%]	Yield diff. [%]
R1.1.1	R2.1.1r	R3.1.1	31440	74.6	32422	74.4	3.1	29888	74.6	-4.9
R1.2.1	R2.2.1r	R3.2.1	31667	75.1	32694	75.0	3.2	30068	75.0	-5.1
R1.3.1m	R2.3.1	R3.3.1	34620	78.2	35652	78	3.0	32786	78	-5.3
R1.1.2	R2.1.2r	R3.1.2	31260	75.4	32237	75.3	3.1	29720	75.5	-4.9
R1.2.2	R2.2.2r	R3.2.2	31504	76.0	32562	76.0	3.4	29946	76.0	-4.9
R1.3.2m	R2.3.2	R3.3.2	35120	79	36264	78.9	3.3	33410	79.1	-4.9
R1.1.3	R2.1.3	R3.1.3	38401	78.4	39899	78.9	3.9	36594	78.6	-4.7
R1.1.4	R2.1.4	R3.1.4	37499	81.4	38689	81.3	3.2	35618	81.4	-5.0
G1			32360	79.5	33319	79.1	3.0	30647	79.4	-5.3
G2			33230	80.3	34205	79.9	2.9	31479	80.2	-5.3
G3			32213	81.6	33274	81.5	3.3	30521	81.5	-5.3
G4			31792	84.2	32746	83.9	3.0	30099	84.1	-5.3

4.2.1 Discussion

As seen in table 4.4, the choice of dataset affects the performance of the systems. The yield increased about 3.0% when using Dataset 1, and decreased about 5% when using Dataset 3. The difference in system yield could have a great effect on the economy of the system, as the electricity produced is a factor when calculating the levelized cost of electricity, payback time and net present value.

The yield differences should be the same for systems having the same orientation, as systems having the same orientation receives the same irradiation amount. The yield difference for systems having the same orientation is more similar for Dataset 3 than Dataset 1. The slight variations observed may be due to minor rounding errors in the simulation.

The performance ratio for each system remains almost the same when simulating with different irradiation data. This is expected, as the PR is independent from irradiation data. Both wind and temperature data are the same for all the datasets, only the irradiation is different. Had the temperatures and wind data differed between the datasets, it would influence the efficiency of the PV modules, and thus affect the PR.

4.3 Soiling loss sensitivity

Table 4.5 compares the performance of the systems when keeping all system parameters constant and only changing the soiling loss. The yield difference is the difference in energy produced by the system when the soiling data is changed. The three soiling cases mentioned in subsection 3.9.2 were used. Soiling Case 2 has the same soiling parameters used for the module inverters in the main simulation.

Table 4.5: Simulation result from soiling loss sensitivity analysis.

System			Main soiling		Soiling Case 1		Soiling Case 2		Soiling Case 3	
			Yield [kWh]	PR [%]	PR [%]	Yield diff. [%]	PR [%]	Yield diff. [%]	PR [%]	Yield diff. [%]
R1.1.1	R2.1.1r	R3.1.1	31440	74.6	77.3	3.7	75.9	1.9	73.2	-1.9
R1.2.1	R2.2.1r	R3.2.1	31667	75.1	77.9	3.7	76.5	1.9	73.7	-1.9
R1.3.1m	R2.3.1	R3.3.1	34620	78.2	79.7	1.9	78.2	0.0	75.3	-3.7
R1.1.2	R2.1.2r	R3.1.2	31260	75.4	78.2	3.6	76.8	1.8	74.0	-1.9
R1.2.2	R2.2.2r	R3.2.2	31504	76.0	78.8	3.7	77.4	1.9	74.6	-1.9
R1.3.2m	R2.3.2	R3.3.2	35120	79.0	80.2	1.6	79.0	0.0	76.2	-3.5
R1.1.3	R2.1.3	R3.1.3	38401	78.4	81.6	4.1	80.0	2.0	76.9	-1.9
R1.1.4	R2.1.4	R3.1.4	37499	81.4	84.6	3.9	83.0	1.9	79.9	-1.9
G1			32360	79.5	82.3	3.6	81.0	1.9	77.8	-2.1
G2			33230	80.3	83.1	3.6	81.8	1.9	78.6	-2.1
G3			32213	81.6	84.7	3.9	83.2	2.0	79.8	-2.1
G4			31797	84.2	87.3	3.7	85.8	1.9	82.4	-2.1

4.3.1 Discussion

When increasing the soiling losses to 6%, a decrease in system yield of 2.1% for ground systems and 1.9% for roof systems were observed. Systems with module inverters showed a higher reduction, as they were simulated with a lower soiling loss in the main simulation. An increase in soiling loss resulted in a marked decrease in system performance.

When decreasing the soiling loss to 0%, an increase in system yield between 3.6% and 4.1% was observed. When decreasing the soiling loss, the performance ratio increased, as expected.

There was a slight variation in yield differences for Soiling Case 1, where systems with thin-film modules had a 0.1% to 0.4% higher yield difference. Both thin-film systems have modules on a larger part of building 2. As seen from table 4.1, building 2 has a slightly higher soiling loss than the other buildings. As building 2 has a 0° tilt angle, it is expected to have larger soiling losses. This may have resulted in a slightly higher yield difference for Soiling Case 1.

In Soiling Case 2, the systems with optimizers were simulated with the same soiling loss as the module inverters had in the main simulation. When using the same soiling losses, the systems with optimizers had a PR of 76.5% and 77.4%. The systems with module inverters had a 2% higher performance ratio, meaning that the difference in performance was reduced, but not eliminated. The module inverters were simulated with a lower soiling loss based on a recommendation from the manufacturer's user guide [42]. When simulating the module inverters with the same soiling loss as the other systems in the main simulation, a PR of 76.8% and 77.6% was achieved. Whether this soiling loss is more realistic, or the soiling loss recommended by the manufacturer, is not known.

As Panthera Africa is located in a rural environment with some agricultural activity and many wine farms, the soiling losses could vary seasonally. The ground also consists of sand, with some low vegetation, which may lead to higher soiling in combination with stronger winds. Table 3.4 shows higher wind speeds during summer months and figure 3.11 shows lower amounts of rainfall during summer months. This combination may lead to higher soiling losses during summer months, and thus seasonal variations.

The effect of soiling is reduced if modules are washed by rainwater. To achieve this, the tilt angle should be at least 19° [14]. As building 2 has a tilt angle of 0°, the effect of washing by rainwater is therefore expected to be minimal. All other buildings and the ground mounted systems have a higher tilt angle than 19°, and the soiling effect should be reduced in winter months.

There are many factors affecting the soiling parameter, and uncertainties regarding the actual value, but a seasonal soiling setting may be a good assumption for Panthera Africa.

4.4 Thermal parameter sensitivity

As the largest losses were the efficiency losses due to operating temperatures different from STC, the effect of different thermal parameters on system performance was analyzed. Table 4.6 compares the system performance when keeping all parameters constant and only changing the thermal parameter. The yield difference is the difference in energy produced by the system when the thermal parameter is changed.

Table 4.6: Simulation result from thermal parameter sensitivity analysis.

System			Main U-value			U-value Case 1			U-value Case 2		
			Yield [kWh]	PR [%]	Temp. loss [%]	PR [%]	Yield diff. [%]	Temp. loss [%]	PR [%]	Yield diff. [%]	Temp. loss [%]
R1.1.1	R2.1.1r	R3.1.1	31440	74.6	7.5	71.7	-3.8	10.8	77.1	3.4	4.5
R1.2.1	R2.2.1r	R3.2.1	31667	75.1	7.5	72.2	-3.8	10.8	77.6	3.3	4.5
R1.3.1m	R2.3.1	R3.3.1	34620	78.2	7.6	75.4	-3.6	11.0	80.8	3.3	4.6
R1.1.2	R2.1.2r	R3.1.2	31260	75.4	6.9	72.8	-3.5	10.0	-	-	-
R1.2.2	R2.2.2r	R3.2.2	31504	76.0	6.9	73.3	-3.6	10.0	-	-	-
R1.3.2m	R2.3.2	R3.3.2	35120	79.0	7.1	76.5	-3.1	10.2	80.9	2.5	4.2
R1.1.3	R2.1.3	R3.1.3	38401	78.4	5.4	76.4	-2.5	7.8	80.2	2.3	3.2
R1.1.4	R2.1.4	R3.1.4	37499	81.4	5.9	79.2	-2.7	8.5	83.5	2.5	3.6
G1			32360	79.5	4.8	76.8	-4.0	8.0	79.8	0.4	4.4
G2			33230	80.3	4.4	77.7	-3.2	7.4	80.6	0.4	4.0
G3			32213	81.6	3.5	79.6	-2.4	5.8	81.8	0.3	3.2
G4			31797	84.2	3.9	82.0	-2.6	6.4	84.5	0.3	3.6

4.4.1 Discussion

The U-values used for Case 1 and 2 are given in table 3.23. The U-values used in the main simulation are given in table 3.21. The systems R1.1.2 R2.1.2r R3.1.2 and R1.2.2 R2.2.2r R3.2.2 were not simulated for U-value Case 2, due to the inverter power being strongly undersized.

Thin-film modules generally show a smaller sensitivity to changes in the U-value than crystalline modules. Systems with the poly-crystalline module from Canadian Solar had the highest yield difference and systems with the First Solar module had the lowest yield difference. This corresponds with the fact that First Solar modules were the least sensitive to temperature changes, while the Canadian Solar poly-crystalline modules was the most sensitive. This is expected, as these modules have the lowest and highest power temperature coefficient, as shown in table 3.14.

A higher thermal parameter increased the yield by 2.3% to 3.4% for roof mounted systems, while a lower thermal parameter decreased the yield by 2.5% to 3.8%. A U-value of 30.7 W/m^2K was used in U-value Case 2 for the ground mounted systems. In a guide provided by First Solar, they recommend a U-value of 30.7 W/m^2K for free standing systems. As

can be observed from table 4.6, the slight increase in U-value for ground mounted systems only increased the yield by 0.3% to 0.4%.

A better performance ratio is observed when the U-value is increased, which is expected, as the efficiency loss due to temperature decreases. When a lower thermal parameter is used, the efficiency loss due to temperature increases, thus decreasing the performance ratio.

4.5 Ageing sensitivity

The ageing loss parameter consists of degradation loss for the individual modules and added mismatch due to the modules ageing at different rates. Only the ageing loss for the first production year was included in the main simulation. To get a better overview of the progression of ageing losses over the lifetime of the different system, the progression was simulated and analyzed. Figure 4.8 shows the progressive ageing loss for the four systems using Canadian Solar CS6U-330P modules. The ageing losses varies depending on if the system uses string inverters, string inverters with optimizers or module inverters.

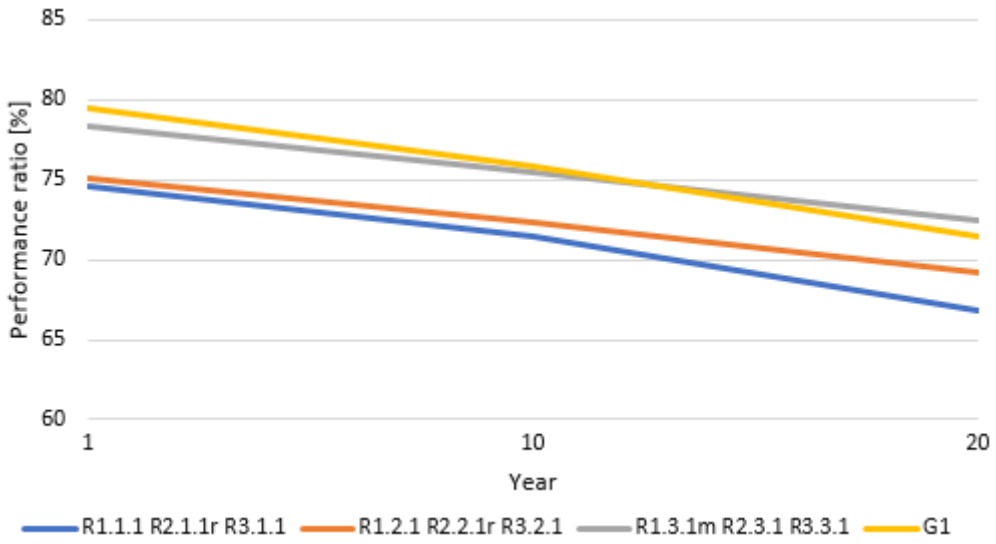

Figure 4.8: The progression of ageing loss for all systems with Canadian Solar CS6U-330P modules. The three roof systems have, respectivly, string inverter, string inverter with optimizer and module inverters. The ground system uses string inverters.

When only considering the degradation rate for the module, and excluding mismatch losses due to uneven degradation, the degradation rate has a linear relationship in PVsyst. Table 4.7 shows the degradation losses associated with different degradation rates for a PV module in PVsyst.

Table 4.7: Degradation losses when using different degradation rates in PVsyst.

	Degradation loss [%]		
Degradation rate [%/year]	Year 1	Year 10	Year 20
0.2	0.1	1.9	3.9
0.4	0.2	3.8	7.8
0.5	0.3	4.8	9.8
0.7	0.4	6.7	13.7

4.5.1 Discussion

From the progressive ageing loss graph in figure 4.8, the ground mounted system has the best performance initially, but after about 10 years, the roof mounted system with module inverters has the same performance ratio. After 20 years, the system with module inverters has the best performance ratio. Both systems using string inverters have an added mismatch loss due to uneven degradation between modules in a string. After 10 years, the added mismatch loss is 0.6% and after 20 years the added mismatch loss is 2.7%. Systems with optimizers and module inverters does not experience mismatch loss, as they maximizes the performance of each module. When simulating the progressive ageing losses for the system, the added benefit of using module inverters or optimizers are therefore displayed.

A degradation rate of 0.4%/year was used in the main simulation. Whether this rate is a good approximation for the actual degradation loss of the system due to module degradation is unknown. PVsyst does not have much reference about the average degradation of modules and they don't have any information about the real loss rate due to mismatch between modules as they age at different rates [19]. According to PVsyst, long time degradation rate measurements are relatively scarce, so there are uncertainties regarding the ageing parameter [19].

The manufacturer's warranty regarding the degradation of the PV module should be seen as a maximum limit for individual modules, according to PVsyst [19]. Both First Solar and Canadian Solar offers linear performance warranties for their modules. First Solar guarantees a maximum degradation loss of 0.5%/year from year 2 to 25 and Canadian Solar guarantees a maximum degradation loss of 0.7%/year from year 2 to 25. Even though these rates are seen as a maximum, they could still occur. Table 4.7 shows the associated PV module efficiency losses due to degradation at different degradation rates. If a Canadian Solar module degrades at the warranty rate, it would have an efficiency loss of 13.7% by year 20, which is considerable, compared to the efficiency loss of 7.8% by year 20, used in the main simulation.

4.6 Ground mounted orientation sensitivity

4.6.1 Inter-row spacing sensitivity

To maximize the area utilization for the ground mounted systems, the sensitivity of system performance to changes in inter-row spacing were analyzed. Changes in inter-row spacing affect the inter row shading, thus affecting the electrical and irradiance loss due to near shading objects. The irradiance loss depends on the orientation of the system and will be the same for all ground mounted systems, as their orientation is the same. The impact of inter-row spacing was only be analyzed for system G1 and G2, as these systems had crystalline modules. Systems with crystalline modules accounts for the electrical losses, while systems with thin-film modules does not. This is because thin-film modules are modeled with linear shading losses in PVsyst.

Figure 4.9a shows the yield drop with decreasing inter-row spacing for system G1. Figure 4.9c shows the resulting drop in PR and increase in electrical and irradiance losses. Figure 4.9b shows the yield drop for system G2 and figure 4.9d shows the drop in PR. All system parameters were kept constant, only the inter-row spacing was changed.

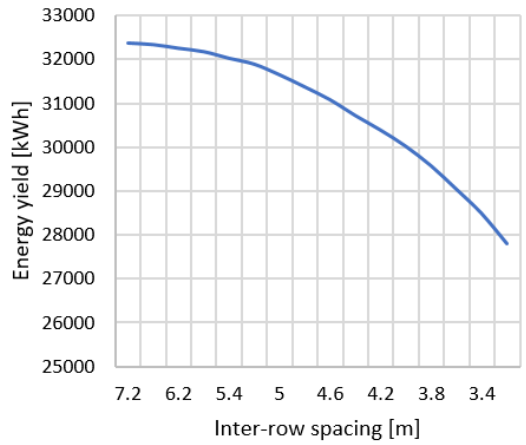

(a) System G1.

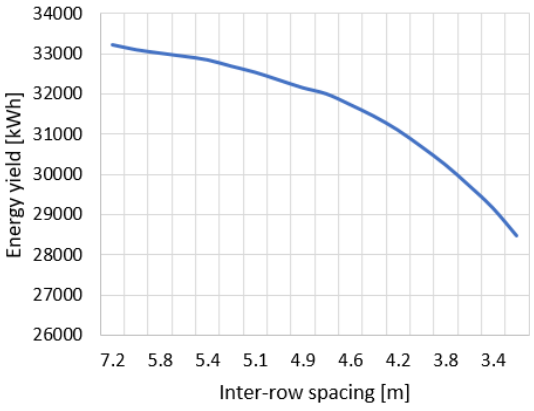

(b) System G2.

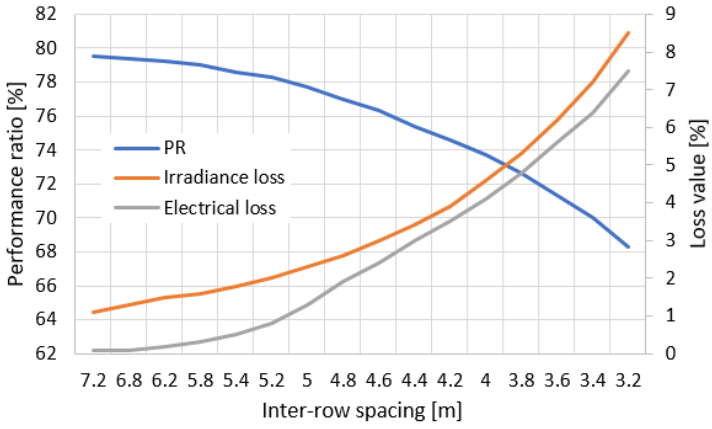

(c) System G1.

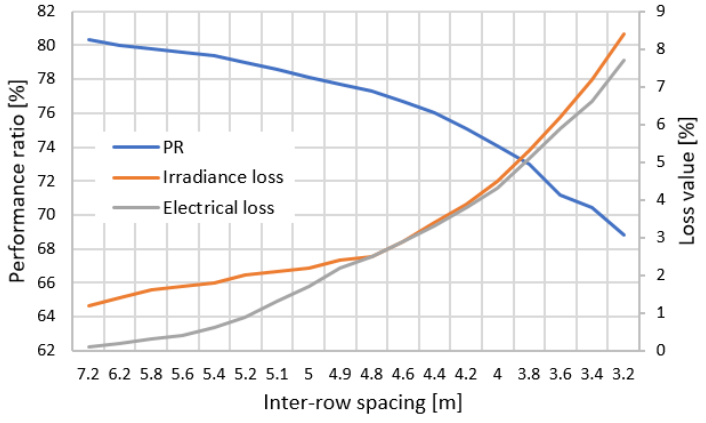

(d) System G2.

Figure 4.9: Variation in (a), (b) energy yield and (c), (d) performance ratio and losses with inter-row spacing for system G1 and G2.

Discussion

As seen in figure 4.9c and figure 4.9d, when the inter-row spacing was decreased, the performance ratio was reduced. When the inter-row spacing decreased, the inter-row shading increased, which increased the electrical and irradiance loss due to near shading. The increase in irradiance loss was the same for both systems, as the irradiance loss only depends on the orientation of the systems. The electrical losses were slightly different, as the electrical loss depends on the string design.

The performance ratio, irradiance loss and electrical loss shown in figure 4.9 are the average values for a year. The values will all be higher during winter months, as the Sun's position is lower in the sky, thus more shading is cast between the rows. The values will be lower in the summer, as the Sun's position is higher in the sky.

It may seem like the energy yield decreases faster than the performance ratio, which is not the case. It is a result of different figure dimensions. The energy yield and performance ratio decreases at the same rate.

4.6.2 Azimuth angle sensitivity

As the available ground area is oriented at 18°, an analysis on the impact of a change in azimuth angle was performed. All other system variables were kept constant and only the azimuth angle of the panels were changed. Table 4.8 shows the resulting system performances.

Table 4.8: Simulation result from changing the azimuth angle from 0° to 18°.

	Main azimuth		An 18° azimuth angle							
System	Yield [kWh]	PR [%]	PR [%]	Yield diff. [%]	GIR [kWh/m^2]	Horizon [%]	Irrad. loss [%]	IAM [%]	Soiling loss [%]	El. loss [%]
G1	32360	79.5	79.2	-1.6	2032	0.9	1.4	2.6	3.9	0.2
G2	33230	80.3	80.0	-1.6	2032	0.9	1.4	2.7	3.9	0.2
G3	32213	81.6	81.4	-1.4	2032	0.9	1.5	2.6	3.9	-
G4	31797	84.2	84.0	-1.5	2032	0.9	1.5	2.6	3.9	-

Discussion

When using an azimuth angle of 18°, there was a yield loss between 1.4% and 1.6%. When changing the azimuth angle, the orientation is changed and the optical losses will be changed. When comparing the optical losses in table 4.8 to the optical losses before changing the azimuth angle, a slight decrease in the global incident irradiation (GIR) and slight increase in the horizon and near shading loss was observed. This was expected, as the azimuth angle was changed from the optimal azimuth angle for the Southern Hemisphere, which is directly North.

There was a slight decrease in performance ratio when changing the azimuth angle, as there was some increases in losses due to horizon and near shading irradiance loss. The

largest effect of changing the azimuth was on the system yield, as changing the azimuth angle resulted in a lower irradiation reaching the modules.

4.7 Economical evaluation

4.7.1 Comparing production and consumption

A comparison of monthly production and consumption was carried out to analyze when a system would have to buy or sell electricity to the grid, and the amount it had to buy or sell. Table 4.9 compares the production of each system with the 2016 consumption for Panthera Africa. As seen in figure 3.8, the 2016 consumption dips to zero in October and peaks in November. The dip is due to the consumption being estimated by Eskom in October and not read from the electricity meter. The peak in November was therefore assumed to be both the consumption from October and November, and was equally divided between the months.

Table 4.9: A comparison of 2016 consumption with production for the systems simulated in the main simulation.

			% of 2016 consumption [%]												
System			Jan	Feb	Mar	Apr	May	Jun	Jul	Aug	Sept	Oct	Nov	Dec	Total
R1.1.1	R2.1.1r	R3.1.1	100	71	77	78	57	54	48	78	78	77	86	84	74
R1.2.1	R2.2.1r	R3.2.1	101	72	77	75	56	55	50	70	79	83	87	85	75
R1.3.1m	R2.3.1	R3.3.1	112	76	84	85	66	58	49	84	80	91	96	94	82
R1.1.2	R2.1.2r	R3.1.2	98	71	77	78	57	54	48	77	78	77	85	83	74
R1.2.2	R2.2.2r	R3.2.2	99	72	77	79	56	53	49	72	78	82	85	84	74
R1.3.2m	R2.3.2	R3.3.2	113	81	86	80	68	58	53	86	87	92	97	89	83
R1.1.3	R2.1.3	R3.1.3	127	90	95	94	63	58	58	92	94	93	109	107	91
R1.1.4	R2.1.4	R3.1.4	123	87	91	91	65	61	54	90	91	93	105	104	89
G1			86	69	79	87	73	68	62	88	79	81	80	69	76
G2			89	71	81	90	75	70	63	91	81	83	82	71	78
G3			92	69	79	80	73	65	58	87	82	75	80	76	76
G4			85	68	78	86	72	67	60	86	78	79	79	68	75

Based on the comparison of production and consumption, a table indicating the energy amount needed to be bought or sold from each system was made. The table is listed in appendix F, table F.1.

Discussion

Most of the systems produced between 75% and 80% of the total 2016 consumption at Panthera Africa. The roof mounted systems had a larger variation in production between winter and summer months. They generally produced more during summer months and less during winter month compared to the ground mounted systems. All ground mounted systems had less variation in production between summer and winter months.

None of the ground mounted systems produced more than what was consumed for any months of the year. The roof mounted systems with optimizers and module inverters produced more than what was consumed only in January. The roof mounted systems with thin-film modules both produced more than what was consumed in January, November and December. As these systems produced more compared with the other systems, it was expected that they would overproduce during some months.

4.7.2 Economical evaluation

Table 4.10 shows the results of the calculation of LCoE, NPV and payback time for the systems simulated in the main simulation. It was assumed that 10% of the produced electricity would be sold to the utility for all systems except module inverter systems and the roof mounted thin-film systems. For systems with module inverters, 15% was assumed to be sold to the utility, as both systems had a slightly higher yearly production. The roof mounted systems with thin-film modules was assumed to sell 20% was to the utility, as these systems had the highest yearly production.

When calculating the payback time, the discounted payback time was used. This means that if a system has a negative net present value, the initial investment will not have been payed back in the defined system lifetime. The calculated investment costs were excluding VAT.

Table 4.10: Investment cost, levelized cost of electricity, net present value and payback time for all base case systems.

System			Investment cost [R]	Investment cost [R/kWp]	LCoE [R/kWh]	NPV [R]	Payback time [year]
R1.1.1	R2.1.1r	R3.1.1	448658	20394	1.6	-58601	25+
R1.2.1	R2.2.1r	R3.2.1	512107	23278	1.8	-102565	25+
R1.3.1m	R2.3.1	R3.3.1	478723	20814	1.6	-64302	25+
R1.1.2	R2.1.2r	R3.1.2	452803	20582	1.6	-63946	25+
R1.2.2	R2.2.2r	R3.2.2	520040	22638	1.8	-110529	25+
R1.3.2m	R2.3.2	R3.3.2	483731	21032	1.5	-59404	25+
R1.1.3	R2.1.3	R3.1.3	511801	24371	1.5	-40500	25+
R1.1.4	R2.1.4	R3.1.4	477054	23853	1.4	-22651	25+
G1			431499	21575	1.5	-15523	25+
G2			444837	22242	1.5	-14339	25+
G3			545518	28711	1.8	-98503	25+
G4			489425	27190	1.6	-59339	25+

Discussion

The economical evaluation shows that the net present value is negative for all systems. This means that the investment cost will not be payed back during the system lifetime. When calculating the net present value, an increase in energy prices was not taken into

account. As Eskom increases their energy tariffs annually, this underestimates the actual savings on the utility bill. If the systems are profitable or not depends on the electricity price, as both the NPV and payback time considers the revenue. The LCoE indicates the minimum electricity price needed for the system to break even. The current utility tariff is 1.2 R/kWh, which is lower than all the calculated LCoE. Had one of the calculated LCoE been lower than this rate, the system would have been profitable.

The LCoE varied from 1.4 - 1.8 R/kWh and system R1.1.4 R2.1.4 R3.1.4 had the lowest levelized cost of electricity of 1.4 R/kWh. The system consists of Solar Frontier modules and SMA string inverters, and is a roof mounted system. The most economical system was not the best performing system overall, but it was the best performing roof mounted system. System G4 had the best performance ratio, but has a LCoE of 1.6 R/kWh.

Systems with optimizers and systems with system G3 had the highest cost per kWp and highest LCoE. Systems using optimizers had an additional expense of 947 R/module, but the system performance did not increase a lot. Systems G3 has First Solar modules, which requires the largest quantity of modules per kWp. The system has a higher total module cost and mounting cost, as the cost of mounting structure is per module based.

Ground mounted systems were generally more expensive per kWp than roof mounted systems based on the estimations in table 4.10. Even though the ground mounted systems had a higher performance ratio, the ground mounting structure cost used in the estimation was 532 R/module more expensive than the roof mounting structure. The result of this cost difference can be seen especially for system G3 and G4, having thin-film modules. As more modules were required in the systems, the ground mounting structure cost was high.

The investment costs were calculated based on the values given in table C.2. All inverter and module costs were found on South African websites selling solar equipment. There are large uncertainties regarding the actual PV module and inverter prices. The PV module costs accounted for about 36% for crystalline modules and 38% for thin-film modules. The inverter cost varied between 14% and 23% depending on inverter type and system configuration. For the ground mounted systems, the percentage inverter cost was slightly lower than in the roof mounted systems. The module and inverter costs in the estimate from Solareff were 20% cheaper than the values used in the economical evaluation for the same components.

The total investment cost and the investment cost per Wp installed power are listed in table 4.10. According to Green Cape, an average PV system cost in 2017 for a 10 kWp rooftop PV systems without battery storage was 20000 R/kWp [10]. The price estimate from Solareff gave an investment cost of 22058 R/kWp for a 13.2 kWp system. The simulated systems had investment costs ranging from 20394 - 28711 R/kWp and a rated power of 18 - 23 kWp.

There were many assumptions and simplifications in the economical evaluation, which makes the results debatable. Loan, interest payments and inflation were not considered

in the economical evaluation. The component prices depend on the quantities bought and the Bos prices depends on the chosen monitoring system. Different inverter manufacturer's have different monitoring systems, so the prices vary. The systems using optimizers were simulated with optimizers on all modules in the entire system, due to limitations in PVsyst. When using Tigo optimizers in real life, only the modules affected by shading need to have an optimizer on, reducing the cost of the system using optimizers.

It is uncertain if the building roofs are able to carry the additional load of the PV systems. The roof mounted systems may therefore have an additional cost to inspect the structure and improve it if needed. If the roof has to be replaced during the lifetime of the PV modules, uninstalling and reinstalling the PV system may be expensive. To avoid this, the roof may have to be changed before installing the PV system, which will increase the overall cost.

System yield and performance ratio will affect the calculated LCoE. As both yield and PR depends on sensitivity factors such as soiling loss, irradiation levels, thermal parameter and degradation rate, the LCoE will wary according to changes in these factors. In the sensitivity analysis, a higher irradiation value increased the yield by 5%.

Chapter 5

Conclusion

There are uncertainties regarding the meteorological data and the available solar resource. The irradiations used in the simulation and sensitivity analysis varied from from 1709 - 1854 kWh/m^2. Changes in irradiation data increased the system yield by 5%. It is difficult to conclude which meteorological dataset is most representative for the climate conditions at Panthera Africa.

The best performing ground system gives a yearly yield of 81.8 kWh and has a performance ratio of 84.2%. The ground system produces 75% of the yearly energy consumed at Panthera Africa. When comparing the roof mounted system and ground mounted system, the ground mounted system has the best performance, as it is experiences less near shading and is optimally tilted, thus receiving more irradiation. The best performing ground and roof systems have Solar Frontier modules. As Solar Frontier modules are less sensitive to changes in temperature, they have lower efficiency losses due to temperatures different than STC. The yearly system yield is sensitive to uncertainties in irradiation data, and the performance ratio is sensitive to soiling losses and the thermal parameter.

When using optimizers, the performance was increased by 0.5%, while module inverters increased the performance by 3.6%, compared to using string inverters. When simulating optimizers and module inverters with the same soiling loss, the increase in performance was reduced to 2.3% for the module inverters.

The best performing roof system was the most profitable system when comparing the calculated levelized costs of electricity. The ground system G4 has the highest performance ratio, but was not the most profitable system. The investment cost of the systems rage from 20394 R/kWp to 28711 R/kWp. When calculating the LCoE for all systems, they ranged from 1.4 R/kWh to 1.8 R/kWh. As the LCoE was calculated based on a number of assumptions, there are several uncertainties regarding the calculated numbers. As the calculated LCoE are higher than the tariff for buying electricity, all the systems have a negative net present value and will not be payed back during the system lifetime.

The best system is a consideration between performance and price. System G4 is the best performing system, while system R1.1.4 R2.1.4 R3.1.4 has the lowest levelized cost of electricity and is the most profitable. Ground mounted systems are easier to expand and maintain, while roof mounted systems does not take up land area and leaves a smaller footprint on the nature. A PV system can also be used for educational purposes regarding energy consumption, renewable energy and energy efficiency.

5.1 Further work

As this is a feasibility study, more detailed information regarding the electrical layout, possible mechanical load the building can handle, dimensioning for the mounting structure and protection, disconnection switches and metering is needed before constructing the system. An analysis of the ground soiling type may also be needed.

The PV modules on building 2 could also be simulated at a tilt angle, which may increase the performance and system yield. It is also possible to explore the option of integrating PV modules on the roof when building the planned educational center. The building could be constructed with and optimal azimuth angle and roof tilt angle to maximize energy production.

There is also a wide selection of other module and inverter technology available on the market today. Other systems could also be evaluated and compared with respect to performance and price. There are local manufacturers of both PV modules and inverters in South Africa which may be explored. Several PV module manufacturers also offer smart solar panels with integrated optimizers or module inverters. Enphase collaborates with JinkoSolar and LG. As the systems were only simulated with three-phase string inverters, it may be interesting to compare the performance if simulating them with one-phase inverters. One-phase inverters could be used to supply three-phase AC by connecting two phases together.

The possibility of a battery storage is another option to be explored. It can store the excess energy produced during the daytime and use it during the night time. The prices for selling electricity to the utility is low and a battery storage can replace the existing diesel aggregate for a lessened environmental impact. A storage option also increases system reliability in case of outages.

The uncertainties in the economical evaluation could be further assessed by collecting information from several PV system companies regarding costs to compare them. A PV system company, such as Solareff, will also have a full overview over the regulations and policies who have to be followed. The will engage with relevant authorities, such as Eskom or minicipalities, on behalf of the customer to ensure that the solution is registered and legal. A sensitivity analysis of the impact of different parameters on the levelized cost of electricity could be performed.

A more in depth analysis of the actual operation and maintenance costs for residential systems could also be interesting to perform. It would be interesting to know what the costs entail and the amounts. A suggested operation and maintenance plan for the system could also be created. Many of the PV system companies in South Africa offer system operation and maintenance for an additional monthly expense.

Bibliography

[1] Eskom. *Company information overview*, . URL http://www.eskom.co.za/OurCompany/CompanyInformation/Pages/Company_Information.aspx. Accessed 27.01.2018.

[2] Eskom. *Electricity generation in South Africa*, . URL http://www.eskom.co.za/news/Pages/Nov2.aspx. Accessed 27.01.2018.

[3] Eskom. *Electricity technologies*, . URL http://www.eskom.co.za/AboutElectricity/ElectricityTechnologies/Pages/Electricity_Technologies.aspx. Accessed 27.01.2018.

[4] Michael Taylor and Eun young So. *Solar PV in Africa: Costs and Markets*, .

[5] James Leigland Anton Eberhard, Joel Kolker. *South Africa's Renewable Energy IPP Procurement Program: Success Factors and Lessons*, May 2014.

[6] Anton Eberhard and Tomas Kåberger. *Renewable energy auctions in South Africa outshine feed-in tariffs*. *Energy Science Engineering*, 4(3):190–193, 2016. ISSN 2050-0505. doi: 10.1002/ese3.118. URL http://dx.doi.org/10.1002/ese3.118.

[7] Emiliano Bellini. *South Africa's PV capacity reaches 1.47 GW, new PV installations for 2016 total 509 MW*. URL https://www.pv-magazine.com/2017/03/17/south-africas-pv-capacity-reaches-1-47-gw-new-pv-installations-for-2016-total-509-mw/. Accessed 12.02.2018.

[8] United Nations. *Report of the Conference of the Parties on its twenty - first session, held in Paris from 30 November to 13 December 2015*. URL http://unfccc.int/resource/docs/2015/cop21/eng/10.pdf#page=30. Accessed 12.02.2018.

[9] Overstrand Municipality. *SSEG guidelines*, . URL https://www.overstrand.gov.za/en/documents/electricity/3347-sseg-guidelines. Accessed 28.01.2018.

[10] Jack Radmore Michael Leighton Seraj Chilwan Pieter Janse van Vuuren Bruce Raw Maloba G. Tshehla, Songo Didiza. *Market Intelligence Report 2017*.

[11] Arno H. M. Smets, Klaus Jäger, Olindo Isabella, René A. C. M. M. van Swaaij, and Miro Zeman. *Solar energy : the physics and engineering of photovoltaic conversion, technologies and systems*. UIT Cambridge, Cambridge, 2016. ISBN 978-1-906860-32-5.

[12] Stuart Bowden Christiana Honsberg. *PVeducation*. URL http://pveducation.org/. Accessed 07.09.2017.

[13] Gilbert M. Masters. *Renewable and Efficient Electric Power Systems*. Wiley - IEEE Ser. Wiley, Hoboken, 2005. ISBN 1-280-27281-3.

[14] Sonnenenergie Deutsche Gesellschaft für. *Planning and installing photovoltaic systems : a guide for installers, architects and engineers*. Planning and installing series. Earthscan Deutsche Gesellschaft für Sonnenenergie, London, 3rd rev. and updated ed. edition, 2013. ISBN 9781849713436.

[15] PVeducation. *Standard Solar Spectra*. URL http://www.pveducation.org/pvcdrom/appendices/standard-solar-spectra. Accessed 18.12.17.

[16] C. Hu. *Modern Semiconductor Devices for Integrated Circuits*. Prentice Hall, 2010. ISBN 9780136085256. URL https://books.google.no/books?id=PosRbWdafnsC.

[17] Heinrich Häberlin. *Photovoltaics : system design and practice*. Wiley-Blackwell, Chichester, 2012. ISBN 9781119992851.

[18] Werner Warmuth Dr. Simon Philipps. *Photovoltaics Report* . URL https://www.ise.fraunhofer.de/en/publications/studies/photovoltaics-report.html. Accessed 21.12.2017.

[19] Pvsyst contextual help (built-in software). URL http://files.pvsyst.com/help/index.html.

[20] S Flex. *A Safe and Strong Support for Photovoltaic Systems on Pitched Roofs*. URL http://www.sflex.com/htdocs/index.php/en/pitched-roof-structures. Accessed 22.01.2018.

[21] Landpower. *Steel Ground Mounting system*. URL http://www.landpowersolar.com/Steel-Gound-Mounting.html?Solar-Roof-Mount=2&Solar-Ground-Mount=74. Accessed 22.01.2018.

[22] PV shop. *PV solar system diagram*. URL http://pvshop.eu/diagrams.html. Accessed 22.01.2018.

[23] SMA. *7 Reasons Why You Should Oversize Your PV Array*. URL http://en.sma-sunny.com/en/7-reasons-why-you-should-oversize-your-pv-array-2/. Accessed 23.01.2018.

[24] V.R.V. *Pnom Ratio - A Well Known Factor For the PV Plant Efficiency*. URL https://www.linkedin.com/pulse/well-known-factor-pv-plant-efficiency-pnom-ratio-v-r-v/. Accessed 23.01.2018.

[25] Johannes Idsø. *Nåverdi*. URL https://snl.no/n%C3%A5verdi. Accessed 27.01.2018.

[26] Seth B. Darling, Fengqi You, Thomas Veselka, and Alfonso Velosa. *Assumptions and the levelized cost of energy for photovoltaics*. *Energy Environ. Sci.*, 4:3133–3139, 2011.

[27] J. Hernández-Moro and J.M. Martínez-Duart. *Analytical model for solar PV and CSP electricity costs: Present LCOE values and their future evolution*. *Renewable and Sustainable Energy Reviews*, 20:119 – 132, 2013. ISSN 1364-0321.

[28] Michael Taylor and Eun young So. *Projected Costs of Generating Electricity 2015 edition*, . URL https://www.iea.org/publications/freepublications/publication/projected-costs-of-generating-electricity-2015-edition.html.

[29] Sandia National Laboratories. *Budgeting for Solar PV Plant Operations & Maintenance: Practices and Pricing*. United States Department of Energy, Office of Energy Efficiency and Renewable Energy, 2015. URL https://books.google.no/books?id=IaaHnQAACAAJ.

[30] South african revenue service (SARS). *Taxation in South Africa 2016/2017*. URL http://www.sars.gov.za/AllDocs/OpsDocs/Guides/LAPD-Gen-G01%20-%20Taxation%20in%20South%20Africa%20-%20External%20Guide.pdf. Accessed 13.02.2018.

[31] PVsyst. *Synthetic hourly irradiance*, . URL http://files.pvsyst.com/help/models_meteo_synthetic_generation_irradiance.htm. Accessed 02.02.2018.

[32] PVsyst. *Synthetic hourly data*, . URL http://forum.pvsyst.com/viewtopic.php?f=18&t=15. Accessed 02.02.2018.

[33] PVsyst. *What is the accuracy of the PVsyst simulation results?*, . URL http://forum.pvsyst.com/viewtopic.php?f=30&t=1649. Accessed 29.11.2017.

[34] Petros J. Axaopoulos, Emmanouil D. Fylladitakis, and Konstantinos Gkarakis. *Accuracy analysis of software for the estimation and planning of photovoltaic installations. International Journal of Energy and Environmental Engineering*, 5(1):1, Jan 2014. ISSN 2251-6832.

[35] J.L van Niekerk P. Gauche C. Leonard Mouzouris M.J. Meyer A.J. van der Westhuizen N. van Dyk E.E. M.J. Brooks, S. du Clou and F Vorster. *SAURAN: A new resource for solar radiometric data in Southern Africa. Journal of Energy in Southern Africa*, 26:2–10, 2015.

[36] The Southern African Universities Radiometric Network (SAURAN). *SUN - Stellenbosch University*. URL http://www.sauran.net/ShowStation.aspx?station=4. Accessed 25.10.2017.

[37] European Comission Joint Research Centre Institute for Energy and Transport (IET). *Photovoltaic Geographical Information System - Interactive Maps - Africa*. URL http://re.jrc.ec.europa.eu/pvgis/apps4/pvest.php?lang=en&map=africa. Accessed 17.10.2017.

[38] Heinrich Häberlin and Herbert Eppel. *Photovoltaics : system design and practice*. Wiley-Blackwell, Chichester, 2012. ISBN 9781119992851.

[39] Finlay Colville. *Top 10 solar module suppliers in 2016*. URL https://www.pv-tech.org/editors-blog/top-10-solar-module-suppliers-in-2016. Accessed 07.01.2018.

[40] PQRS. Solar pv investment and equipment report, . URL http://pqrs.co.za/data/february-2017-solar-pv-investment-and-equipment-report/. Accessed 01.02.2018.

[41] PQRS. *Solar PV March 2016 PQRS Industry Report* , . URL http://pqrs.co.za/data/s-a-solar-pv-list-2/. Accessed 06.12.2017.

[42] Enphase. *Guide to Modeling Enphase Microinverter Systems with PVsyst v6.* URL https://enphase.com/en-us/support/guide-modeling-enphase-microinverter-systems-pvsyst-v6. Accessed 01.02.2018.

[43] PVsyst. *How to adjust the design temperatures*, . URL http://forum.pvsyst.com/viewtopic.php?f=29&t=1516. Accessed 02.02.2018.

[44] Tigo. *PVsyst guide.* URL https://support.tigoenergy.com/hc/en-us/articles/215348938-PVsyst. Accessed 07.02.2018.

[45] J. R. Caron and B. Littmann. *Direct monitoring of energy lost due to soiling on first solar modules in California.* In *2012 IEEE 38th Photovoltaic Specialists Conference (PVSC) PART 2*, pages 1–5. doi: 10.1109/PVSC-Vol2.2012.6656732.

[46] A. Massi Pavan, A. Mellit, and D. De Pieri. *The effect of soiling on energy production for large-scale photovoltaic plants. Solar Energy*, 85(5):1128–1136, 2011. ISSN 0038-092X.

[47] Felipe A. Mejia and Jan Kleissl. *Soiling losses for solar photovoltaic systems in California. Solar Energy*, 95(Supplement C):357–363, 2013. ISSN 0038-092X.

[48] Mari Benedikte Øgaard. *Effect of Soiling on the Performance of Photovoltaic Modules in Kalkbult, South Africa.*, 2016.

[49] Sunflare renewable systems. *Products.* URL https://www.sunflare.co.za/products. Accessed 29.01.2018.

[50] Sustainable Online Eco Store. *Solar power products.* URL https://www.sustainable.co.za/solar-power.html. Accessed 29.01.2018.

[51] GW store. *GW store - your online renewable energy product partner.* URL https://www.gwstore.co.za/. Accessed 09.02.2018.

[52] *NREL U.S. Solar Photovoltaic System Cost Benchmark Q1 2017 Report.*

[53] Eskom. *2017/18 Tariffs and charges* , . URL http://www.eskom.co.za/CustomerCare/TariffsAndCharges/Pages/Tariffs_And_Charges.aspx. Accessed 29.01.2018.

[54] Overstrand Municipality. E*lectricity Tariffs (after NERSA approval June 2017)*, . URL https://www.overstrand.gov.za/en/documents/electricity/4486-electricity-tariffs-after-nersa-approval-june-2017. Accessed 29.01.2018.

[55] K. Branker, M.J.M. Pathak, and J.M. Pearce. *A review of solar photovoltaic levelized cost of electricity. Renewable and Sustainable Energy Reviews*, 15(9):4470 – 4482, 2011. ISSN 1364-0321.

[56] Seth B. Darling, Fengqi You, Thomas Veselka, and Alfonso Velosa. *Assumptions and the levelized cost of energy for photovoltaics.* 4:3133–3139, 08 2011.

[57] D.C. Jordan, Ryan Smith, C.R. Osterwald, E Gelak, and S.R. Kurtz. *Outdoor PV degradation comparison*, 07 2010.

[58] D. C. Jordan and S. R. Kurtz. *Photovoltaic Degradation Rates—an Analytical Review. Progress in Photovoltaics: Research and Applications*, 21(1). ISSN 1099-159X.

[59] Janosch Ondraczek. *Are we there yet? Improving solar PV economics and power planning in developing countries: The case of Kenya. Renewable and Sustainable Energy Reviews*, 30:604 – 615, 2014. ISSN 1364-0321.

[60] National Renewable Energy Laboratory (NREL). *Distributed Generation Energy Technology Operations and Maintenance Costs.* URL https://www.nrel.gov/analysis/tech-cost-om-dg.html. Accessed 29.01.2018.

[61] Stefan Reichelstein and Michael Yorston. *The prospects for cost competitive solar PV power. Energy Policy*, 55:117 – 127, 2013. ISSN 0301-4215. Special section: Long Run Transitions to Sustainable Economic Structures in the European Union and Beyond.

[62] Solar Frontier. *Light Soaking Effect.* URL https://www.solar-frontier.eu/en/cis-technology/light-soaking-effect/. Accessed 09.02.2018.

[63] Standard Bank. Market rates and tools. URL https://corporateandinvestment.standardbank.com/CIB/Products/Global-Markets/Market-Rates. Accessed 29.01.2018.

[64] FreeCleanSolar. *Free clean solar - power for less.* URL http://www.freecleansolar.com/Default.asp. Accessed 09.02.2018.

Appendix A
Meteorological data

The meteorological datasets used in this thesis were Dataset 1, Dataset 2 and Dataset 3. Dataset 1 is given in table A.1, Dataset 2 is given in table A.2 and Dataset 3 is given in table A.3. Dataset 1 has the highest yield, Dataset 2 has a weighted average yield and Dataset 3 has the most conservative yield.

Table A.1: Dataset 1 consists of temperature and wind speed data from Stanford weather station and irradiation data from the PVgis SAF database.

	Dataset1			
Month	Global [kWh/m^2]	Diffuse [kWh/m^2]	T [°C]	Wind speed [m/s]
Jan	233.4	65.4	21.3	3.1
Feb	182.6	54.8	21.2	2.9
Mar	183.5	66.1	19.8	2.8
Apr	122.4	40.4	17.6	2.7
May	91.1	32.8	15.5	2.6
Jun	76.2	27.4	13.3	2.8
Jul	85.6	28.2	12.8	2.8
Aug	110.4	37.5	12.9	3.1
Sep	145.5	48.0	14.3	3.2
Oct	184.8	68.4	16.1	3.3
Nov	207.6	68.5	17.7	3.2
Dec	231.3	74.0	20.0	3.1
Year	1854.3	611.5	16.9	3.0

Table A.2: Dataset 2 consists of temperature and wind speed data from Stanford weather station and constructed irradiation data as a weighted average.

	Dataset2			
Month	Global [kWh/m^2]	Diffuse [kWh/m^2]	T [°C]	Wind speed [m/s]
Jan	225.5	71.4	21.3	3.1
Feb	178.5	57.8	21.2	2.9
Mar	166.4	56.1	19.8	2.8
Apr	118.6	40.4	17.6	2.7
May	90.3	32.6	15.5	2.6
Jun	75.1	26.7	13.3	2.8
Jul	84.3	29.0	12.8	2.8
Aug	107.3	38.4	12.9	3.1
Sep	139.3	50.1	14.3	3.2
Oct	178.6	66.3	16.1	3.3
Nov	205.9	68.9	17.7	3.2
Dec	227.0	76.6	20.0	3.1
Year	1796.9	614.2	16.9	3.0

Table A.3: Dataset 3 consists of temperature and wind speed data from Stanford weather station and irradiation data from the Solargis database.

	Dataset1			
Month	Global [kWh/m^2]	Diffuse [kWh/m^2]	T [°C]	Wind speed [m/s]
Jan	215.0	69.0	21.3	3.1
Feb	168.0	55.0	21.2	2.9
Mar	155.0	52.0	19.8	2.8
Apr	114.0	40.0	17.6	2.7
May	86.0	34.0	15.5	2.6
Jun	72.0	28.0	13.3	2.8
Jul	81.0	31.0	12.8	2.8
Aug	103.0	40.0	12.9	3.1
Sep	134.0	52.0	14.3	3.2
Oct	171.0	64.0	16.1	3.3
Nov	196.0	68.0	17.7	3.2
Dec	214.0	75.0	20.0	3.1
Year	1709.0	608.0	16.9	3.0

Appendix B
Component specifications

The data sheet for the modules, inverters and optimizer used in the simulation are listed in this appendix. All data sheets are from the manufacturers website.

The data sheets are listed in the following order:

- Canadian Solar Maxpower CS6U-series
- Canadian Solar Superpower CS6K-series
- First Solar series 4
- Solar Frontier SF170-S
- SMA Sunny Tripower series
- Tigo TS4-R optimizers
- Enphase IQ6 and IQ6+

NEW

CanadianSolar

MAXPOWER
CS6U-315 | 320| 325| 330P

Canadian Solar's modules use the latest innovative cell technology, increasing module power output and system reliability, ensured by 15 years of experience in module manufacturing, well-engineered module design, stringent BOM quality testing, an automated manufacturing process and 100% EL testing.

25 years linear power output warranty

10 years product warranty on materials and workmanship

KEY FEATURES

- Excellent module efficiency of up to 16.97 %
- Cell efficiency of up to 18.8 %
- Outstanding low irradiance performance: 96.0 %
- No. 1 PTC — High PTC rating of up to 91.55 %
- IP67 — IP67 junction box for long-term weather endurance
- Heavy snow load up to 5400 Pa, wind load up to 2400 Pa

MANAGEMENT SYSTEM CERTIFICATES*

ISO 9001:2008 / Quality management system
ISO 14001:2004 / Standards for environmental management system
OHSAS 18001:2007 / International standards for occupational health & safety

PRODUCT CERTIFICATES*

IEC 61215 / IEC 61730: VDE / CE / CQC / MCS
UL 1703 / IEC 61215 performance: CEC listed (US)
UL 1703: CSA / IEC 61701 ED2: VDE / IEC 62716: VDE / Take-e-way
UNI 9177 Reaction to Fire: Class 1

* As there are different certification requirements in different markets, please contact your local Canadian Solar sales representative for the specific certificates applicable to the products in the region in which the products are to be used.

CANADIAN SOLAR INC. is committed to providing high quality solar products, solar system solutions and services to customers around the world. As a leading PV project developer and manufacturer of solar modules with over 15 GW deployed around the world since 2001, Canadian Solar Inc. (NASDAQ: CSIQ) is one of the most bankable solar companies worldwide.

CANADIAN SOLAR INC.
2430 Camino Ramon, Suite 240 San Ramon, CA, USA 94583-4385 | www.canadiansolar.com/na | sales.us@canadiansolar.com

ENGINEERING DRAWING (mm)

Rear View

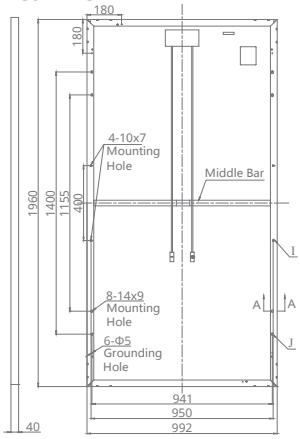

Frame Cross Section A-A

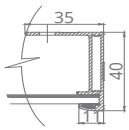

Mounting Hole

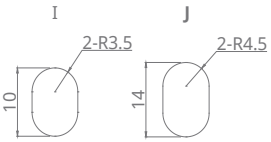

CS6U-320P / I-V CURVES

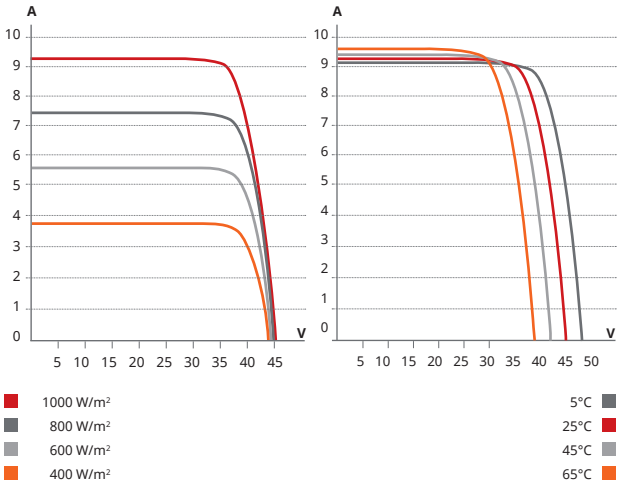

ELECTRICAL DATA / STC*

CS6U	315P	320P	325P	330P
Nominal Max. Power (Pmax)	315 W	320 W	325 W	330 W
Opt. Operating Voltage (Vmp)	36.6 V	36.8 V	37.0 V	37.2 V
Opt. Operating Current (Imp)	8.61 A	8.69 A	8.78A	8.88 A
Open Circuit Voltage (Voc)	45.1 V	45.3 V	45.5 V	45.6 V
Short Circuit Current (Isc)	9.18 A	9.26 A	9.34 A	9.45 A
Module Efficiency	16.20%	16.46%	16.72%	16.97%
Operating Temperature	-40°C ~ +85°C			
Max. System Voltage	1000 V (IEC) or 1000 V (UL)			
Module Fire Performance	TYPE 1 (UL 1703) or CLASS C (IEC 61730)			
Max. Series Fuse Rating	15 A			
Application Classification	Class A			
Power Tolerance	0 ~ + 5 W			

* Under Standard Test Conditions (STC) of irradiance of 1000 W/m², spectrum AM 1.5 and cell temperature of 25°C.

MECHANICAL DATA

Specification	Data
Cell Type	Poly-crystalline, 6 inch
Cell Arrangement	72 (6×12)
Dimensions	1960×992×40 mm (77.2×39.1×1.57 in)
Weight	22.4 kg (49.4 lbs)
Front Cover	3.2 mm tempered glass
Frame Material	Anodized aluminium alloy
J-Box	IP67, 3 diodes
Cable	4 mm² (IEC) or 4 mm² & 12 AWG 1000V (UL), 1160 mm (45.7 in)
Connector	T4 (IEC/UL)
Per Pallet	26 pieces, 635kg (1400lbs)
Per container (40' HQ)	624 pieces

ELECTRICAL DATA / NOCT*

CS6U	315P	320P	325P	330P
Nominal Max. Power (Pmax)	228 W	232 W	236 W	239 W
Opt. Operating Voltage (Vmp)	33.4 V	33.6 V	33.7 V	33.9 V
Opt. Operating Current (Imp)	6.84 A	6.91 A	6.98 A	7.05 A
Open Circuit Voltage (Voc)	41.5 V	41.6 V	41.8 V	41.9 V
Short Circuit Current (Isc)	7.44 A	7.50 A	7.57 A	7.66 A

* Under Nominal Operating Cell Temperature (NOCT), irradiance of 800 W/m², spectrum AM 1.5, ambient temperature 20°C, wind speed 1 m/s.

TEMPERATURE CHARACTERISTICS

Specification	Data
Temperature Coefficient (Pmax)	-0.41 % / °C
Temperature Coefficient (Voc)	-0.31 % / °C
Temperature Coefficient (Isc)	0.053 % / °C
Nominal Operating Cell Temperature	45±2 °C

PERFORMANCE AT LOW IRRADIANCE

Outstanding performance at low irradiance, average relative efficiency of 96.0 % from an irradiance of 1000 W/m² to 200 W/m² (AM 1.5, 25°C).

The specification and key features described in this datasheet may deviate slightly and are not guaranteed. Due to on-going innovation, research and product enhancement, Canadian Solar Inc. reserves the right to make any adjustment to the information described herein at any time without notice. Please always obtain the most recent version of the datasheet which shall be duly incorporated into the binding contract made by the parties governing all transactions related to the purchase and sale of the products described herein.

Caution: For professional use only. The installation and handling of PV modules requires professional skills and should only be performed by qualified professionals. Please read the safety and installation instructions before using the modules.

PARTNER SECTION

SUPERPOWER
CS6K-290|295|300|305MS

*Black frame product can be provided upon request.

Canadian Solar's new SuperPower modules with Mono-PERC cells significantly improve efficiency and reliability. The innovative technology offers superior low irradiance performance in the morning, in the evening and on cloudy days, increasing the energy output of the module and the overall yield of the solar system.

25 years **linear power output warranty**

10 years **product warranty on materials and workmanship**

KEY FEATURES

- 11 % more power than conventional modules
- Excellent performance at low irradiance of up to: 97.5 %
- High PTC rating of up to: 91.90 %
- Improved energy production due to low temperature coefficients
- IP68 junction box for long-term weather endurance
- Heavy snow load up to 6000 Pa, wind load up to 4000 Pa *

MANAGEMENT SYSTEM CERTIFICATES*

ISO 9001:2008 / Quality management system
ISO 14001:2004 / Standards for environmental management system
OHSAS 18001:2007 / International standards for occupational health & safety

PRODUCT CERTIFICATES*

IEC 61215 / IEC 61730: TÜV-Rheinland / VDE / CE / MCS / CEC AU / JET
UL 1703 / IEC 61215 performance: CEC listed (US) / FSEC (US Florida)
UL 1703: CSA / IEC 61701 ED2: VDE / IEC 62716: VDE
UNI 9177 Reaction to Fire: Class 1
IEC 60068-2-68: SGS
Take-e-way

* Please contact your local Canadian Solar sales representative for the specific product certificates applicable in your market.

CANADIAN SOLAR INC. is committed to providing high quality solar products, solar system solutions and services to customers around the world. As a leading PV project developer and manufacturer of solar modules with over 21 GW deployed around the world since 2001, Canadian Solar Inc. (NASDAQ: CSIQ) is one of the most bankable solar companies worldwide.

*For detail information, please refer to Installation Manual.

CANADIAN SOLAR INC.
545 Speedvale Avenue West, Guelph, Ontario N1K 1E6, Canada, www.canadiansolar.com, support@canadiansolar.com

ENGINEERING DRAWING (mm)

Rear View

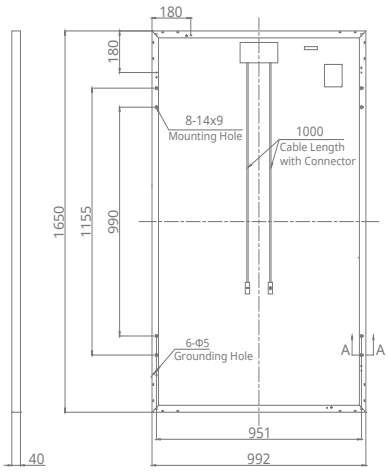

Frame Cross Section A-A

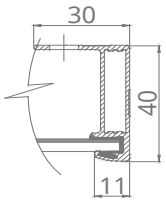

Mounting Hole

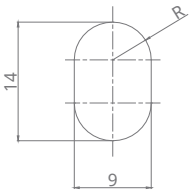

CS6K-295MS / I-V CURVES

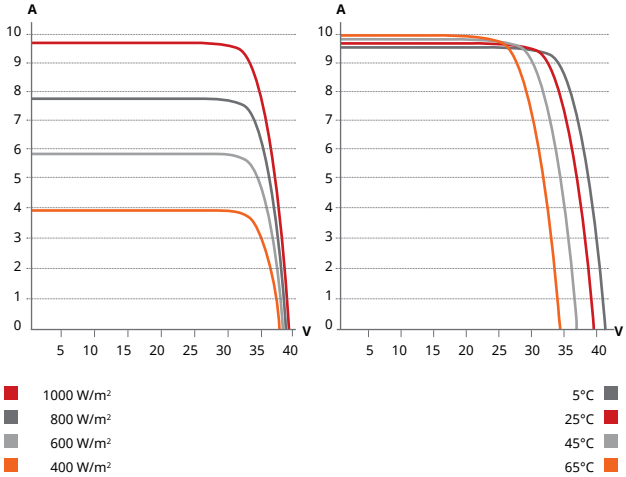

ELECTRICAL DATA | STC*

CS6K	290MS	295MS	300MS	305MS
Nominal Max. Power (Pmax)	290 W	295 W	300 W	305 W
Opt. Operating Voltage (Vmp)	32.1 V	32.3 V	32.5 V	32.7 V
Opt. Operating Current (Imp)	9.05 A	9.14 A	9.24 A	9.33 A
Open Circuit Voltage (Voc)	39.3 V	39.5 V	39.7 V	39.9 V
Short Circuit Current (Isc)	9.67 A	9.75 A	9.83 A	9.91 A
Module Efficiency	17.72%	18.02%	18.33%	18.63%
Operating Temperature	-40°C ~ +85°C			
Max. System Voltage	1000 V (IEC) or 1000 V (UL)			
Module Fire Performance	TYPE 1 (UL 1703) or CLASS C (IEC 61730)			
Max. Series Fuse Rating	15 A			
Application Classification	Class A			
Power Tolerance	0 ~ + 5 W			

* Under Standard Test Conditions (STC) of irradiance of 1000 W/m², spectrum AM 1.5 and cell temperature of 25°C.

MECHANICAL DATA

Specification	Data
Cell Type	Mono-crystalline, 6 inch
Cell Arrangement	60 (6×10)
Dimensions	1650×992×40 mm (65.0×39.1×1.57 in)
Weight	18.2 kg (40.1 lbs)
Front Cover	3.2 mm tempered glass
Frame Material	Anodized aluminium alloy
J-Box	IP68, 3 diodes
Cable	4.0 mm² (IEC), 12 AWG (UL), 1000 mm (39.4 in)
Connector	T4 series
Per Pallet	27 pieces, 538 kg (1186.1 lbs)
Per Container (40' HQ)	756 pieces

ELECTRICAL DATA | NMOT*

CS6K	290MS	295MS	300MS	305MS
Nominal Max. Power (Pmax)	215 W	218 W	222 W	226 W
Opt. Operating Voltage (Vmp)	29.7 V	29.8 V	30.0 V	30.2 V
Opt. Operating Current (Imp)	7.24 A	7.32 A	7.40 A	7.48 A
Open Circuit Voltage (Voc)	36.8 V	37.0 V	37.2 V	37.4 V
Short Circuit Current (Isc)	7.81 A	7.87 A	7.93 A	8.00 A

* Under Nominal Module Operating Temperature (NMOT), irradiance of 800 W/m², spectrum AM 1.5, ambient temperature 20°C, wind speed 1 m/s.

TEMPERATURE CHARACTERISTICS

Specification	Data
Temperature Coefficient (Pmax)	-0.39 % / °C
Temperature Coefficient (Voc)	-0.29 % / °C
Temperature Coefficient (Isc)	0.05 % / °C
Nominal Module Operating Temperature (NMOT)	42 ± 2 °C

PERFORMANCE AT LOW IRRADIANCE

Excellent performance at low irradiance, with an average relative efficiency of 97.5 % for irradiances between 200 W/m² and 1000 W/m² (AM 1.5, 25°C).

PARTNER SECTION

The aforesaid datasheet only provides the general information on Canadian Solar products and, due to the on-going innovation and improvement, please always contact your local Canadian Solar sales representative for the updated information on specifications, key features and certification requirements of Canadian Solar products in your region.

Please be kindly advised that PV modules should be handled and installed by qualified people who have professional skills and please carefully read the safety and installation instructions before using our PV modules.

First Solar Series 4™ PV Module

ADVANCED THIN FILM SOLAR TECHNOLOGY

122.5 WATT MODULE EFFICIENCY OF 17.0%

INDUSTRY BENCHMARK SOLAR MODULES

As a global leader in PV energy, First Solar's advanced thin film solar modules have set the industry benchmark with over 17 gigawatts (GW) installed worldwide and a proven performance advantage over conventional crystalline silicon solar modules. Generating more energy than competing modules with the same power rating, First Solar's Series 4™ and Series 4A™ PV Modules deliver superior performance and reliability to our customers.

PROVEN ENERGY YIELD ADVANTAGE

- Generates more energy than conventional crystalline silicon solar modules with the same power due to superior temperature coefficient and superior spectral response
- Anti-reflective coated glass (Series 4A™) enhances energy production

ADVANCED PERFORMANCE & RELIABILITY

- Compatible with advanced 1500V plant architectures
- Independently certified for reliable performance in high temperature, high humidity, extreme desert and coastal environments
- Visit PlantPredict.com - The only Energy Prediction Software designed for Utility Scale PV

CERTIFICATIONS & TESTS

- PID-Free, Thresher Test, Long-Term Sequential Test, and ATLAS 25+[1]
- IEC 61215/61646 1500V, IEC 61730 1500V, CE
- IEC 61701 Salt Mist Corrosion, IEC 60068-2-68 Dust and Sand Resistance
- ISO 9001:2008 and ISO 14001:2004
- UL 1703 Listed Fire Performance PV Module Type 10[2]
- CSI Eligible, FSEC, MCS, CEC Listed (Australia), SII, InMetro

END-OF-LIFE RECYCLING

- Recycling services available through First Solar's industry-leading recycling program or customer-selected third party.

MODULE WARRANTY[3]

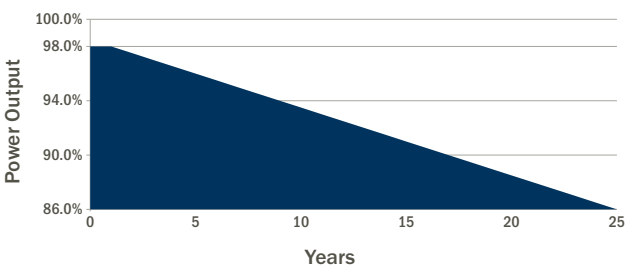

- 25-Year Linear Performance Warranty[4]
- 10-Year Limited Product Warranty

FIRST SOLAR SERIES 4™ PV MODULE

MECHANICAL DESCRIPTION	
Length	1200mm
Width	600mm
Weight	12kg
Thickness	6.8mm
Area	0.72m^2
Individual Leadwire	2.5mm^2, 657mm (minimum from strain relief to connector mating surface)
Connectors	MC4 or MC4-EVO 2[9]
Bypass Diode	None
Cell Type	Thin-film CdTe semiconductor, up to 216 cells
Frame Material	None
Front Glass	3.2mm heat strengthened Series 4A™ includes anti-reflective coating
Back Glass	3.2mm tempered
Encapsulation	Laminate material with edge seal
Load Rating	2400Pa[10]

MODULE NUMBERS AND RATINGS AT STANDARD TEST CONDITIONS (1000W/m^2, AM 1.5, 25°C)[5]							
NOMINAL VALUES		FS-4110-3 FS-4110A-3	FS-4112-3 FS-4112A-3	FS-4115-3 FS-4115A-3	FS-4117-3 FS-4117A-3	FS-4120-3 FS-4120A-3	FS-4122-3 FS-4122A-3
Nominal Power[6] (-0/+5W)	P_{MPP} (W)	110.0	112.5	115.0	117.5	120.0	122.5
Voltage at P_{MAX}	V_{MPP} (V)	67.8	68.5	69.3	70.1	70.8	71.5
Current at P_{MAX}	I_{MPP} (A)	1.62	1.64	1.66	1.68	1.70	1.71
Open Circuit Voltage	V_{OC} (V)	86.4	87.0	87.6	88.1	88.7	88.7
Short Circuit Current	I_{SC} (A)	1.82	1.83	1.83	1.83	1.84	1.85
Module Efficiency	%	15.3	15.6	16.0	16.3	16.7	17.0
Maximum System Voltage	V_{SYS} (V)	1500 [7,8]					
Limiting Reverse Current	I_R (A)	4.0					
Maximum Series Fuse	I_{CF} (A)	4.0					
RATINGS AT NOMINAL OPERATING CELL TEMPERATURE OF 45°C (800W/m^2, 20°C air temperature, AM 1.5, 1m/s wind speed)[5]							
Nominal Power	P_{MPP} (W)	83.2	85.1	87.0	89.0	90.8	92.7
Voltage at P_{MAX}	V_{MPP} (V)	63.5	64.5	64.9	65.9	66.3	67.2
Current at P_{MAX}	I_{MPP} (A)	1.31	1.32	1.34	1.35	1.37	1.38
Open Circuit Voltage	V_{OC} (V)	81.6	82.1	82.7	83.2	83.7	83.7
Short Circuit Current	I_{SC} (A)	1.47	1.47	1.48	1.48	1.48	1.49
TEMPERATURE CHARACTERISTICS							
Module Operating Temperature Range	(°C)	-40 to +85					
Temperature Coefficient of P_{MPP}	T_K (P_{MPP})	-0.28%/°C [Temperature Range: 25°C to 75°C]					
Temperature Coefficient of V_{OC}	T_K (V_{OC})	-0.28%/°C					
Temperature Coefficient of I_{SC}	T_K (I_{SC})	+0.04%/°C					

SUPERIOR SPECTRAL RESPONSE

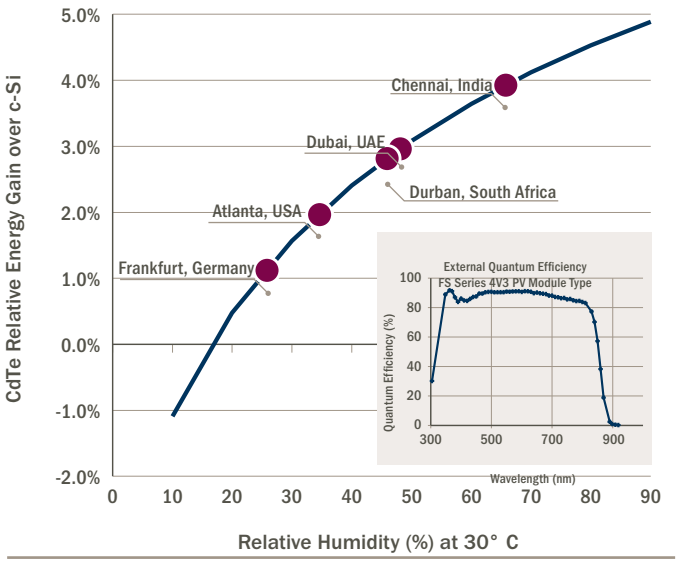

SUPERIOR TEMPERATURE COEFFICIENT

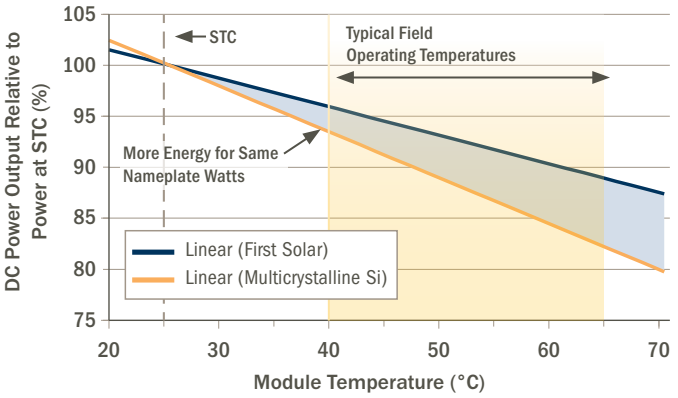

MECHANICAL DRAWING

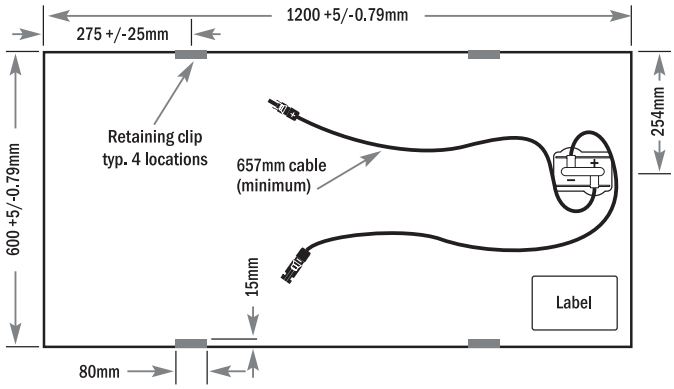

1 Device package meets Atlas 25+
2 Class A Spread of Flame / Class B Burning Brand. Roof mounted fire rating is established by assessing rack and solar module as a unit
3 Limited power output and product warranties subject to warranty terms and conditions
4 Ensures 98% rated power in first year, -0.5%/year through year 25
5 All ratings ± 10%, unless specified otherwise. Specifications are subject to change
6 Measurement uncertainty applies
7 UL 1703 1500V Listed / ULC 1703 1000V Listed
8 Application Class A for 1000V (class II), Application Class B for 1500V (class 0) with MC4; Application Class A for 1000V and 1500V (class II) with MC4-EVO 2
9 Multi-Contact: MC4 (PV-KST4/PV-KBT4) or MC4-EVO 2 (PV-KST-EVO 2 / PV-KBT-EVO 2).
10 Higher load ratings can be met with additional clips or wider clips, subject to testing

Solar Frontier K.K.

Product Data Sheet　SF170-S

SF170-S 170 W Module Data Sheet

1. Electrical Characteristics

1.1 Electrical Performance at Standard Test Conditions (STC)*[1]

		SF170-S
Maximum Power	Pmax	170 W
Tolerance of Pmax		+10 % / -5 %
Open Circuit Voltage	Voc	112 V
Short Circuit Current	Isc	2.20 A
Maximum Power Voltage	Vmpp	87.5 v
Maximum Power Current	Impp	1.95 A

Note *[1]

Standard Test Conditions (STC): 1000 W/m^2 irradiance, cell temperature 25°C and a spectral distribution of irradiance according to air mass 1.5. Isc and Voc are within ±10% tolerance of the rated values at STC.

1.2 Electrical Performance at Nominal Operating Cell Temperature (NOCT) Conditions*[2]

		SF170-S
Maximum Power	Pmax	126 W
Open Circuit Voltage	Voc	102 V
Short Circuit Current	Isc	1.76 A
Maximum Power Voltage	Vmpp	82.1 V
Maximum Power Current	Impp	1.55 A

Note *[2]

Nominal Operating Cell Temperature Conditions: Module operating temperature at 800 W/m^2 irradiance, ambient temperature 20°C, wind speed 1 m/s and open circuit condition.

1.3 Performance at Low Irradiance

Efficiency reduction of maximum power from an irradiance of 1000 W/m^2 to 200W/m^2 at 25°C is typically 2.0%.

The standard deviation for the reduction of efficiency is 1.9%.

1.4 Dependence of Irradiance

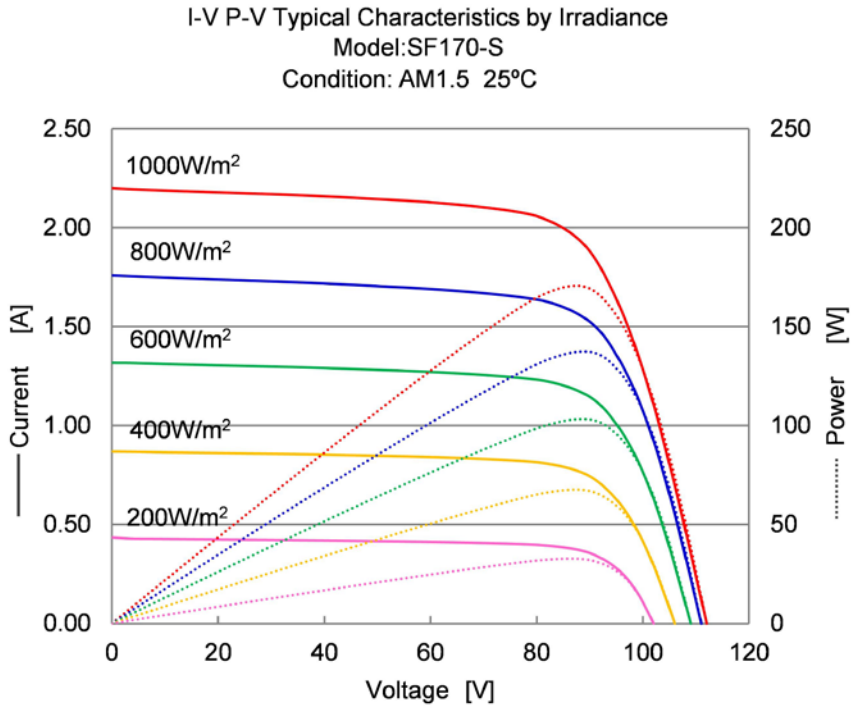

1.5 Thermal Characteristics

NOCT		47°C
Temperature Coefficient of Isc	α	+0.01 % / K
Temperature Coefficient of Voc	β	-0.30 % / K
Temperature Coefficient of Pmax	δ	-0.31 % / K

These thermal characteristics are for reference only.

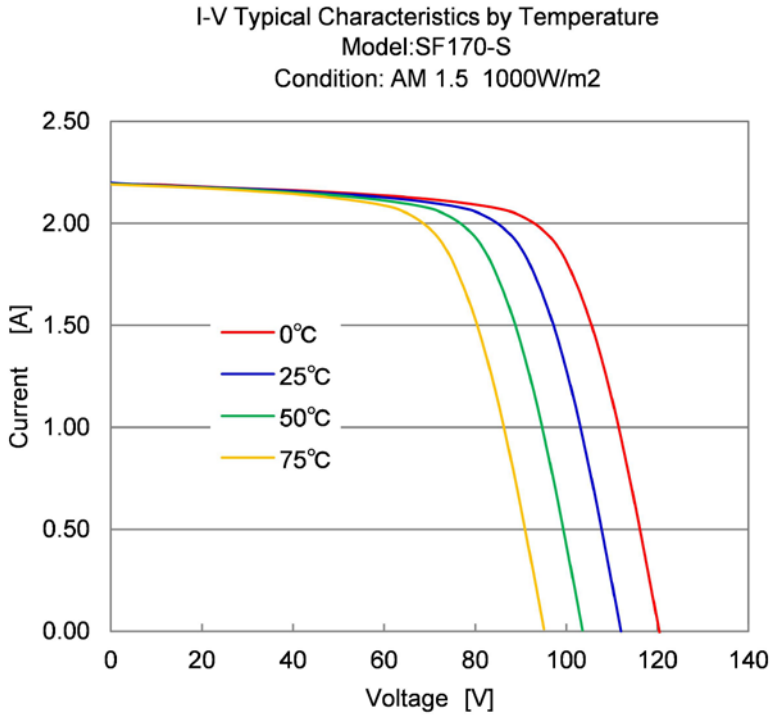

1.6 Characteristics for System Design

Maximum System Voltage	Vsys	1,000V DC
Limiting Reverse Current	Ir	7 A
Maximum Series Fuse Rating	Isf	4 A

2. Mechanical Characteristics

Dimensions (L x W x H)*[3]	1257 x 977 x 35 mm (49.5 x 38.5x 1.4 inch)
Weight	20 kg (44.1 lbs)
Module Operating Temperature	-40°C to 85°C
Application Class on IEC61730	Class A
Fire Safety Class on IEC61730	Class C
Safety Class on IEC61140	II
Snow Load (to the front of the module) *[4]	2400 Pa (IEC61646) / 1600Pa design load (UL1703)
Wind Load (to the back of the module)	2400 Pa (IEC61646) / 1600Pa design load (UL1703)

Cell Type	CIS substrate glass (Cadmium free)
Front Cover	3.2 mm clear tempered glass
Encapsulant	EVA
Back Sheet	Weatherproof plastic film
Frame	Anodized aluminum alloy (Color: black)
Edge Sealant	Butyl rubber
Junction Box	Protection rating: IP67 (with bypass diode)
Adhesive	Silicone
Output Cables (Conductor)	2.5 mm^2 /14AWG (Halogen free)
Cable Lengths (Symmetrical)	1200 mm (47.2 inch)
Connectors	MC4 compatible

Note *3
Dimensional tolerances are stated in the drawing section of this product data sheet.
Note *4
UL: 1.5 times design load is applied to the module. Accordingly, 2400 Pa (50.1lbs /ft^2) is loaded to test the 1600 Pa (33.4 lbs /ft^2) UL design load

3. Qualifications and Compliance

IEC 61646 / IEC 61730 / UL1703 certified

CE-Mark Declaration

No conflict with ROHS

4. Disclaimers

The data contained in this Product Data Sheet indicates nominal data of our products.

Any warranty with respect to the quality or performance of our products will be provided only based on a limited warranty certificate separately issued by Solar Frontier. See the Installation and Maintenance Guide or contact the Technical Service for further information on approved installation and use of this product.

5. Contact

Solar Frontier K.K.

Address: 2-3-2 Daiba, Minato-ward Tokyo, 135-8074 JAPAN

Email: info@solarfrontier.co.jp

Website: www.solar-frontier.com

6. Module Drawing

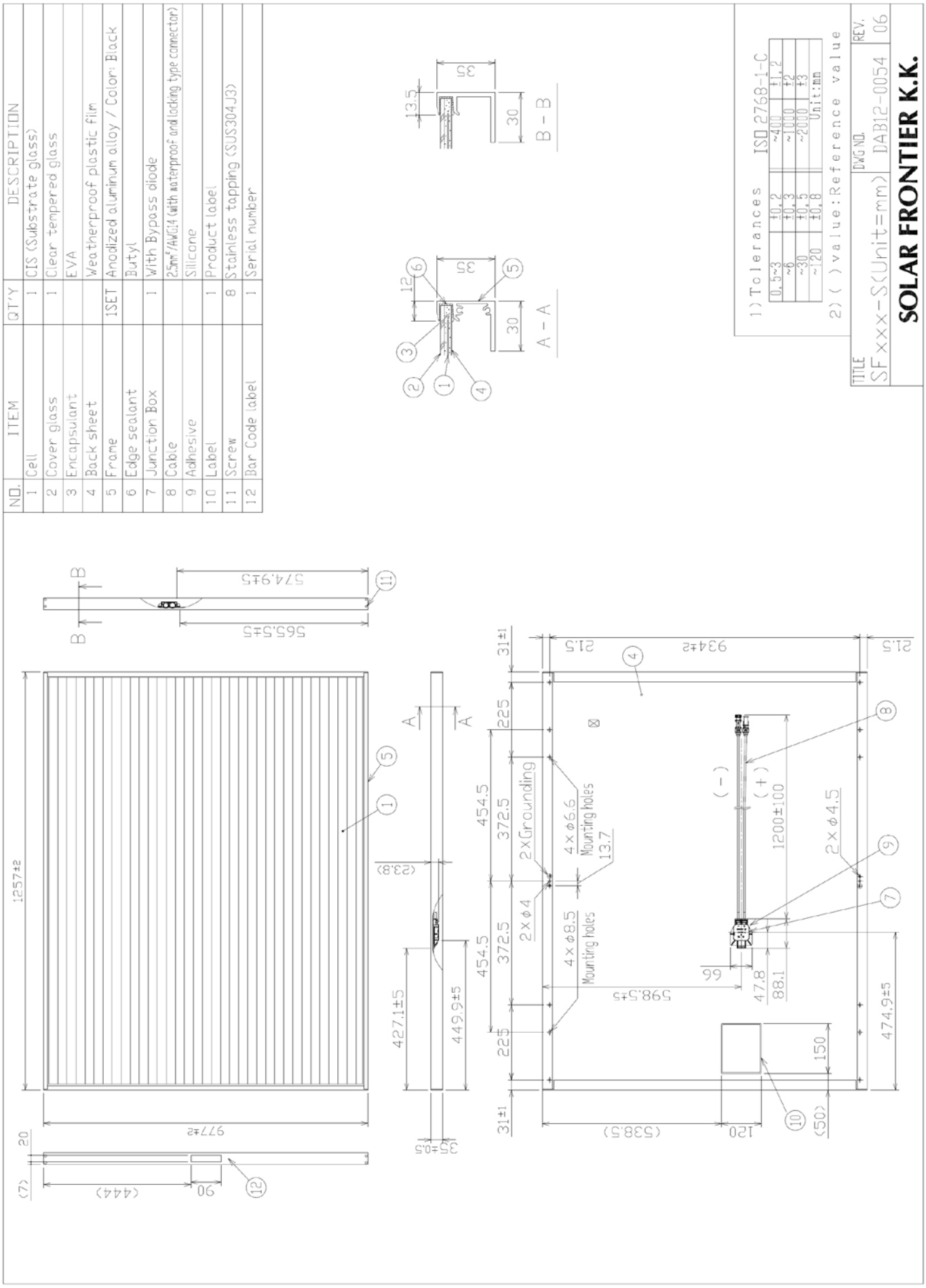


SOLAR
FRONTIER

SUNNY TRIPOWER 5000TL – 12000TL

STP 5000TL-20 / STP 6000TL-20 / STP 7000TL-20 / STP 8000TL-20 / STP 9000TL-20 / STP 10000TL-20 / STP 12000TL-20

Economical

- Maximum efficiency of 98.3 %
- Shade management with OptiTrac Global Peak
- Active temperature management with OptiCool

Flexible

- DC input voltage of up to 1,000 V
- Integrated grid management functions
- Reactive power supply
- Module-tailored system design with Optiflex

Communicative

- SMA Webconnect
- Sunny Portal communication
- SMA and SunSpec Modbus communication
- Simple country configuration
- Multifunction relay comes standard

Easy-to-Use

- Three-phase feed-in
- Cable connection without tools
- SUNCLIX DC plug-in system
- Integrated ESS (Electronic Solar Switch)
- Easy wall mounting

SUNNY TRIPOWER 5000TL – 12000TL

The Three-Phase Inverter – Not Only for Your Home...

...but also perfectly suited to the design of the traditional residential PV system up to the higher power outage range. After all, with the addition of the new 10 kVA and 12 kVA versions to the portfolio, the Sunny Tripower product range covers a broad spectrum of applications. Users benefit from numerous tried-and-tested product features. Highly flexible with its proven Optiflex technology and asymmetrical multistring, it delivers maximum yields with a top efficiency rating and OptiTrac Global Peak. In addition to SMA and Sunspec Modbus communication, it also comes standard with a direct Sunny Portal connection via SMA Webconnect. Other standard features include integrated grid management functions, reactive power supply and suitability for operation with a 30 mA RCD. In summary, when it comes to system design in the 5 kW to 12 kW power classes, the Sunny Tripower is the optimum product solution – for applications ranging from use in your own home and larger PV rooftop systems to implementation of smaller-scale PV farms.

SUNNY TRIPOWER
5000TL / 6000TL / 7000TL / 8000TL / 9000TL / 10000TL / 12000TL

Technical Data	Sunny Tripower 5000TL	Sunny Tripower 6000TL
Input (DC)		
Max. generator power	9000 Wp	9000 Wp
Max. input voltage	1000 V	1000 V
MPP voltage range / rated input voltage	245 V to 800 V/580 V	295 V to 800 V/580 V
Min. input voltage / start input voltage	150 V / 188 V	150 V / 188 V
Max. input current input A / input B	11 A / 10 A	11 A / 10 A
Max. short-circuit current input A / input B	17 A / 15 A	17 A / 15 A
Number of independent MPP inputs / strings per MPP input	2 / A:2; B:2	2 / A:2; B:2
Output (AC)		
Rated power (at 230 V, 50 Hz)	5000 W	6000 W
Max. AC apparent power	5000 VA	6000 VA
Nominal AC voltage	3 / N / PE; 220 / 380 V 3 / N / PE; 230 / 400 V 3 / N / PE; 240 / 415 V	3 / N / PE; 220 / 380 V 3 / N / PE; 230 / 400 V 3 / N / PE; 240 / 415 V
Nominal AC voltage range	160 to 280 V	160 V to 280 V
AC grid frequency / range	50 Hz, 60 Hz / -5 Hz to +5 Hz	50 Hz, 60 Hz / -5 Hz to +5 Hz
Rated power frequency / rated grid voltage	50 Hz / 230 V	50 Hz / 230 V
Max. output current	7.3 A	8.7 A
Power factor at rated power	1	1
Adjustable displacement power factor	0.8 overexcited to 0.8 underexcited	0.8 overexcited to 0.8 underexcited
Feed-in phases / connection phases	3 / 3	3 / 3
Efficiency		
Max. efficiency / European efficiency	98 % / 97.1 %	98 % / 97.4 %
Protective devices		
DC disconnect device	●	●
Ground fault monitoring / grid monitoring	● / ●	● / ●
DC reverse polarity protection / AC short-circuit current capability / galvanically isolated	● / ● / –	● / ● / –
All-pole sensitive residual-current monitoring unit	●	●
Protection class (according to IEC 62103)/overvoltage category (according to IEC 60664-1)	I / III	I / III
General data		
Dimensions (W / H / D)	470 / 730 / 240 mm (18.5 / 28.7 / 9.5 inch)	470 / 730 / 240 mm (18.5 / 28.7 / 9.5 inch)
Weight	37 kg (81.6 lb)	37 kg (81.6 lb)
Operating temperature range	-25 °C to +60 °C (-13 °F to +140 °F)	-25 °C to +60 °C (-13 °F to +140 °F)
Noise emission (typical)	40 dB(A)	40 dB(A)
Self-consumption (at night)	1 W	1 W
Topology / cooling concept	Transformerless / Opticool	Transformerless / Opticool
Degree of protection (according to IEC 60529)	IP65	IP65
Climatic category (according to IEC 60721-3-4)	4K4H	4K4H
Maximum permissible value for relative humidity (non-condensing)	100 %	100 %
Features		
DC connection / AC connection	SUNCLIX / spring-cage terminal	SUNCLIX / spring-cage terminal
Display	Graphic	Graphic
Interface: RS485, Modbus, Speedwire / Webconnect	○ / ● / ●	○ / ● / ●
Multifunction relay / Power Control Module	● / ○	● / ○
Guarantee: 5 / 10 / 15 / 20 years	● / ○ / ○ / ○	● / ○ / ○ / ○
Certificates and permits (more available on request)	AS 4777.2:2015, CE, CEI 0-21:2016, C10/11:2012, DIN EN 62109-1, EN 50438[1], G59/3, G83/2, IEC 61727/MEA[2], IEC 62109-2, NEN EN 50438, NRS 097-2-1, PPC, PPDS, RD 661/2007, RD 1699:2011, SI 4777, UTE C15-712-1, VDE0126-1-1, VDE AR-N 4105, VFR 2013, VFR 2014	
Type designation	STP 5000TL-20	STP 6000TL-20

Sunny Tripower 7000TL	Sunny Tripower 8000TL	Sunny Tripower 9000TL
13500 Wp	13500 Wp	13500 Wp
1000 V	1000 V	1000 V
290 V to 800 V / 580 V	330 V to 800 V / 580 V	370 V to 800 V / 580 V
150 V / 188 V	150 V / 188 V	150 V / 188 V
15 A / 10 A	15 A / 10 A	15 A / 10 A
25 A / 15 A	25 A / 15 A	25 A / 15 A
2 / A:2; B:2	2 / A:2; B:2	2 / A:2; B:2
7000 W	8000 W	9000 W
7000 VA	8000 VA	9000 VA
3 / N / PE; 220 / 380 V 3 / N / PE; 230 / 400 V 3 / N / PE; 240 / 415 V	3 / N / PE; 220 / 380 V 3 / N / PE; 230 / 400 V 3 / N / PE; 240 / 415 V	3 / N / PE; 220 / 380 V 3 / N / PE; 230 / 400 V 3 / N / PE; 240 / 415 V
160 V to 280 V	160 V to 280 V	160 V ... 280 V
50 Hz, 60 Hz / -5 Hz to +5 Hz	50 Hz, 60 Hz / -5 Hz to +5 Hz	50 Hz, 60 Hz / -5 Hz ... +5 Hz
50 Hz / 230 V	50 Hz / 230 V	50 Hz / 230 V
10.2 A	11.6 A	13.1 A
1	1	1
0.8 overexcited to 0.8 underexcited	0.8 overexcited to 0.8 underexcited	0.8 overexcited to 0.8 underexcited
3 / 3	3 / 3	3 / 3
98 % / 97.5 %	98 % / 97.6 %	98 % / 97.6 %
●	●	●
● / ●	● / ●	● / ●
● / ● / –	● / ● / –	● / ● / –
●	●	●
I / III	I / III	I / III
470 / 730 / 240 mm (18.5 / 28.7 / 9.5 inch)	470 / 730 / 240 mm (18.5 / 28.7 / 9.5 inch)	470 / 730 / 240 mm (18.5 / 28.7 / 9.5 inch)
37 kg (81.6 lb)	37 kg (81.6 lb)	37 kg (81.6 lb)
-25 °C to +60 °C (-13 °F to +140 °F)	-25 °C to +60 °C (-13 °F to +140 °F)	-25 °C to +60 °C (-13 °F to +140 °F)
40 dB(A)	40 dB(A)	40 dB(A)
1 W	1 W	1 W
Transformerless / Opticool	Transformerless / Opticool	Transformerless / Opticool
IP65	IP65	IP65
4K4H	4K4H	4K4H
100 %	100 %	100 %
SUNCLIX / spring-cage terminal	SUNCLIX / spring-cage terminal	SUNCLIX / spring-cage terminal
Graphic	Graphic	Graphic
○ / ● / ●	○ / ● / ●	○ / ● / ●
● / ○	● / ○	● / ○
● / ○ / ○ / ○	● / ○ / ○ / ○	● / ○ / ○ / ○
AS 4777.2:2015, CE, CEI 0-21:2016, C10/11:2012, DIN EN 62109-1, EN 50438[1], G59/3, G83/2, IEC 61727/MEA[2], IEC 62109-2, NEN EN 50438, NRS 097-2-1, PPC, PPDS, RD 661/2007, RD 1699:2011, SI 4777, UTE C15-712-1, VDE0126-1-1, VDE AR-N 4105, VFR 2013, VFR 2014		
STP 7000TL-20	STP 8000TL-20	STP 9000TL-20

Efficiency curve

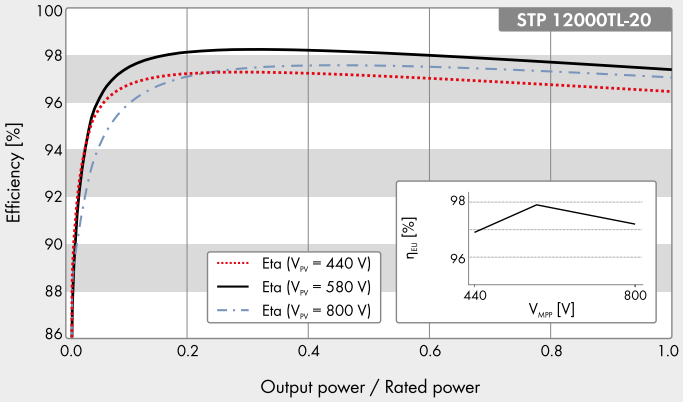

Accessories

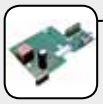

Power Controle Module
PWCBRD-10

RS485 interface
485BRD-10

[1] Does not apply to all national appendices of EN 50438
[2] Only STP 9000TL-20

● Standard feature ○ Optional feature – Not available
Last updated: May 2017
Data at nominal conditions

Sunny Tripower 10000TL	Sunny Tripower 12000TL	
13500 Wp	18000 Wp	
1000 V	1000 V	
370 V to 800 V / 580 V	440 V to 800 V / 580 V	
150 V / 188 V	150 V / 188 V	
18 A / 10 A	18 A / 10 A	
25 A / 15 A	25 A / 15 A	
2 / A:2; B:2	2 / A:2; B:2	
10000 W	12000 W	
10000 VA	12000 VA	
3 / N / PE; 220 / 380 V 3 / N / PE; 230 / 400 V 3 / N / PE; 240 / 415 V	3 / N / PE; 220 / 380 V 3 / N / PE; 230 / 400 V 3 / N / PE; 240 / 415 V	
160 V to 280 V	160 V to 280 V	
50 Hz, 60 Hz / -5 Hz to +5 Hz	50 Hz, 60 Hz / -5 Hz to +5 Hz	
50 Hz / 230 V	50 Hz / 230 V	
14.5 A	17.4 A	
1	1	
0.8 overexcited to 0.8 underexcited	0.8 overexcited to 0.8 underexcited	
3 / 3	3 / 3	
98 % / 97.6 %	98.3 % / 97.9 %	
●	●	
● / ●	● / ●	
● / ● / –	● / ● / –	
●	●	
I / III	I / III	
470 / 730 / 240 mm (18.5 / 28.7 / 9.5 inches)	470 / 730 / 240 mm (18.5 / 28.7 / 9.5 inch)	
37 kg (81.6 lb)	38 kg / 84 lbs	
-25°C to +60 °C (-13 °F to +140 °F)	-25°C to +60 °C (-13 °F to +140 °F)	
40 dB(A)	40 dB(A)	
1 W	1 W	
Transformerless / Opticool	Transformerless / Opticool	
IP65	IP65	
4K4H	4K4H	
100 %	100 %	
SUNCLIX / spring-cage terminal	SUNCLIX / spring-cage terminal	
Graphic	Graphic	
○ / ● / ●	○ / ● / ●	
● / ○	● / ○	
● / ○ / ○ / ○	● / ○ / ○ / ○	
AS 4777.2:2015, CE, CEI 0-21:2016, C10/11:2012, DIN EN 62109-1, EN 50438[1], G59/3, G83/2, IEC 61727/MEA[2], IEC 62109-2, NEN EN 50438, NRS 097-2-1, PPC, PPDS, RD 661/2007, RD 1699:2011, SI 4777, UTE C15-712-1, VDE0126-1-1, VDE AR-N 4105, VFR 2013, VFR 2014		
STP 10000TL-20	STP 12000TL-20	

SUNNY PORTAL

www.SunnyPortal.com
Professional management, monitoring and presentation of PV plants

SUNNY PLACES

www.SunnyPlaces.com
The community portal for private end customers

ENERGY
THAT
CHANGES

SMA

www.SMA-Solar.com

Status: May 2017

Tigo® Flex MLPE

TS4-R
PV Module Retrofit or Add-On

SMART MODULE RETROFIT PLATFORM

The TS4-R is a retrofit solution that brings smart module functionality to standard PV modules, for upgrading underperforming PV systems or adding smart features to new installations. The TS4-R retrofit base can be matched with one of several electronic covers to address a range of functions and budgets. Together they form a new generation of module-level power electronics: flexible, replaceable, upgradeable, and accompanied by a powerful PV 2.0 communication backend.

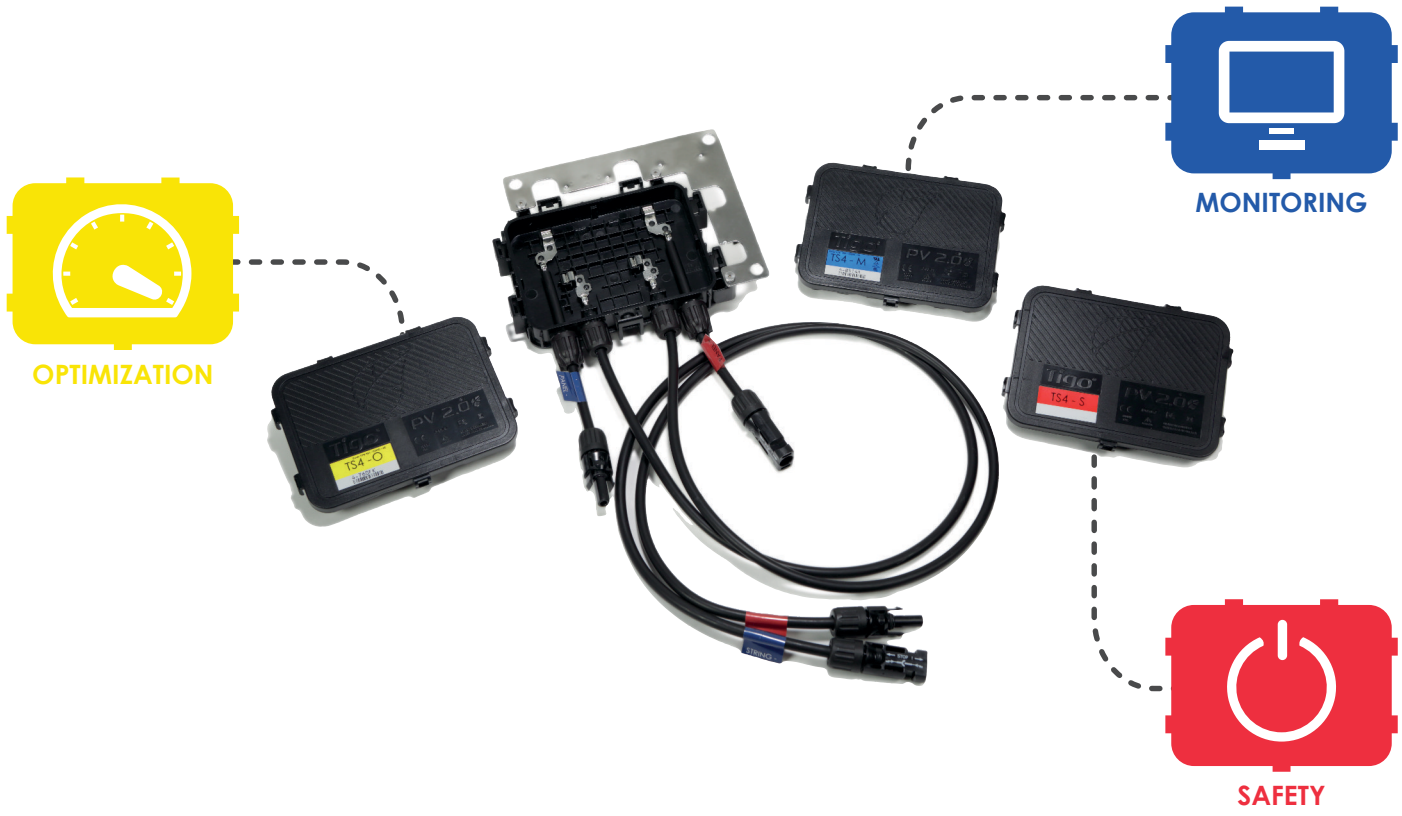

PV 2.0

RETROFIT MODULAR PLATFORM

TS4-R

Type: TS4-R (base up to 1500V)

RETROFIT ADD-ON BASE

Mounting Bracket
Snaps to standard module frame

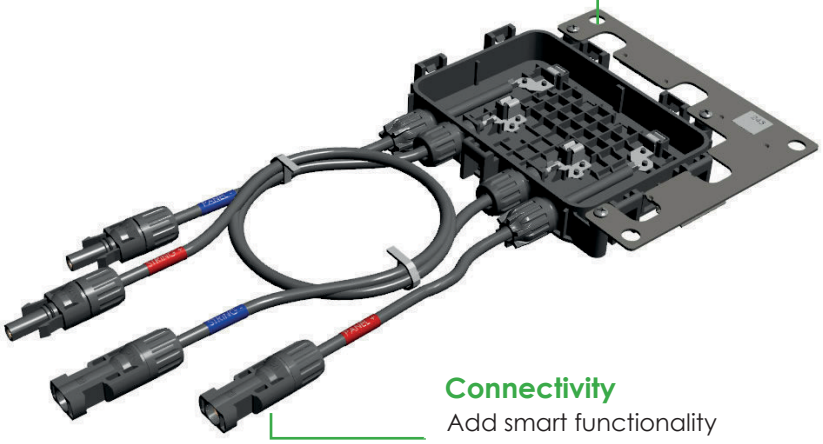

Choice of Electronic Covers
Removable TS4 covers with different levels of functionality

Connectivity
Add smart functionality to a standard module

MECHANICAL SPECIFICATIONS

Mechanical	
Operating Temperature Range	-40°C to +70°C (-40°F to +158°F)
Storage Temperature Range	-40°C to +70°C (-40°F to +158°F)
Cooling Method	Natural Convection
Dimensions (with cover)	152.5mm x 108mm x 25.3mm
Weight (base and cover)	610g (M or S cover), 670g (O cover)
Outdoor Rating	IP67, NEMA 3R
Cabling	
Type	H1Z2Z2-K
Output Length	Standard 1.0m, other lengths on request
Cable Options	1000V rated 1500V rated
Cable Cross-Section	7.15 ± 0.25 mm (1000V) 6.4 ± 0.2mm, 7.05 ± 0.2mm (1500V)
Connectors	MC4, MC4 compatible, Amphenol, EVO2
UV Resistance	500hr with UV light between 300-400nm @65°C
Maximum String Voltage	1500V UL/IEC[1]

[1] All TS4 covers are 1500V compatible. Specify max system voltage when ordering TS4-R bases for appropriate cables & connectors.

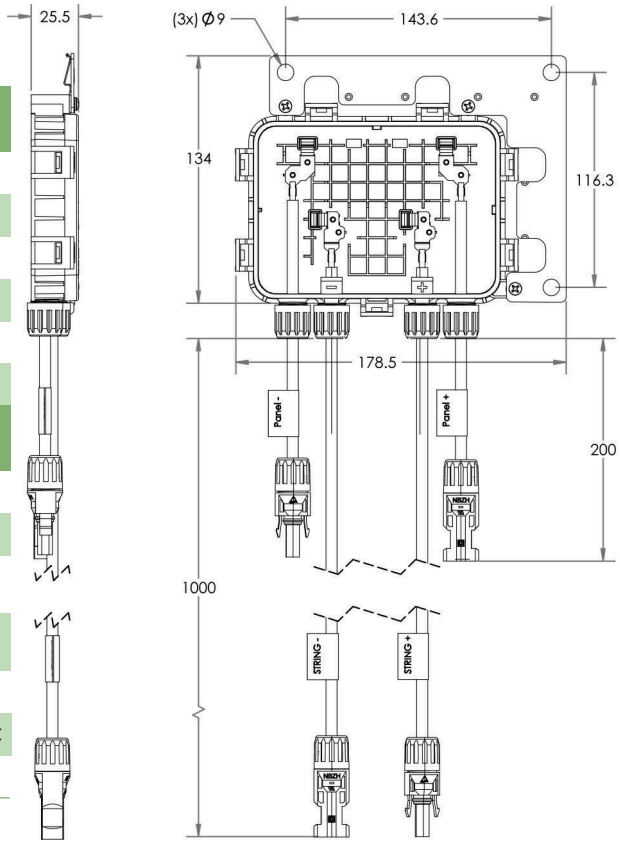

*All dimensions are in mm

UPGRADE YOUR FLEET WITH TS4-R

Tigo has expanded its smart module retrofit platform to provide three levels of customization. With a universal base and a range of covers containing the Flex MLPE, TS4 increases your freedom of choice when selecting features for a particular project and budget. TS4 retrofit cover options include monitoring, safety, and optimized performance features.

OPTIMIZATION

TS4-O

- Shade and mismatch tolerance
- Enhanced energy yield
- Greater design flexibility
- Maximized roof usage
- Plus all the benefits of Safety and Monitoring

SAFETY

TS4-S

- NEC 2014 & 2017 690.12 rapid shutdown compliant
- Module-level deactivation
- Automatic or manual shutdown
- Plus all the benefits of Monitoring

MONITORING

TS4-M

- Reduced O&M costs
- PV-2.0 data synchronization
- Module bar code tracking
- CRM integration
- Warranty tracking
- Fleet management

TS4 COVERS

ELECTRICAL RATINGS	MONITORING TS4-M	SAFETY TS4-S	OPTIMIZATION TS4-O
INPUT			
Rated DC Input Power	475W	475W	475W
Maximum Input Voltage	90V	90V	90V
Maximum Continuous Input Current (I_{MAX})	12A	12A	12A
Maximum V_{OC} @ STC	75V	75V	75V
Minimum V_{MP}	16V	16V	16V
OUTPUT			
Output Power Range	0 - 475W	0 - 475W	0 - 475W
Output Voltage Range	0 - V_{OC}	0 - V_{OC}	0 - V_{OC}
Communication Type	802.15.4 2.4GHz	802.15.4 2.4GHz	802.15.4 2.4GHz
Rapid Shutdown UL Listed[1] (NEC 2014 & 2017 690.12)	No	Yes	Yes
Impedance Matching Capability	No	No	Yes
Output Voltage Limit	No	No	No
Maximum System Voltage	1500V	1500V	1500V
Recommended Fuse Rating	15A	15A	15A

[1] Cloud Connect and Gateway required for rapid shutdown compliance.

ORDERING INFORMATION

Add-on / Retrofit Unit	
TS4-R	1000V TÜV / UL, MC4 compatible, 1m cable
Options	
☐	Connectors (1000V TÜV / UL): MC4, Amphenol, EVO2
☐	1500V TÜV / UL, EVO2 or MC compatible
Pre-Assembled	**Features**
TS4-R-M	Monitoring
TS4-R-S	Safety
TS4-R-O	Optimization

All TS4 covers are 1500V compatible. Specify max system voltage when ordering TS4-R bases for appropriate cables & connectors.

For sales info:
sales@tigoenergy.com or 1.408.402.0802

For product info:
Visit www.tigoenergy.com/products

For TS4-R retrofit units:
Contact your local distributor or sales@tigoenergy.com

For technical info:
http://support.tigoenergy.com

For additional info and product selection assistance, use Tigo's online design tool at www.tigoenergy.com/design

Tigo®

PV 2.0

Tigo Energy, Inc. 420 Blossom Hill Rd, Los Gatos, California 95032 USA | www.tigoenergy.com
P: +1.408.402.0802 F: +1.408.358.6279 | sales@tigoenergy.com

Enphase IQ 6 and IQ 6+ Microinverters

The high-powered smart grid-ready **Enphase IQ 6 Micro™** and **Enphase IQ 6+ Micro™** dramatically simplify the installation process while achieving the highest efficiency for module-level power electronics.

Part of the Enphase IQ System, the IQ 6 and IQ 6+ Micro integrate seamlessly with the Enphase IQ Envoy™, Enphase Q Aggregator™, Enphase IQ Battery™, and the Enphase Enlighten™ monitoring and analysis software.

The IQ 6 and IQ 6+ Micro extend the reliability standards set forth by previous generations and undergo over a million hours of power-on testing, enabling Enphase to provide an industry-leading warranty of up to 25 years.

Easy to Install

- Lightweight and simple
- Faster installation with improved two-wire cabling
- Built-in rapid shutdown compliant (NEC 2014 & 2017)

Productive and Reliable

- Optimized for high powered 60-cell and 72-cell* modules
- More than a million hours of testing
- Class II double-insulated enclosure
- UL listed

Smart Grid Ready

- Complies with fixed power factor, voltage and frequency ride-through requirements
- Remotely updates to respond to changing grid requirements
- Configurable for varying grid profiles
- Meets CA Rule 21 (UL 1741-SA)

* The IQ 6+ Micro is required to support 72-cell modules

UL CERTIFIED SAFETY US-CA E341165

To learn more about Enphase offerings, visit **enphase.com**

ENPHASE

Enphase IQ 6 and IQ 6+ Microinverters

INPUT DATA (DC)	IQ6-60-2-US	IQ6PLUS-72-2-US
Commonly used module pairings[1]	195 W - 330 W +	235 W - 400 W +
Module compatibility	60-cell PV modules only	60-cell and 72-cell PV modules
Maximum input DC voltage	48 V	62 V
Peak power tracking voltage	27 V - 37 V	27 V - 45 V
Operating range	16 V - 48 V	16 V - 62 V
Min/Max start voltage	22 V / 48 V	22 V / 62 V
Max DC short circuit current (module Isc)	15 A	15 A
Overvoltage class DC port	II	II
DC port backfeed under single fault	0 A	0 A
PV array configuration	1 x 1 ungrounded array; No additional DC side protection required; AC side protection requires max 20A per branch circuit	

OUTPUT DATA (AC)	IQ 6 Microinverter		IQ 6+ Microinverter	
Peak output power	240 VA		290 VA	
Maximum continuous output power	230 VA		280 VA	
Nominal (L-L) voltage/range[2]	240 V / 211-264 V	208 V / 183-229 V	240 V / 211-264 V	208 V / 183-229 V
Maximum continuous output current	0.96 A	1.11 A	1.17 A	1.35 A
Nominal frequency	60 Hz		60 Hz	
Extended frequency range	47 - 68 Hz		47 - 68 Hz	
Power factor at rated power	1.0		1.0	
Maximum units per 20 A (L-L) branch circuit	16 (240 VAC) 14 (208 VAC)		13 (240 VAC) 11 (208 VAC)	
Overvoltage class AC port	III		III	
AC port backfeed under single fault	0 A		0 A	
Power factor (adjustable)	0.7 leading ... 0.7 lagging		0.7 leading ... 0.7 lagging	

EFFICIENCY	@240 V	@208 V	@240 V	@208 V
CEC weighted efficiency	97.0 %	97.0 %	97.0 %	97.0 %

MECHANICAL DATA	
Ambient temperature range	-40°C to +65°C
Relative humidity range	4% to 100% (condensing)
Connector type	MC4 locking type
Dimensions (WxHxD)	219 mm x 191 mm x 37.9 mm (without bracket)
Weight	1.29 kg (2.84 lbs)
Cooling	Natural convection - No fans
Approved for wet locations	Yes
Pollution degree	PD3
Enclosure	Class II double-insulated
Environmental category / UV exposure rating	NEMA Type 6 / outdoor

FEATURES	
Communication	Power line
Monitoring	Enlighten Manager and MyEnlighten monitoring options Compatible with Enphase IQ Envoy
Disconnecting means	The AC and DC connectors have been evaluated and approved by UL for use as the load-break disconnect required by NEC 690.
Compliance	CA Rule 21 (UL 1741-SA) UL 62109-1, UL1741/IEEE1547, FCC Part 15 Class B, ICES-0003 Class B, CAN/CSA-C22.2 NO. 107.1-01 This product is UL Listed as PV Rapid Shut Down Equipment and conforms with NEC-2014 and NEC-2017 section 690.12 and C22.1-2015 Rule 64-218 Rapid Shutdown of PV Systems, for AC and DC conductors, when installed according manufacturer's instructions.

1. No enforced DC/AC ratio. See the compatibility calculator at https://enphase.com/en-us/support/module-compatibility.
2. Nominal voltage range can be extended beyond nominal if required by the utility.

To learn more about Enphase offerings, visit **enphase.com**

2018-01-25

ENPHASE.

Appendix C
Economical assumptions

The exchange rates used in this thesis are given in table C.1. The system component costs, installation costs and general feed used in the calculation of the investment cost are given in table C.2.

Table C.1: Exchange rates used in the thesis as the national currency unit per rand. South Africa uses rand (R) as their currency. Exchange rates from 29.01.2018 [63].

Country	Currency [symbol]	Exchange rate [R/currency]
Norway	NOK [kr]	1.5
Euro area	EUR [€]	14.6
United States	USD [$]	11.8
United Kingdom	GBP[£]	16.6

Table C.2: System component cost, installation cost and general feed used in the investment cost calculation. The *Explanation* section explains prices that are assumed and states were the prices are from.

PV system component costs			
Component description	Unit	Price	Explanation
CanadianSolar CS6U-330P	R	2450	Price from a South African store called *sustainable* [50].
CanadianSolar CS6K-305MS	R	2352	At *freecleansolar* [64] the CS6K-305MS module is 4% cheaper than the CS6U-330P module. The same price difference was assumed, and the price was calculated based on the price for the CS6U-330P module in South Africa.
First Solar FS-4120-2	R	1134	Assumes the same price per Wp as the SF170-S module.
Solar Frontier SF170-S	R	1606	Price from South African store called *GW store* [51].
SMA Sunny Tripower 5kW	R	28547	Price from a South African store called *sustainable* [50].
SMA Sunny Tripower 7kW	R	34972	Assumes a linear reduction in price per kW, based on prices for the other SMA inverters.
SMA Sunny Tripower 9kW	R	38780	Price from a South African store called *sustainable* [50].
Optimizer	R	947	Price for the SolarEdge P350 optimizer at the *sustainable* store [50], as a reliable price for the Tigo TS4-R-O optimizer was not found.
Enphase IQ6	R	1416	From an American store called *freecleansolar* [64].
Enphase IQ6+	R	1593	From an American store called *freecleansolar* [64].
Ground mount structure	R/module	840	Price from Solareff.
Roof mount structure	R/module	308	Price from a South African store called *sustainable* [50].
Cabling and general	R/kWp	1620	Price from Solareff.

Balance of system components			
Description	Unit	Price	Explanation
SMA Sunny Home Manager	R	4320	Price from Solareff.
SMA Energy Meter	R	6960	Price from Solareff.
Industrial router	R	4800	Price from Solareff.
Irradiance sensor	R	6059	Price from Solareff.
PT 1000 Temp Sensor	R	2580	Price from Solareff.
Bulk Supply Meter	R	7800	Price from Solareff.

Installation costs and fees			
Description	Unit	Price	Explanation
Electrical installation	R/kWp	1092	Price from Solareff.
Engineering and draughting	R/kWp	820	Price from Solareff.
Project management	R/kWp	446	Price from Solareff.
Transport and site establishment	R/kWp	203	Price from Solareff.
Lightning protection	R/kWp	240	Price from Solareff.
Health and safety allowance	R	6000	Price from Solareff.
Structural Engineering	R	6000	Price from Solareff.
Commissioning	R	3600	Price from Solareff.
Eskom application fee	R	20000	Price from Solareff.

Appendix D

Roof mounted system results for the individual buildings

The simulation results for the roof mounted system configurations listed in table 3.19. The simulation results are presented in table D.1.

Table D.1: Simulation results for the roof mounted systems presented in table 3.19. The simulation results are for the individual buildings. Systems marked with an r are the same as the system above, only with reduced amounts of modules.

System	System yield [kWh]	Specific yield [kWh/kWp]	PR [%]	Efficiency loss temp. [%]	Electrical loss [%]	Inverter loss [%]	Unavailability loss [%]
Building 1 and 1.2							
R1.1.1	11059	1396	72.4	7.6	2.7	2.9	1.8
R1.2.1	11244	1420	73.6	7.6	1.5	2.9	1.6
R1.3.1	11537	1457	75.5	7.8	1.6	3.3	1.4
R1.1.2	11222	1415	73.1	7	2.4	3	2.6
R1.2.2	11387	1436	74.2	7	1.4	3	1.7
R1.3.2	11737	1480	76.5	7.2	1.7	3.1	1.7
R1.1.3	11292	1494	77.4	5.5	-	2.4	1.6
R1.1.4	10957	1535	79.5	6.1	-	2.5	1.6
Building 2							
R2.1.1	19704	1389	77.3	7	0.2	3.1	1.6
R2.1.1r	11525	1397	77.7	7	0.1	2.7	1.6
R2.2.1	19722	1390	77.4	7	0.1	3.1	1.8
R2.3.1	20400	1435	79.9	7.2	0	3.3	1.4
R2.1.2	19251	1403	78.1	6.4	0.1	3.3	1.8
R2.1.2r	10760	1411	78.5	6.4	0	3	1.8
R2.2.2	19326	1408	78.4	6.4	0.1	3.2	1.8
R2.3.2	19960	1454	80.9	6.6	0.1	2.9	1.8
R2.1.3	19261	1433	79.8	5.1	-	2.6	1.8
R2.1.4	18709	1487	82.8	5.6	-	2.6	1.8
Building 3							
R3.1.1	8690	1463	72	7.9	2.2	3.7	2
R3.2.1	8765	1476	72.6	7.9	1.5	3.6	2
R3.3.1	9140	1539	75.7	8.2	1.3	3.3	1.5
R3.1.2	9054	1484	73	7.2	2	3.7	2
R3.2.2	9125	1496	73.6	7.3	1.3	3.7	2
R3.3.2	9447	1549	76.2	7.5	0.9	3.3	2.5
R3.1.3	7889	1565	77.0	5.8	-	2.6	2
R3.1.4	7680	1614	79.4	6.4	-	2.6	2

Appendix E
Simulation results

PV syst produces a six page report from each simulation, and as over a 100 simulations were performed, it would be unfeasible to show them all in the thesis. The most important results were shown in the result and discussion section. This section shows an example of a simulation report for system R1.1.1 R2.1.1r R3.1.1.

The following information is given in the report:

- The first page shows the location for the simulated system, the albedo value and the weather data used.
- The system string design are then displayed on page two and three. It lists the design for each sub-array used in the simulation. It also gives information about the module and inverter types, and the number of each that are used in the simulation.
- The loss factors used in the simulation are stated at the end of page two and page three.
- Page four gives information about the horizon used.
- Page five shows the 3D scene used in the simulation and the iso-shading diagram for the scene.
- Page six illustrates the monthly system performance and yield. The figures also show the system losses and array losses each month. At the end of the page, monthly values of the main simulation results are given.
- Page seven shows the loss diagram over the whole year.

Grid-Connected System: Simulation parameters

Project : **Panthera Africa roof system**

Geographical Site	**Panthera Africa**		Country	**South Africa**	
Situation		Latitude	-34.46° S	Longitude	19.53° E
Time defined as		Legal Time	Time zone UT+2	Altitude	113 m

Monthly albedo values

	Jan.	Feb.	Mar.	Apr.	May	June	July	Aug.	Sep.	Oct.	Nov.	Dec.
Albedo	0.25	0.25	0.25	0.25	0.25	0.20	0.20	0.20	0.25	0.25	0.25	0.25

Meteo data: **Panthera Africa** Weighted average, Stanford weather station - Synthetic

Simulation variant : **R1.1, R2.1, R3.1 SMA, CS6U-330P v4 smaller building 2**

Simulation date 05/02/18 00h50
Simulation for the **first year of operation**

Simulation parameters

4 orientations	Tilts/Azimuths	35°/20°, 5°/20°, 0°/18°, 23°/-7°		
Models used	Transposition	Perez	Diffuse	Perez, Meteonorm
Horizon	Average Height	2.8°		
Near Shadings	Detailed electrical calculation	(acc. to module layout)		

PV Arrays Characteristics (6 kinds of array defined)

PV module Si-poly	Model	**CS6U - 330P 1000V**		
Original PVsyst database	Manufacturer	Canadian Solar Inc.		
Sub-array "Building 1"	Orientation	#1	Tilt/Azimuth	35°/20°
Number of PV modules	In series	10 modules	In parallel	1 strings
Total number of PV modules	Nb. modules	10	Unit Nom. Power	330 Wp
Array global power	Nominal (STC)	**3300 Wp**	At operating cond.	2964 Wp (50°C)
Array operating characteristics (50°C)	U mpp	332 V	I mpp	8.9 A
Sub-array "Building 1.2"	Orientation	#2	Tilt/Azimuth	5°/20°
Number of PV modules	In series	14 modules	In parallel	1 strings
Total number of PV modules	Nb. modules	14	Unit Nom. Power	330 Wp
Array global power	Nominal (STC)	**4620 Wp**	At operating cond.	4149 Wp (50°C)
Array operating characteristics (50°C)	U mpp	465 V	I mpp	8.9 A
Sub-array "Building 2.3"	Orientation	#3	Tilt/Azimuth	0°/18°
Number of PV modules	In series	15 modules	In parallel	1 strings
Total number of PV modules	Nb. modules	15	Unit Nom. Power	330 Wp
Array global power	Nominal (STC)	**4950 Wp**	At operating cond.	4445 Wp (50°C)
Array operating characteristics (50°C)	U mpp	498 V	I mpp	8.9 A
Sub-array "Building 2.4"	Orientation	#3	Tilt/Azimuth	0°/18°
Number of PV modules	In series	10 modules	In parallel	1 strings
Total number of PV modules	Nb. modules	10	Unit Nom. Power	330 Wp
Array global power	Nominal (STC)	**3300 Wp**	At operating cond.	2964 Wp (50°C)
Array operating characteristics (50°C)	U mpp	332 V	I mpp	8.9 A
Sub-array "Building 3.1"	Orientation	#4	Tilt/Azimuth	23°/-7°
Number of PV modules	In series	9 modules	In parallel	1 strings
Total number of PV modules	Nb. modules	9	Unit Nom. Power	330 Wp
Array global power	Nominal (STC)	**2970 Wp**	At operating cond.	2667 Wp (50°C)
Array operating characteristics (50°C)	U mpp	299 V	I mpp	8.9 A

Grid-Connected System: Simulation parameters (continued)

Sub-array "Building 3.2"	Orientation	#4	Tilt/Azimuth	23°/-7°
Number of PV modules	In series	9 modules	In parallel	1 strings
Total number of PV modules	Nb. modules	9	Unit Nom. Power	330 Wp
Array global power	Nominal (STC)	**2970 Wp**	At operating cond.	2667 Wp (50°C)
Array operating characteristics (50°C)	U mpp	299 V	I mpp	8.9 A
Total Arrays global power	Nominal (STC)	**22 kWp**	Total	67 modules
	Module area	**130 m²**	Cell area	117 m²

Sub-array "Building 1" : Inverter	Model	**Sunny Tripower 7000TL-20**		
Original PVsyst database	Manufacturer	SMA		
Characteristics	Operating Voltage	290-800 V	Unit Nom. Power	7.00 kWac
Inverter pack	Nb. of inverters	1 * MPPT 0.40	Total Power	2.9 kWac
Sub-array "Building 1.2" : Inverter	Model	**Sunny Tripower 7000TL-20**		
Original PVsyst database	Manufacturer	SMA		
Characteristics	Operating Voltage	290-800 V	Unit Nom. Power	7.00 kWac
Inverter pack	Nb. of inverters	1 * MPPT 0.60	Total Power	4.1 kWac
Sub-array "Building 2.3" : Inverter	Model	**Sunny Tripower 7000TL-20**		
Original PVsyst database	Manufacturer	SMA		
Characteristics	Operating Voltage	290-800 V	Unit Nom. Power	7.00 kWac
Inverter pack	Nb. of inverters	1 * MPPT 0.60	Total Power	4.2 kWac
Sub-array "Building 2.4" : Inverter	Model	**Sunny Tripower 7000TL-20**		
Original PVsyst database	Manufacturer	SMA		
Characteristics	Operating Voltage	290-800 V	Unit Nom. Power	7.00 kWac
Inverter pack	Nb. of inverters	1 * MPPT 0.40	Total Power	2.8 kWac
Sub-array "Building 3.1" : Inverter	Model	**Sunny Tripower 5000TL-20**		
Original PVsyst database	Manufacturer	SMA		
Characteristics	Operating Voltage	245-800 V	Unit Nom. Power	5.00 kWac
Inverter pack	Nb. of inverters	1 * MPPT 0.52	Total Power	2.5 kWac
Sub-array "Building 3.2" : Inverter	Model	**Sunny Tripower 5000TL-20**		
Original PVsyst database	Manufacturer	SMA		
Characteristics	Operating Voltage	245-800 V	Unit Nom. Power	5.00 kWac
Inverter pack	Nb. of inverters	1 * MPPT 0.48	Total Power	2.5 kWac
Total	Nb. of inverters	3	Total Power	19 kWac

PV Array loss factors

Array Soiling Losses

Jan.	Feb.	Mar.	Apr.	May	June	July	Aug.	Sep.	Oct.	Nov.	Dec.
6.0%	6.0%	3.0%	3.0%	2.0%	2.0%	2.0%	2.0%	3.0%	3.0%	6.0%	6.0%

Thermal Loss factor	Uc (const)	20.0 W/m²K	Uv (wind)	0.0 W/m²K / m/s
Wiring Ohmic Loss	Array#1	418 mOhm	Loss Fraction	1.0 % at STC
	Array#2	585 mOhm	Loss Fraction	1.0 % at STC
	Array#3	627 mOhm	Loss Fraction	1.0 % at STC
	Array#4	418 mOhm	Loss Fraction	1.0 % at STC
	Array#5	376 mOhm	Loss Fraction	1.0 % at STC
	Array#6	376 mOhm	Loss Fraction	1.0 % at STC
	Global		Loss Fraction	1.0 % at STC
LID - Light Induced Degradation			Loss Fraction	2.0 %
Module Quality Loss			Loss Fraction	-0.4 %
Module Mismatch Losses			Loss Fraction	1.0 % at MPP
Module average degradation	Year no	1	Loss factor	0.4 %/year
Mismatch due to degradation	Imp RMS dispersion	0.4 %/year	Voc dispersion RMS	0.4 %/year
Incidence effect, ASHRAE parametrization	IAM =	1 - bo (1/cos i - 1)	bo Param.	0.05

Grid-Connected System: Simulation parameters (continued)

System loss factors

Wiring Ohmic Loss	Wires: 3x10.0 mm² 40 m	Loss Fraction 1.0 % at STC
Unavailability of the system	7.3 days, 3 periods	Time fraction 2.0 %

User's needs : Unlimited load (grid)

Grid-Connected System: Horizon definition

Project : **Panthera Africa roof system**

Simulation variant : **R1.1, R2.1, R3.1 SMA, CS6U-330P v4 smaller building 2**

Simulation for the first year of operation

Main system parameters		System type	**Grid-Connected**		
Horizon		Average Height	2.8°		
Near Shadings		Detailed electrical calculation	(acc. to module layout)		
PV Field Orientation		4 orientations	Tilt/Azimuth = 35°/20°, 5°/20°, 0°/18°, 23°/-7°		
PV modules		Model	CS6U - 330P 1000V	Pnom	330 Wp
PV Array		Nb. of modules	67	Pnom total	**22.11 kWp**
Inverter		Model	Sunny Tripower 7000TL-20	Pnom	7.00 kW ac
Inverter		Model	Sunny Tripower 5000TL-20	Pnom	5.00 kW ac
Inverter pack		Nb. of units	3.0	Pnom total	**19.00 kW ac**
User's needs		Unlimited load (grid)			

Horizon

Average Height	2.8°	Diffuse Factor	0.98
Albedo Factor	100 %	Albedo Fraction	0.85

Height [°]	3.0	3.0	2.0	2.0	3.0	3.0	2.0	2.0	3.0	3.0	4.0	4.0
Azimuth [°]	-180	-147	-146	-126	-125	-118	-117	-109	-108	-83	-82	-70
Height [°]	5.0	5.0	4.0	4.0	3.0	3.0	4.0	4.0	3.0	3.0	2.0	2.0
Azimuth [°]	-69	-57	-56	-43	-42	-18	-17	-12	-11	11	12	23
Height [°]	3.0	3.0	2.0	2.0	1.0	1.0	3.0	2.0	3.0	2.0	2.0	3.0
Azimuth [°]	24	26	27	75	76	111	113	114	115	116	119	120
Height [°]	3.0	4.0	4.0	5.0	5.0	4.0	4.0	3.0	3.0			
Azimuth [°]	146	147	150	151	154	155	163	164	180			

Meteonorm horizon for, Lat. = 0.000°, Long. = 0.000°

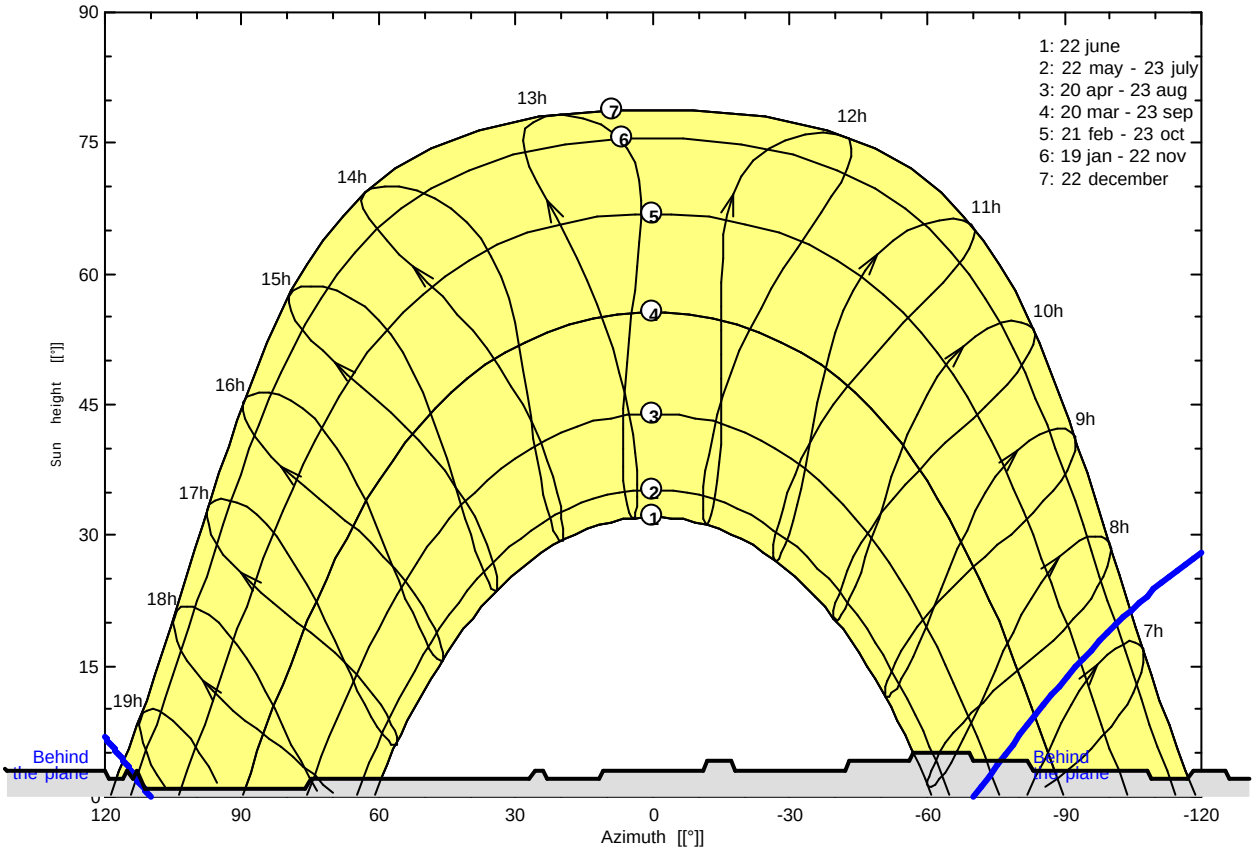

Grid-Connected System: Near shading definition

Project : **Panthera Africa roof system**

Simulation variant : **R1.1, R2.1, R3.1 SMA, CS6U-330P v4 smaller building 2**

Simulation for the first year of operation

Main system parameters	System type	**Grid-Connected**			
Horizon	Average Height	2.8°			
Near Shadings	Detailed electrical calculation	(acc. to module layout)			
PV Field Orientation	4 orientations	Tilt/Azimuth = 35°/20°, 5°/20°, 0°/18°, 23°/-7°			
PV modules	Model	CS6U - 330P 1000V	Pnom	330 Wp	
PV Array	Nb. of modules	67	Pnom total	**22.11 kWp**	
Inverter	Model	Sunny Tripower 7000TL-20	Pnom	7.00 kW ac	
Inverter	Model	Sunny Tripower 5000TL-20	Pnom	5.00 kW ac	
Inverter pack	Nb. of units	3.0	Pnom total	**19.00 kW ac**	
User's needs	Unlimited load (grid)				

Perspective of the PV-field and surrounding shading scene

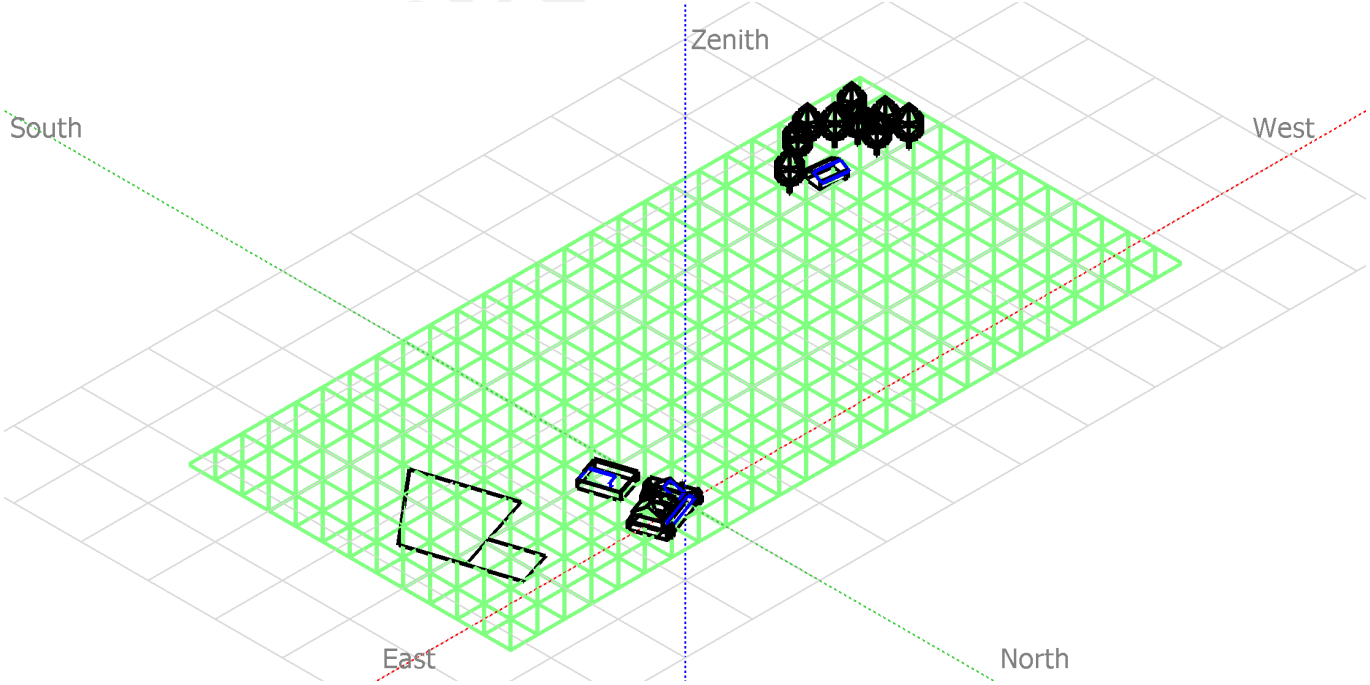

Iso-shadings diagram

Panthera Africa roof system

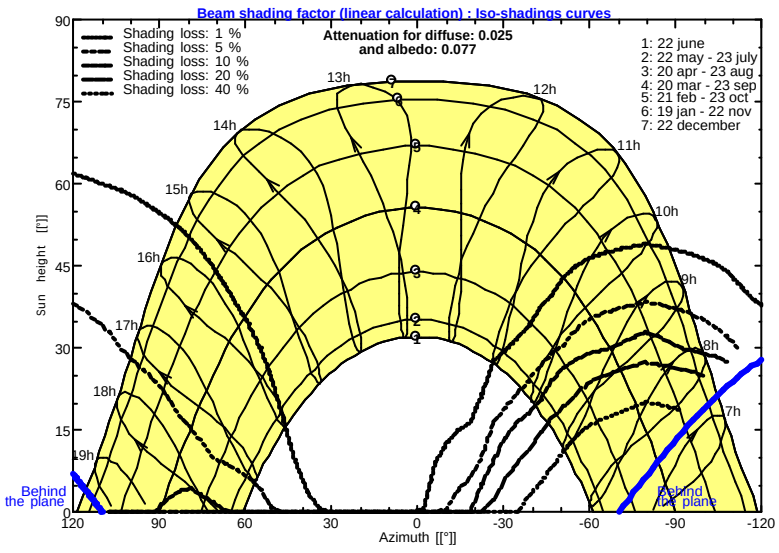

Grid-Connected System: Main results

Project : **Panthera Africa roof system**

Simulation variant : **R1.1, R2.1, R3.1 SMA, CS6U-330P v4 smaller building 2**

Simulation for the first year of operation

Main system parameters	System type	**Grid-Connected**			
Horizon	Average Height	2.8°			
Near Shadings	Detailed electrical calculation	(acc. to module layout)			
PV Field Orientation	4 orientations	Tilt/Azimuth = 35°/20°, 5°/20°, 0°/18°, 23°/-7°			
PV modules	Model	CS6U - 330P 1000V	Pnom	330 Wp	
PV Array	Nb. of modules	67	Pnom total	**22.11 kWp**	
Inverter	Model	Sunny Tripower 7000TL-20	Pnom	7.00 kW ac	
Inverter	Model	Sunny Tripower 5000TL-20	Pnom	5.00 kW ac	
Inverter pack	Nb. of units	3.0	Pnom total	**19.00 kW ac**	
User's needs	Unlimited load (grid)				

Main simulation results

System Production — **Produced Energy** **31.44 MWh/year** Specific prod. 1422 kWh/kWp/year

Performance Ratio PR 74.55 %

Normalized productions (per installed kWp): Nominal power 22.11 kWp

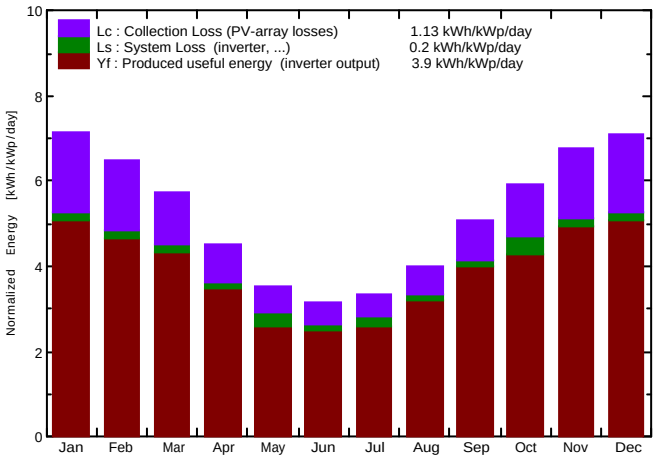

Performance Ratio PR

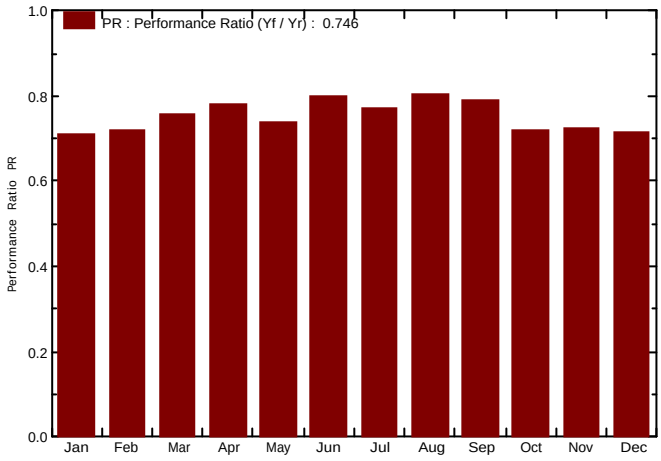

R1.1, R2.1, R3.1 SMA, CS6U-330P v4 smaller building 2

Balances and main results

	GlobHor kWh/m²	DiffHor kWh/m²	T Amb °C	GlobInc kWh/m²	GlobEff kWh/m²	EArray MWh	E_Grid MWh	PR
January	225.5	71.40	21.30	221.1	192.8	3.606	3.471	0.710
February	178.5	57.80	21.20	181.3	159.4	2.998	2.890	0.721
March	166.4	56.10	19.80	177.8	162.2	3.093	2.981	0.758
April	118.6	40.40	17.60	134.9	123.3	2.410	2.325	0.779
May	90.3	32.60	15.50	109.0	99.9	1.992	1.782	0.739
June	75.1	26.70	13.30	94.3	85.8	1.734	1.662	0.797
July	84.3	29.00	12.80	104.2	95.0	1.923	1.774	0.770
August	107.3	38.40	12.90	123.8	114.1	2.286	2.206	0.806
September	139.3	50.10	14.30	152.1	138.8	2.746	2.653	0.789
October	178.6	66.30	16.10	184.4	167.9	3.233	2.940	0.721
November	205.9	68.90	17.70	203.9	178.1	3.386	3.265	0.724
December	227.0	76.60	19.99	220.6	192.0	3.623	3.492	0.716
Year	1796.8	614.30	16.85	1907.4	1709.4	33.031	31.439	0.746

Legends:

GlobHor	Horizontal global irradiation	GlobEff	Effective Global, corr. for IAM and shadings
DiffHor	Horizontal diffuse irradiation	EArray	Effective energy at the output of the array
T Amb	Ambient Temperature	E_Grid	Energy injected into grid
GlobInc	Global incident in coll. plane	PR	Performance Ratio

Grid-Connected System: Loss diagram

Project : **Panthera Africa roof system**

Simulation variant : **R1.1, R2.1, R3.1 SMA, CS6U-330P v4 smaller building 2**

Simulation for the first year of operation

Main system parameters	System type	**Grid-Connected**			
Horizon	Average Height	2.8°			
Near Shadings	Detailed electrical calculation	(acc. to module layout)			
PV Field Orientation	4 orientations	Tilt/Azimuth = 35°/20°, 5°/20°, 0°/18°, 23°/-7°			
PV modules	Model	CS6U - 330P 1000V	Pnom	330 Wp	
PV Array	Nb. of modules	67	Pnom total	**22.11 kWp**	
Inverter	Model	Sunny Tripower 7000TL-20	Pnom	7.00 kW ac	
Inverter	Model	Sunny Tripower 5000TL-20	Pnom	5.00 kW ac	
Inverter pack	Nb. of units	3.0	Pnom total	**19.00 kW ac**	
User's needs	Unlimited load (grid)				

Loss diagram over the whole year

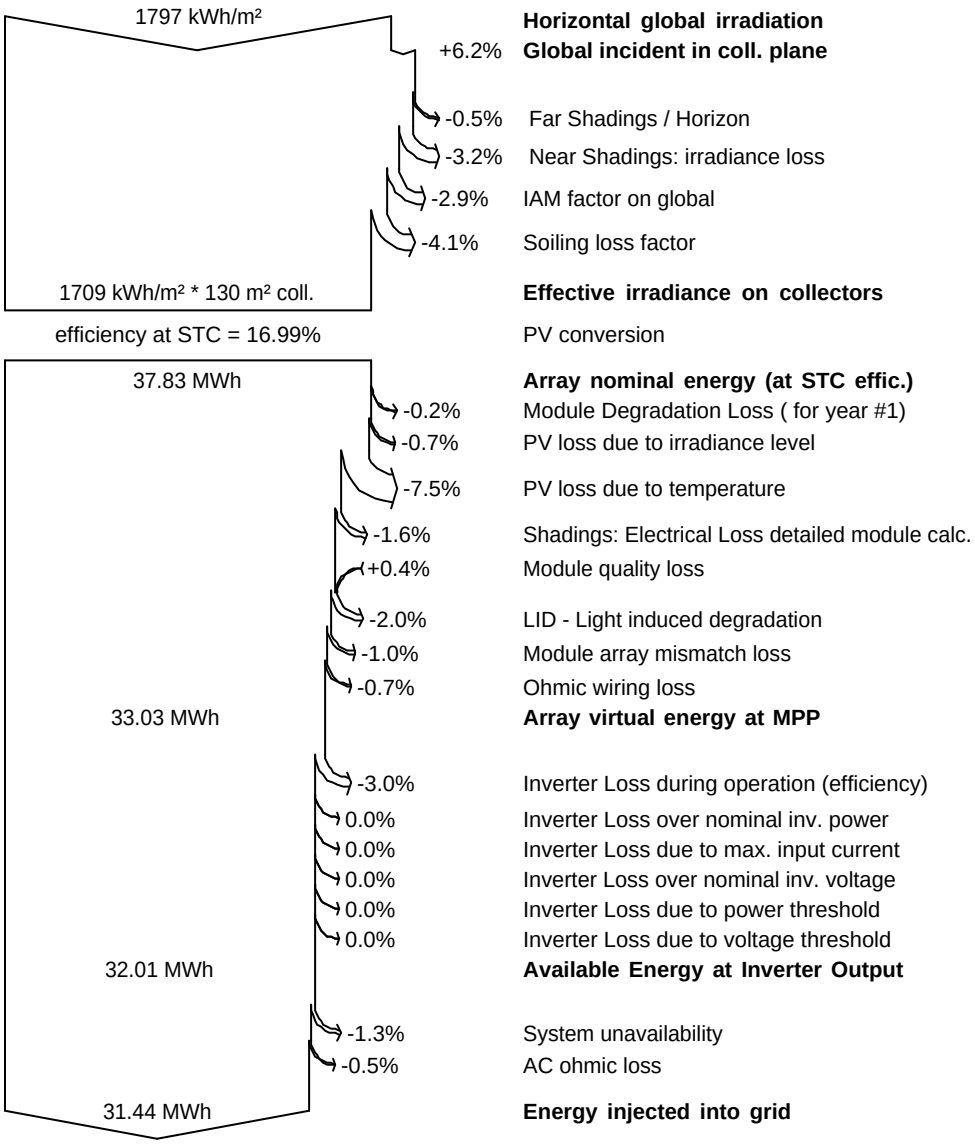

Appendix F
Energy amount to buy or sell

The energy each system simulated in the main simulation needs to buy or sell for each month of the year is listed in table F.1. The energy amount is calculated based on the 2016 consumption at Panthera Africa and the system production from table 4.2 and 4.3. The system production numbers are from the main simulation.

Table F.1: Energy needed to buy or sell for each system. A negative sign indicates a need to buy and a positive value indicates a need to sell the energy.

	Energy amount needed to buy or sell [kWh]											
	R1.1	R1.2	R1.3m	R1.4	R1.5	R1.6m	R1.7	R1.8	G1.1	G2.1	G3.1	G4.1
Jan	-16	26	420	-65	-20	462	958	796	-479	-395	-280	-521
Feb	-1167	-1131	-967	-1180	-1151	-776	-409	-533	-1252	-1175	-1250	-1290
Mar	-905	-875	-610	-902	-885	-542	-210	-333	-803	-721	-797	-847
Apr	-644	-742	-445	-652	-632	-603	-191	-262	-377	-307	-579	-422
May	-1361	-1370	-1073	-1360	-1380	-1008	-1157	-1102	-838	-776	-863	-880
Jun	-1401	-1374	-1272	-1398	-1439	-1286	-1279	-1183	-971	-916	-1087	-1009
Jul	-1939	-1841	-1897	-1941	-1900	-1760	-1576	-1700	-1426	-1365	-1550	-1471
Aug	-628	-844	-450	-642	-790	-386	-235	-294	-334	-268	-366	-391
Sept	-754	-726	-679	-757	-737	-439	-205	-293	-704	-633	-616	-755
Oct	-872	-657	-357	-878	-677	-296	-282	-270	-730	-649	-952	-788
Nov	-547	-513	-154	-586	-553	-111	336	186	-765	-683	-777	-819
Dec	-665	-625	-231	-718	-674	-474	311	146	-1303	-1225	-1009	-1349
Total buy	-10899	-10698	-8135	-11079	-10838	-7681	-5544	-5970	-9982	-9113	-10126	-10542
Total sell	0	26	420	0	0	462	1605	1128	0	0	0	0

Appendix G
Economical evaluation

As only the main financial results and financial assumptions are shown in the economical evaluation, the Excel spreadsheet used to calculate the investment cost and the economical values are shown in this appendix. The spreadsheet is only shown for the system R1.1.1 R2.1.1r R3.1.1, as it is not feasible to show all ten spreadsheets.

Figure G.1 shows the spreadsheet used to calculate the investment cost. Figure G.2 shows the spreadsheet used to calculate the levelized cost of electricity. Figure G.3 shows the spreadsheet for calculating the NPV and payback time.

			R1.1 Number of components	Total price
	Unit	Price		
CS6U-330P module	R/module	2450	67	164150
SMA 5kW	R	28547	1	28547
SMA 7kW	R	34972	2	69944
SMA 9 kW	R	38780	0	0
Optimizer	R	947	0	0
Enphase IQ6	R	1416	0	0
Enphase IQ6+	R	1593	0	0
Ground mount structure	R/module	840	0	0
Roof mount structure	R/module	308	67	20636
Cabling	R/kWp	1620	22	35640
Other BoS				
SMA monitoring	R	24718.8	1	24718.8
Bulk Supply Meter	R	7800	1	7800
Installation				
Variable	R/kWp	2801	22	61622
Fixed	R	35600	1	35600
Total				448658

Figure G.1: Spreadsheet used in the economical evaluation to calculate investment costs.

System inputs										Electricity charges		
System lifetime	25	year	Installed capacity	22	kW					Network Demand	0.2369	R/kWh
Discount rate	7	%	Electricity sold to utility	0.1						Ancillary service	0.0037	R/kWh
Annual degradation	0.4	%/year	Electricity consumed	0.3						Energy charge	0.3483	R/kWh
RV	10	%investment cost	Electricity produced	31441	kWh/year					Total energy charge	1.1689	R/kWh
O&M	260	R/kW	Inverter replacement cost	36491	R							
Investment support	28	%investment cost	Investment cost	448658	R					Feed-in-tariff	0.5724	R/kWh

LCoE calculation

Year	Discount factor	Degradation factor	Electricity produced	Discounted electricity	Investment cost	Operation and maintenance	Inverter replacement	Annual cash flow	Discounted cash flow	Residual value	Discounted residual value
0	1	1			448658						
1	0.935	0.996	31441	29384		5720	6566	12286	11482		
2	0.873	0.992	31315	27352		5720	6566	12286	10731		
3	0.816	0.988	31190	25460		5720	6566	12286	10029		
4	0.763	0.984	31065	23700		5720	6566	12286	9373		
5	0.713	0.980	30941	22060		5720	6566	12286	8760		
6	0.666	0.976	30817	20535		5720	6566	12286	8187		
7	0.623	0.972	30694	19115		5720	6566	12286	7651		
8	0.582	0.968	30571	17793		5720	6566	12286	7151		
9	0.544	0.965	30449	16562		5720	6566	12286	6683		
10	0.508	0.961	30327	15417		5720	6566	12286	6246		
11	0.475	0.957	30206	14351		5720	6566	12286	5837		
12	0.444	0.953	30085	13358		5720	6566	12286	5455		
13	0.415	0.949	29965	12434		5720	6566	12286	5098		
14	0.388	0.945	29845	11574		5720	6566	12286	4765		
15	0.362	0.942	29725	10774		5720	6566	12286	4453		
16	0.339	0.938	29606	10029		5720	0	5720	1938		
17	0.317	0.934	29488	9335		5720	0	5720	1811		
18	0.296	0.930	29370	8690		5720	0	5720	1692		
19	0.277	0.927	29253	8089		5720	0	5720	1582		
20	0.258	0.923	29136	7529		5720	0	5720	1478		
21	0.242	0.919	29019	7008		5720	0	5720	1381		
22	0.226	0.916	28903	6524		5720	0	5720	1291		
23	0.211	0.912	28787	6073		5720	0	5720	1207		
24	0.197	0.908	28672	5653		5720	0	5720	1128		
25	0.184	0.905	28558	5262		5720	0	5720	1054	44866	8266
Sum				354059					126462		

Figure G.2: Spreadsheet used in the economical evaluation to calculate LCoE.

Paynack time and NPV

Depreciation tax savings	Electricity bill saving	Electricity sold to utility	Annual cash flow	Discounted cash flow	Cumulative savings
					-448658
125624	33642	1800	148780	133047	-309611
	33508	1792	23014	20101	-289510
	33374	1785	22873	18671	-270839
	33240	1778	22732	17342	-253496
	33107	1771	22592	16108	-237389
	32975	1764	22453	14961	-222427
	32843	1757	22314	13896	-208532
	32711	1750	22175	12906	-195625
	32581	1743	22037	11987	-183638
	32450	1736	21900	11133	-172506
	32320	1729	21763	10340	-162166
	32191	1722	21627	9603	-152563
	32062	1715	21492	8918	-143645
	31934	1708	21356	8282	-135363
	31806	1701	21222	7692	-127671
	31679	1695	27654	9367	-118304
	31552	1688	27520	8712	-109591
	31426	1681	27387	8103	-101488
	31301	1674	27255	7536	-93952
	31175	1668	27123	7009	-86943
	31051	1661	26992	6519	-80424
	30926	1654	26861	6063	-74361
	30803	1648	26731	5639	-68723
	30680	1641	26601	5244	-63478
	30557	1635	26471	4877	-58601
				390057	

Figure G.3: Spreadsheet used in the economical evaluation to calculate NPV and payback time. Additional information from the spreadsheet in figure G.2 was used in the calculations.

Norges miljø- og biovitenskapelige universitet
Noregs miljø- og biovitskapelege universitet
Norwegian University of Life Sciences

Postboks 5003
NO-1432 Ås
Norway